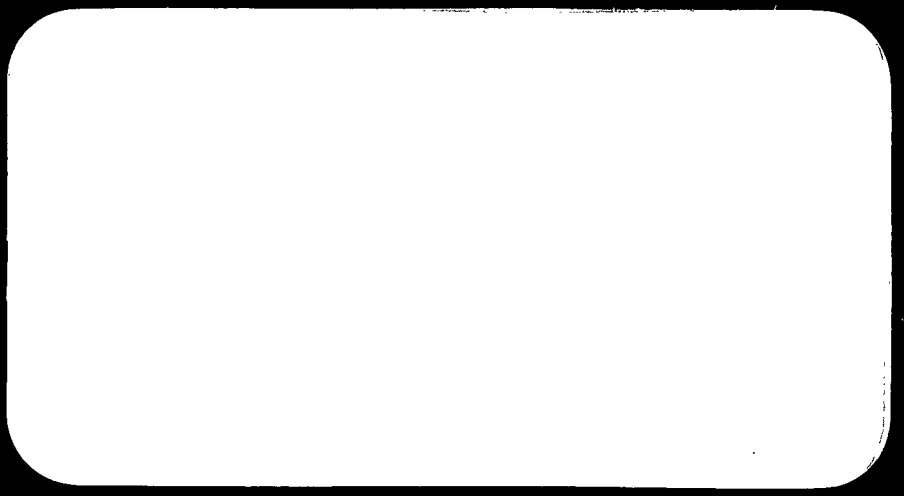

*Grumman*

# ADVANCED DEVELOPMENT

GRUMMAN AIRCRAFT ENGINEERING CORPORATION
BETHPAGE NEW YORK

GRUMMAN AIRCRAFT ENGINEERING CORPORATION, Bethpage, N.Y.

ADVANCED DEVELOPMENT

Copy 58

# AN ENGINEERING EVALUATION OF AIRPLANE GUST LOAD ANALYSIS METHODS

## VOLUME I - THEORETICAL DEVELOPMENT

REPORT NO. ADR 06-14-63.1 DATE OCTOBER 1963

PREPARED UNDER BUREAU OF NAVAL WEAPONS
CONTRACT NOw 60-0449-c

Final rept.

by DINO GEORGE
JOHN B. SMEDFJELD and
DYNAMIC ANALYSIS SECTION

GEORGE R. SCHIRO,
AERODYNAMICS SECTION



APPROVED BY Eugene F. Baird
CHIEF OF DYNAMIC ANALYSIS

APPROVED BY Robert E. Sauer
CHIEF OF ADVANCED DEVELOPMENT

## FOREWARD

This report was prepared by the Grumman Aircraft Engineering Corporation, Bethpage, New York, for the Bureau of Naval Weapons, Washington, D.C., under contract NOw 60-0449-c, dated 8 June 1960.

The work was performed under the cognizance of Grumman Advanced Development by the Dynamic Analysis and Aerodynamics Sections of the Grumman Engineering Department. The project was monitored initially by Mr. E. J. Griffin and subsequently by Mr. J. H. Walls, RAAD-223, Loads and Dynamics Branch, Airframe Design Division, Bureau of Naval Weapons.

This report is the final report on the project, and supersedes previous progress reports. It is presented in three complementary volumes as follows:

Volume I - Theoretical Development (Unclassified)

Volume II - Calculation Procedure (Confidential)

Volume III - Results (Confidential)

All three volumes have the same basic title, An Engineering Evaluation of Airplane Gust Load Analysis Methods. The theoretical development and calculation procedures have general application to subsonic aircraft. The illustrative examples, data, and specific results are for the A-6A airplane.

## TABLE OF CONTENTS

## SUMMARY

Airplane longitudinal motion is described by a linear, multi-degree-of-freedom system of forced response equations in terms of normal modes, where the basic inputs to the system are the generalized aerodynamic forces due to motion and gust. The modes considered in the analysis are two symmetric rigid-body modes (vertical translation and pitch) and an arbitrary number of symmetric vibration modes of the wing and fuselage with the stabilizer assumed rigid. In formulating the generalized forces, strip theory, appropriately modified to yield experimental complete-airplane steady-state stability derivatives, is used. The lifting elements (strips) of the airplane are an arbitrary number of wing and tail panels per side. Aerodynamic loading of the fuselage is assumed to be acting on the wing sections obtained by extending the wing to the centerline of the airplane.

Development of the generalized force variations is carried out through use of Duhamel's integral, with the unsteady aerodynamics due to motion, gust, and downwash being described by indicial lift functions which include both compressibility and aspect ratio effects. The unsteady aerodynamics of swept planforms is considered by developing indicial generalized force functions which account for the sweep of the leading edge of the wing and tail by a transport time delay to the leading edge of each panel. Auxiliary differential equations derived from exponential and/or damped trigonometric approximations to the indicial functions are used to represent the aerodynamics due to arbitrary motion and gusts in either the time or the frequency domain.

Control system dynamics, including stick motion, stabilizer rotation, and autopilot control, is also provided.

Incremental structural loads (shear, bending moment, and torque) are determined for several wing spanwise stations and one tail station. The wing loads are determined using the mode acceleration method, with the aerodynamic forces being approximated by the rigid-body airload distribution which

would produce the previously calculated rigid-body vertical acceleration. The tail incremental shear is based on the force summation method, with the aerodynamic forces being summed over the panels. The associated tail torque and bending moment due to the aerodynamic forces are obtained by multiplying the lift by appropriate moment arms.

The response in each of the variables considered may be obtained either in the form of time histories, frequency responses, or in the statistical forms of power spectra and/or response peaks per unit time.

# INTRODUCTION

Early airplane gust response investigations were based on relatively simple mathematical models of the disturbance and the disturbed vehicle. The gust models consisted of simplified representative shapes, such as the sharp-edged gust and the ramp-type gust. The resultant airplane motion was computed primarily on the basis of the vertical response, with correction factors added to account for pitching motion, flexibility, and unsteady aerodynamics.

With advances in the state of the art of aircraft design, gust response analysis methods were of course gradually improved. And, in the late 1950's, with the introduction of power-spectral methods in the gust response field and the subsequent measurement of actual atmospheric turbulence characteristics, it became possible to base gust response analyses on a more realistic description of the gust input.

To complement this advance, it was also desirable to obtain additional information on analytical techniques required for a realistic description of the airplane response. To provide such information for subsonic attack- and fighter-type aircraft, the project on which this report is based was established.

A set of equations of motion was formulated which includes control system dynamics, a relatively large number of structural modes, and a fairly comprehensive treatment of the unsteady aerodynamics. Thereafter, successive simplifications in these equations were introduced to obtain information on the degree of analytical sophistication required to obtain gust response data of reasonable engineering accuracy. Finally, a comparison was made between results from the power-spectral approach and those from the one-minus-cosine discrete-gust method.

This volume, Volume I, presents the development of the equations of motion used in the study. The translation of these equations into working digital computer programs is presented in Volume II. Finally, in Volume III, the numerical results of the project are presented and discussed.

## REFERENCES


1. Hobbs, N. P., Indicial Downwash and Its Structural Effect on the Horizontal Tail, Wright Air Development Center Technical Report 56-154, August 1956.

2. Press, H., Mazelsky, B., A Study of the Application of Power Spectral Methods of Generalized Harmonic Analysis to Gust Loads on Airplanes, National Advisory Committee for Aeronautics Technical Report 1172, 1954.

3. Press, H., Meadows, M. T., Hadlock, I., A Reevaluation of Data on Atmospheric Turbulence and Airplane Gust Loads for Application in Spectral Calculations, National Advisory Committee for Aeronautics Technical Report 1272, 1956.

4. Diederich, F. W., Drischler, J. A., Effect of Spanwise Variations in Gust Intensity on the Lift Due to Atmospheric Turbulence, National Advisory Committee for Aeronautics Technical Note 3920, April 1957.

5. Press, H., Tukey, J. W., Power Spectral Methods of Analysis and Application in Airplane Dynamics, Agard Flight Test Manual, Volume IV, Part IVC, June 1956.

6. Press, H., Steiner, R., An Approach to the Problem of Estimating Severe and Repeated Gust Loads for Missile Operations, National Advisory Committee for Aeronautics Technical Note 4332, September 1958.

7. Zetkov, G., Block Diagram Description of A2F-1 Autopilot and Related Systems, Grumman Aircraft Engineering Corporation Report DAN 128-388.2, April 1960.

8. Wiesinger, G. C., Control System Design Report for A2F-1 Airplane, Grumman Aircraft Engineering Corporation Report MD-416400-A1, October 1958.

9. Spiegler, S., Equations of Motion and Data for the A2F-1 Mission Simulator, Grumman Aircraft Engineering Corporation Report DAN 128-258.1, July 1959.

10. Kress, R. W., Mayer, G. F., Dynamic Longitudinal Stability Analysis of the Model F9F-6 Airplane, Grumman Aircraft Engineering Corporation Report RE-68, July 1954.

11. Conners, C. R., Stability and Performance Analysis of the A2F-1 Power Operated Flight Control Systems, Grumman Aircraft Engineering Corporation Report DA 128-368.1, April 1960.

12. Mazelsky, B., Drischler, J. A., Numerical Determination of Indicial Lift and Moment Functions for a Two-Dimensional Sinking and Pitching Airfoil at Mach Numbers of 0.5 and 0.6, National Advisory Committee for Aeronautics Technical Note 2739, 1952.

13. Drischler, J. A., Approximate Indicial Lift Functions for Several Wings of Finite Span in Incompressible Flow as Obtained from Oscillatory Lift Coefficients, National Advisory Committee for Aeronautics Technical Note 3639, 1956.

14. Jones, L. A., Cronk, E. A., Lamb, P. O., Christopherson, D. C., Nichols, C. D., Gust Alleviation Study, Part I, Estimation of the Control Derivatives for Flaps, Spoilers, and Other Control Devices Intended for Use as Gust Alleviators, Wright Air Development Center Technical Report 57-750, Pt. I, January 1958.

15. Bisplinghoff, R. L., Ashley, H., Halfman, R. L., Aeroelasticity, Addison-Wesley Publishing Co., Inc., 1955.

16. Hildebrand, F. B., Introduction to Numerical Analysis, McGraw-Hill Book Company Inc., 1956.

17. Williams, D., Displacements of a Linear Elastic System Under a Given Transient Load, The Aeronautical Quarterly, Volume I, August 1954.

# DISCUSSION AND SUMMARY OF THEORETICAL DEVELOPMENT

## I. Introduction

The detailed theoretical development of the equations for the solution of the flexible-airplane longitudinal gust response problem is carried out in Appendices A to F. The development is so arranged that the reader interested in acquiring a complete understanding of the details involved in the development may continue from Appendix A right through Appendix F. Symbols are listed in Appendix G.

Appendix A presents the development of the autopilot and control system equations which consist of the autopilot signal, the stick and sprashpot signals, and the stabilizer rotation. In Appendix B, the concept of the indicial lift function is discussed, and the method by which these functions are evaluated including compressibility and aspect-ratio effects is described. The indicial lift functions presented herein account for the unsteady aerodynamics of subsonic rectangular planforms due to a stationary step gust, a step change in angle of attack caused by motion, and the downwash at the tail caused by wing motion and gust on the wing. In Appendix C, the unsteady aerodynamics of swept planforms is considered by developing indicial generalized force functions which account for the sweep of the leading edge of the wing and tail. The development of these functions is dependent upon the indicial lift functions due to gust and downwash developed in Appendix B. Appendices D and E develop the generalized forces which are the inputs to the equations of motion. These generalized forces are divided into the following six groupings: (1) motion of the wing, (2) motion of the tail and rotation of the stabilizer, (3) downwash at the tail due to motion of the wing, (4) downwash at the tail due to gust on the wing, (5) gust on the tail, and (6) gust on the wing. Finally in Appendix F, expressions for the airplane structural loads are developed. These expressions are specifically developed for several wing spanwise stations and for one tail station defined by the juncture of the fuselage side and the stabilizer torque tube.

The final form of the equations summarized in the subsequent sections of the main part of the report are reproduced from these appendices after a certain amount

of algebraic manipulation. Also, the time-history differential-equations representation of the variables is converted to a frequency-dependent algebraic-equations representation through the assumption of a sinusoidal form of the variables as given by the following expression:

$$f(s-s_{TD}) = f_a(\omega)e^{i(\kappa s + f_\alpha(\omega)-\kappa s_{TD})} \tag{1}$$

The function $f_a(\omega)$ represents the steady-state harmonic amplitude of the assumed sinusoidal variable on the left-hand side of equation (1). The constant $f_\alpha(\omega)$ is the phase angle of the variable f(s) with respect to a reference forcing function and $\kappa$ is the reduced frequency in radians per wing reference semichord. The time delay $s_{TD}$ is included for those special cases where a physical time delay is associated with a particular function, such as the gust on the tail. Equation (1) may be rearranged as follows:

$$f(s-s_{TD}) = f(\omega)[e^{-i\kappa s_{TD}}][e^{i\kappa s}] \tag{2}$$

where

$$\left.\begin{aligned} f(\omega) &= f_a(\omega)e^{if_\alpha(\omega)} \\ &= f_a(\omega)[\cos(f_\alpha(\omega)) + i\sin(f_\alpha(\omega))] \\ \kappa &= \omega b_R/V = \omega t/s \end{aligned}\right\} \tag{3}$$

and

Now let the Greek letter rho, $\rho$, be used as a subscript to represent the real part and the Greek letter iota, $\iota$, be used to represent the imaginary part. Equation (3) is now written as

$$f(\omega) = f_\rho(\omega) + if_\iota(\omega) \tag{4}$$

where

$$\left.\begin{aligned} f_\rho(\omega) &= f_a(\omega)\ \cos(f_\alpha(\omega)) \\ f_\iota(\omega) &= f_a(\omega)\ \sin(f_\alpha(\omega)) \end{aligned}\right\} \qquad (5)$$

The magnitude of the function is given by

$$f_a(\omega) = [f_\rho^2(\omega) + f_\iota^2(\omega)]^{\frac{1}{2}} \qquad (6)$$

and the phase relationship is

$$f_\alpha(\omega) = \tan^{-1}[f_\iota(\omega)/f_\rho(\omega)] \qquad (7)$$

Equation (2) may be rearranged further as

$$f(s-s_{TD}) = f(\bar{\omega})[\cos \kappa s_{TD} - i \sin \kappa s_{TD}]e^{i\kappa s} \qquad (8)$$

Equations (4) and (8) are the primary equations which will be used in converting the time history expressions to simple harmonic motion. Furthermore, the required first and second derivatives may be evaluated from equation (8) as follows:

$$\mathring{f}(s-s_{TD}) = i\kappa f(\omega)[\cos \kappa s_{TD} - i \sin \kappa s_{TD}]e^{i\kappa s} \qquad (9)$$

$$\mathring{\mathring{f}}(s-s_{TD}) = -\kappa^2 f(\omega)[\cos \kappa s_{TD} - i \sin \kappa s_{TD}]e^{i\kappa s} \qquad (10)$$

where a circle over the variable indicates differentiation with respect to the non-dimensional time, s.

## II. Autopilot and Control System Equations

The A-6A (A2F-1) automatic flight control system has three basic modes of operation: manual with stability augmentation, pilot relief, and command. In the present study, which is restricted to longitudinal perturbations at constant velocity, only the manual mode with stability augmentation and the pilot relief mode in attitude hold will be considered. For these cases, autopilot signals are integrated into the longitudinal control system so as to effect stabilizer motion independently of stick motion. The autopilot signal equation given herein is written in general form to accommodate either one of the above cases. Signals from the motion sensing devices are written in terms of the normal mode components of airplane motion. The equation describing the autopilot signal is reproduced from equation (A5) as

$$\dot{\mu}(s) + L_{10}\mu(s) = \sum_{n=1}^{N} [L_{1n}\ddot{\xi}_n(s) + L_{2n}\dot{\xi}_n(s) + L_{3n}\xi_n(s)] \qquad (11)$$

Simple harmonic motion substitution yields for the autopilot equation

$$\mu(\omega) = \sum_{n=1}^{N} [N_{\mu n}/D_{\mu}]\xi_n(\omega) \qquad (12)$$

where

$$\mu(\omega) = \mu_{\rho}(\omega) + i\mu_{\iota}(\omega) \qquad (13)$$

and

$$\left.\begin{aligned} N_{\mu n} &= (L_{10} - i\kappa)[(L_{3n} - \kappa^2 L_{1n}) + i\kappa L_{2n}] \\ D_{\mu} &= L_{10}^2 + \kappa^2 \end{aligned}\right\} \qquad (14)$$

In the stick-free condition, the stick deflection resulting from aircraft motion is determined by an artificial feel system consisting of a feel spring, a sprashpot, and

two bobweights. The feel spring and the stick inertia are represented by the left side of the stick equation, while the reaction force from the sprashpot and the inertial forces from the bobweights (in terms of normal mode components) are contained on the right side. The sprashpot equation represents a spring and dashpot in series connected to the stick below the stick pivot point. Nonlinearities in the control system due to friction have been neglected. The stick and sprashpot signal equations are given by equations (A17) and (A18) which are reproduced below.

$$\overset{\circ\circ}{\tau}(s) + H_{30}\tau(s) = \sum_{n=1}^{N} H_{3n}\overset{\circ\circ}{\xi}_n(s) + H_{3\eta}\overset{\circ}{\eta}(s) \tag{15}$$

$$\overset{\circ}{\eta}(s) + H_{40}\eta(s) = H_{40}\tau(s) \tag{16}$$

Simple harmonic motion input into these expressions reduces them to the following relationships:

$$\tau(\omega) = [-\kappa^2 \sum_{n=1}^{N} H_{3n}\xi_n(\omega) + i\kappa H_{3\eta}\eta(\omega)]/[H_{30} - \kappa^2] \tag{17}$$

$$\eta(\omega) = [H_{40}(H_{40} - i\kappa)/(H_{40}^2 + \kappa^2)]\tau(\omega) \tag{18}$$

where

$$\left.\begin{aligned} \tau(\omega) &= \tau_\rho(\omega) + i\tau_\iota(\omega) \\ \eta(\omega) &= \eta_\rho(\omega) + i\eta_\iota(\omega) \end{aligned}\right\} \tag{19}$$

The stabilizer deflection results from a superposition of input signals from the autopilot and the stick. The equation describing the stabilizer rotation is reproduced below from equation (A26).

$$\overset{\circ\circ}{\gamma}(s) + H_{20}\overset{\circ}{\gamma}(s) + H_{21}\gamma(s) = H_{21}\mu(s) + H_{22}\tau(s) \tag{20}$$

Substitution of simple harmonic motion into the above equation yields,

$$\gamma(\omega) = [N_{\gamma 1}\mu(\omega) + N_{\gamma 2}\tau(\omega)]/D_{\gamma} \tag{21}$$

where

$$\gamma(\omega) = \gamma_{\rho}(\omega) + i\gamma_{i}(\omega) \tag{22}$$

and

$$\left.\begin{aligned} N_{\gamma 1} &= [(H_{21} - \kappa^2) - i\kappa H_{20}]H_{21} \\ N_{\gamma 2} &= [(H_{21} - \kappa^2) - i\kappa H_{20}]H_{22} \\ D_{\gamma} &= (H_{21} - \kappa^2)^2 + \kappa^2 H_{20}^2 \end{aligned}\right\} \tag{23}$$

## III. Indicial Lift and Generalized Force Functions

Indicial lift functions describe the unsteady lift build up on rectangular planforms due to planform motion, gust on the planform, and downwash effects on an aft planform due to either gust or motion of the forward planform. In the case of a swept planform, a gust or downwash envelops successive spanwise portions of the planform at different times, and therefore, the lift variation on the planform is changed by the sweep of the planform leading edge. The effect of sweep is introduced through the development of indicial generalized force functions for each mode (rigid-body and flexible modes) which depend upon the indicial lift functions, planform sweep, mode shapes, and aerodynamics.

A discussion emphasizing some of the more significant aspects of the analysis for the indicial lift and generalized force functions follows.

The present analysis is based on indicial lift functions for the lift build up on rectangular planforms due to a stationary step gust and a step change in angle of attack due to motion. The lift build up on a rectangular planform due to a step change in angle of attack as a result of a vertical gust with zero gust front velocity, normalized with respect to the steady-state lift and including compressibility and aspect ratio effects, is referred to as the Küssner-type function. This function is approximated by an analytical expression made up of the sum of exponential terms as given by either of equations (B7) or (B10) .

$$\psi(s) = \psi(0) + \sum_{k=1}^{K_\psi} a_k (1 - e^{-\alpha_k s}) \qquad (24)$$

where the letters W and T in equations (B7) and (B10) representing gust on the wing and gust on the tail, respectively, are deleted here for convenience. The maximum index, $K_\psi$, designates the number of exponentials used in approximating the indicial lift function due to gust. The purpose of the constant, $\psi(0)$, is to permit the reduction of the equation to the limiting case where the lift build up due to gust is assumed instantaneous, that is, where no transient effects are present. The reduction

of the equation to this instantaneous lift build up may be accomplished by letting $\psi(0) = 1.0$ and $a_k = 0$ for $k = 1, 2, \ldots, K_\psi$. The constants $a_k$ and $\alpha_k$ will be a function of the Mach number and aspect ratio (see Figure B2).

The lift build up on a rectangular planform due to a step change in angle of attack as a result of motion, normalized with respect to the steady-state lift and including compressibility and aspect ratio effects, is referred to as the Wagner-type function. This function is also approximated by an analytical expression consisting of a constant plus the sum of a number of exponential terms. (See equations (B15) and (B17)). Once again the expression is reproduced below without the identifying letters W or T.

$$\phi(s) = \phi(0) + \sum_{k=1}^{K_\phi} b_k (1 - e^{-\beta_k s}) \tag{25}$$

The constant term arises from the instantaneous lift at time zero, which for incompressible flow and infinite aspect ratio, is equal to one-half. The other coefficients and exponents appearing in the Wagner-type function are evaluated in a manner similar to the constants in the Küssner-type function. A typical plot of a Wagner-type function, and a comparison with a Küssner-type function is shown in Figure B4.

The normalized unsteady downwash experienced at the tail due to step gust on the wing or a step change in angle of attack due to wing motion is referred to as an indicial downwash function (see Figure B5). Since the downwash has the characteristics of a gust disturbance, the lift build up on the tail due to downwash is assumed to be given by Duhamel's integral in terms of the indicial downwash function,

$$w(M_g, M, AR_W, s_T^x, s_T^z, s_\lambda',$$

and the tail Küssner-type function. (See equations (B20) and (B21)).

$$\delta(s) = \int_0^s w(M_g, M, AR_W, s_T^x, s_T^z, \sigma)\psi_T'(s-\sigma)\,d\sigma \tag{26}$$

where, for downwash due to motion, the gust front Mach number is taken as $M_g = \infty$, and for downwash due to a stationary gust, $M_g = 0$. The parameters $s_T^x$ and $s_T^z$ in the indicial downwash function are defined in Figure B1 , and $AR_W$ is the aspect ratio of the wing. The time history variation given by equation (26) is indicated in Figure B7.

The indicial generalized force functions developed herein are defined in terms of a strip theory representation of the unsteady aerodynamics. The indicial generalized force functions describe the normalized time variation of the generalized forces on a swept planform, assuming a lift build up variation on each strip given by the Küssner-type function, as a step gust envelops succeeding spanwise portions of the planform. In the present analysis, which is for a stationary gust, it is assumed that the spanwise rate of gust envelopment is a function of wing and tail leading-edge sweep. Similarly, the rate of downwash envelopment of the tail is assumed to be a function of the tail leading-edge sweep.

To develop the indicial generalized force functions, the wing and tail are divided into a number of panels, where the lift and pitching moment about the reference axis on each panel, determined by the local geometry and aerodynamic properties, are assumed to start at the time the gust (or downwash) reaches the panel spanwise midpoint at the leading edge. Assuming a Küssner-type variation of the lift build up, the total generalized force after the gust or downwash has progressed to a given outboard station is determined by the sum of the generalized forces over all the inboard panels.

Analytical approximations to the indicial generalized force functions are obtained by considering each function to consist of a number of damped trigonometric and/or pure exponential terms. For gust on the wing, the expression for the indicial generalized force function is given by equation (C13) which is reproduced below.

$$\psi_m^W(s) = \psi_W(0) + \sum_{k=1}^{2} a_{mk}^W (1 - e^{-\alpha_{mk}^W s}) + \left[ a_{m3}^W [1 - e^{-\alpha_{m3}^W s} \cos(\omega_{m3}^W s)] - b_{m3}^W e^{-\alpha_{m3}^W s} \sin(\omega_{m3}^W s) \right] \quad (27)$$

In the case of gust on the tail, the indicial generalized force function is similar to equation (27) with the letter W being replaced by T. Furthermore, the downwash effects are represented by the same type of expression, where now the left hand side of equation (27) is replaced by $\delta_m^M(s)$ for downwash due to motion, and by $\delta_m^G(s)$ for downwash due to gust; also, the symbol W is replaced by M and G, respectively. It is noted that the assumption of rigid tail in the present study renders the tail indicial generalized force functions for all modes nearly identical numerically to those for the first mode, that is, according to equations (C15), (C17), and (C19),

$$\left.\begin{aligned} \psi_m^T(s) &\cong \psi_1^T(s) \\ \delta_m^G(s) &\cong \delta_1^G(s) \\ \delta_m^M(s) &\cong \delta_1^M(s) \end{aligned}\right\} \text{ for all m} \qquad (28)$$

Therefore, the functions $\psi_1^T(s)$, $\delta_1^G(s)$, $\delta_1^M(s)$ are used for the other modes as well.

For motion of the wing and tail, the lift build up occurs simultaneously over the entire planform. Therefore, sweep effects do not modify the wing and tail Wagner-type functions, and equation (25) is also a valid approximation to the indicial generalized force functions.

## IV. Equations of Motion and Associated Aerodynamic Lag Equations

In this analysis it is assumed that the airplane encounters a stationary gust symmetrically, and that no spanwise variation in the gust exists. The dynamic response of the airplane due to the gust is obtained by a modal analysis in which the airframe is allowed six degrees of freedom: two symmetric rigid-body modes (vertical translation and pitch), and four symmetric vibration modes of the wing and fuselage with the stabilizer assumed rigid. Note that the flexible modes considered here are coupled bending-torsion modes, and that the word "bending" in a designation such as "first symmetric wing bending mode" is intended only as an indication of the dominant feature of that mode.

Airplane longitudinal motion is described by a linear, multi-degree-of-freedom system of forced response equations in terms of the aforementioned modes, where the basic inputs to the system are the generalized forces due to motion and gust. Structural damping is conservatively neglected throughout the analysis. In formulating the generalized forces, strip theory, appropriately modified to yield correct complete-airplane steady-state stability derivatives, is used. The lifting elements (strips) of the airplane are ten wing panels and six tail panels per side. Aerodynamic loading of the fuselage is assumed to be acting on the wing sections obtained by extending the wing to the centerline of the airplane. The differential equations used in obtaining the airplane response are derived from the following special form of Lagrange's equations of motion,

$$\frac{d}{dt}\left(\frac{\partial T(t)}{\partial \dot{\xi}_m(t)}\right) + \frac{\partial V(t)}{\partial \xi_m(t)} = Q_m^M(t) + Q_m^G(t) \qquad (29)$$

$$\text{for } m = 1, 2, \ldots N$$

where $T(t)$ and $V(t)$ are the kinetic and potential energies, and $Q_m^M(t)$ and $Q_m^G(t)$ are the generalized forces in the $m^{th}$ mode due to motion and gust, respectively.

In converting equation (29) to non-dimensional time, the following substitutions are made:

$$s = \left(\frac{V}{b_R}\right)t \tag{30}$$

$$\frac{d}{dt} = \left(\frac{V}{b_R}\right)\frac{d}{ds} \tag{31}$$

It is noted, for example, that the generalized force due to motion, $Q_m^M(t)$, after conversion should be expressed $Q_m^M\left(\frac{b_R s}{V}\right)$, but for brevity and to reduce excessive symbols for new functional notations, it is designated simply as $Q_m^M(s)$. After conversion, $V(t)$, $\xi_m(t)$, and $Q_m^G(t)$ are simply expressed as $V(s)$, $\xi_m(s)$ and $Q_m^G(s)$. The kinetic energy terms, after substitution of equation (31), become

$$\left(\frac{V}{b_R}\right)\frac{d}{ds}\left(\frac{\partial T(s)}{\left(\frac{V}{b_R}\right)\partial\mathring{\xi}_m(s)}\right) = \frac{d}{ds}\left(\frac{\partial T(s)}{\partial\mathring{\xi}_m(s)}\right) \tag{32}$$

where the circle over the variable indicates differentiation with respect to the non-dimensional time, s. Equation (29) becomes

$$\frac{d}{ds}\left(\frac{\partial T(s)}{\partial\mathring{\xi}_m(s)}\right) + \frac{\partial V(s)}{\partial\xi_m(s)} = Q_m^M(s) + Q_m^G(s) \tag{33}$$

The kinetic energy is expressed in terms of the normal velocity coordinates, $\mathring{\xi}_m(s)$, the stabilizer rotation velocity, $\mathring{\gamma}(s)$, and the generalized mass terms as follows:

$$T(s) = (V/b_R)^2\left\{\sum_{m=1}^{N}\left[M_{mm}\mathring{\xi}_m^2(s) + 2M_{m\gamma}\mathring{\gamma}(s)\mathring{\xi}_m(s)\right] + M_{\gamma\gamma}\mathring{\gamma}^2(s)\right\}/2g \tag{34}$$

Note that the factor "g" is introduced because the generalized mass, as used herein, is defined in terms of pounds mass rather than slugs.

The potential energy is expressed in terms of the normal coordinates, $\xi_m(s)$, and the generalized spring terms as follows:

$$V(s) = \tfrac{1}{2} \sum_{m=1}^{N} [\omega_m^2 M_{mm} \xi_m^2(s)]/g \tag{35}$$

The generalized force in the $m^{th}$ mode due to motion, $Q_m^M(s)$, is composed of the four distinct inputs associated with wing motion, tail motion, stabilizer rotation, and downwash on the tail due to wing motion. The wing and tail generalized forces due to wing motion and tail motion are made up of non-circulatory contributions (apparent mass effects) described in terms of acceleration and velocity, and circulatory contributions given in terms of velocity and displacement. The circulatory contribution is included in the analysis through the use of Duhamel's integral in conjunction with the Wagner-type function given by equation (25). Use of Laplace transform techniques results in an expression for the generalized force due to motion which is made up of a constant term, due to $\phi(0)$ in equation (25) and a set of first order differential equations due to its exponential terms. The downwash on the tail due to wing motion is assumed to result from the rigid-body airplane response only, the reasoning being that downwash due to flexible wing motion, which has relatively small amplitude and high frequency, decays before it reaches the tail. The downwash is assumed to be constant across the tail span and to be defined in terms of the wing motion at a spanwise station corresponding to the tail mean aerodynamic chord. In the equations presented herein, the indicial lift functions due to tail motion and stabilizer rotation, have been assumed equal. Thus, these two motions are combined in a single set of equations.

The expression for the total generalized force due to wing motion, $Q_{1m}(s)$, tail motion and stabilizer rotation, $Q_{2m}(s)$, and downwash on the tail due to wing motion, $Q_{3m}(s)$, is given by the sum of the three component generalized forces:

$$Q_m^M(s) = \sum_{r=1}^{3} Q_{rm}(s), \quad 1 \leq m \leq N \tag{36}$$

The equations of the generalized forces for the three types of inputs are summarized below.

For wing motion, (r = 1), the generalized force consists of a non-circulatory contribution, $\Phi_m^{WN}(s)$, plus a circulatory contribution, $\Phi_m^{WC}(s)$, multiplied by a constant, $-C_V$, which is factored out of the final equations.

$$Q_{1m}(s) = -C_V[\Phi_m^{WN}(s) + \Phi_m^{WC}(s)] \tag{37}$$

$$\text{for } m = 1, 2, \ldots N$$

where $C_V = V^2/(b_R^2 g)$. The expression for the non-circulatory contribution to generalized force is

$$\Phi_m^{WN}(s) = \sum_{n=1}^{N} [A_{mn}^{WN} \overset{\circ\circ}{\xi}_n(s) + B_{mn}^{WN} \overset{\circ}{\xi}_n(s)] \tag{38}$$

where the coefficients in the above expression are defined by equation (E24) and (E25). The circulatory contributions to the generalized force are separated into two parts, the instantaneous lift term and the unsteady lift which is approximated by two term exponential representation of the Wagner-type function. From equations (E38) to (E40),

$$\Phi_m^{WC}(s) = \Phi_{m0}^{W}(s) + \Phi_m^{W}(s) \tag{39}$$

where

$$\Phi_{m0}^{W}(s) = \phi_W(0) F_m^W(s) \tag{40}$$

$$\Phi_m^{W}(s) = \sum_{k=1}^{2} \Phi_{mk}^{W}(s) \tag{41}$$

The unsteady lift terms of equation (41) are defined by the solutions to the differential equations given by equation (E41),

$$\overset{\circ}{\Phi}{}^{W}_{mk}(s) + \beta^{W}_{k}\Phi^{W}_{mk}(s) = b^{W}_{k}\beta^{W}_{k}F^{W}_{m}(s), \quad k = 1, 2 \tag{42}$$

The input to both equations (40) and (42) is defined in terms of the wing motion by the following relationship:

$$F^{W}_{m}(s) = \sum_{n=1}^{N} [B^{WC}_{mn}\overset{\circ}{\xi}_{n}(s) + C^{WC}_{mn}\xi_{n}(s)] \tag{43}$$

The coefficients in these expressions are defined by equations (E28) and (E29).

The expressions for the generalized forces for tail motion and stabilizer rotation (r = 2) are similar to those for wing motion. These expressions are reproduced from Appendix E, Section II. The generalized force is

$$Q_{2m}(s) = -C_{V}[\Phi^{TN}_{m}(s) + \Phi^{TC}_{m}(s)] \tag{44}$$

for m = 1, 2, 3, ...N. The non-circulatory contribution to the generalized force is given by

$$\Phi^{TN}_{m}(s) = \sum_{n=1}^{N} [A^{TN}_{mn}\overset{\circ\circ}{\xi}_{n}(s) + B^{TN}_{mn}\overset{\circ}{\xi}_{n}(s)] + A^{TN}_{m\gamma}\overset{\circ\circ}{\gamma}(s)$$

$$+ B^{TN}_{m\gamma}\overset{\circ}{\gamma}(s) \tag{45}$$

In a manner similar to the circulatory contributions to the wing generalized force, the expressions for the tail are

$$\Phi^{TC}_{m}(s) = \Phi^{T}_{m0}(s) + \Phi^{T}_{m}(s) \tag{46}$$

$$\Phi^{T}_{m0}(s) = \phi_{T}(0)F^{T}_{m}(s) \tag{47}$$

$$\Phi^{T}_{m}(s) = \sum_{k=1}^{2} \Phi^{T}_{mk}(s) \tag{48}$$

where $\Phi^{T}_{mk}(s)$ are solutions to the differential equations

$$\dot{\Phi}^{T}_{mk}(s) + \beta^{T}_{k}\Phi^{T}_{mk}(s) = b^{T}_{k}\beta^{T}_{k}F^{T}_{m}(s), \quad k = 1, 2 \tag{49}$$

and

$$F^{T}_{m}(s) = \sum_{n=1}^{N} [B^{TC}_{mn}\dot{\xi}_{n}(s) + C^{TC}_{mn}\xi_{n}(s)] + B^{TC}_{m\gamma}\dot{\gamma}(s) + C^{TC}_{m\gamma}\gamma(s) \tag{50}$$

Finally the generalized force due to downwash on the tail caused by wing motion ($r = 3$) is defined in terms of the downwash of the wing three quarter chord point and an assumed lift build up which includes the unsteady downwash as described by Hobbs in Reference 1 . The expression for the generalized force is reproduced from equation (E83).

$$Q_{3m}(s) = -C_{V}D^{M}_{m}\Delta^{M}_{m}(s) \tag{51}$$

The constant $D^{M}_{m}$ is defined (equation (E84)) in terms of the stabilizer geometry and aerodynamics. The generalized force variation, $\Delta^{M}_{m}(s)$, is given as the sum of the component parts, $\Delta^{M}_{mk}(s)$, obtained as the solutions to a set of three differential equations. The input to these equations is the wing motion, composed of normal mode velocity and displacement terms, modified by the downwash slope, $\partial\varepsilon/\partial\alpha$. Because of the assumption of a rigid tail, the generalized force variation is numerically nearly independent of mode and is therefore approximated by

$$\left.\begin{aligned} \Delta^{M}_{m}(s) &= \sum_{k=0}^{3} \Delta^{M}_{mk}(s) && \text{for } m = 1 \\ \Delta^{M}_{m}(s) &= \Delta^{M}_{1}(s) && 2 \leq m \leq N \end{aligned}\right\} \tag{52}$$

The right side of the first of equations (52) is obtained from the solution to the following set of differential equations under the assumption that the indicial generalized force function may be represented analytically by a constant plus a maximum of three terms, two of which are pure exponentials and the other a damped sinusoid.

These differential equations are reproduced from equations (E88) to (E90) as follows:

$$\Delta_{10}^{M}(s) = \delta_M(0)F_M(s-s_M) \tag{53}$$

$$\left.\begin{aligned} &\dot{\Delta}_{11}^{M}(s) + R_1\Delta_{11}^{M}(s) = R_2F_M(s-s_M), \quad k = 1 \\ &\dot{\Delta}_{12}^{M}(s) + R_3\Delta_{12}^{M}(s) = R_4F_M(s-s_M), \quad k = 2 \\ &\dot{\Delta}_{13}^{M}(s) + R_5\Delta_{13}^{M}(s) + R_6\int_0^s[\Delta_{13}^{M}(\sigma) + R_7F_M(\sigma-s_M)]d\sigma = \\ &\qquad R_8F_M(s-s_M), \quad k = 3 \end{aligned}\right\} \tag{54}$$

Note that in the case where three exponential terms, rather that two exponentials and a damped sinusoid, approximate the indicial generalized force function the last of equations (54) may be reduced to this condition by letting $R_6 = 0$. The input to equations (53) and (54) is given by equation (E91) as

$$F_M(s) = \sum_{n=1}^{2}[B_n^M\dot{\xi}_n(s) + C_n^M\xi_n(s)] \tag{55}$$

where the coefficients in equation (55) are defined by equations (E92) and (E93). The $R_i$ coefficients in equation (54) are easily evaluated by comparing equations (54) with equations (E88) to (E90). Therefore,

$$\left.\begin{aligned} &R_1 = \alpha_{11}^M \\ &R_2 = a_{11}^M\alpha_{11}^M \end{aligned}\right\} \quad k = 1$$

$$\left.\begin{aligned} &R_3 = \alpha_{12}^M \\ &R_4 = a_{12}^M\alpha_{12}^M \end{aligned}\right\} \quad k = 2$$

$$\left.\begin{aligned} &R_5 = 2\alpha_{13}^M \qquad R_7 = -a_{13}^M \\ &R_6 = (\alpha_{13}^M)^2 + (\omega_{13}^M)^2 \qquad R_8 = a_{13}^M\alpha_{13}^M - b_{13}^M\omega_{13}^M \end{aligned}\right\} \quad k = 3 \tag{56}$$

The time delay $s_M$ is the time between wing motion and the assumed start of the resulting tail lift build up due to downwash.

The generalized force in the $m^{th}$ mode due to gust, $Q_m^G(s)$ in equation (33), consists of the following three parts: gust on the tail, gust on the wing, and downwash on the tail due to gust on the wing. Transport time delays required for the gust front to travel (the gust front is actually stationary in space but does "travel" relative to the airplane) from the assumed zero reference time to the wing and tail and for the wing downwash to reach the tail are also included in the definition of the generalized forces.

The total generalized force due to gust may now be defined in terms of the following contributions: downwash on the tail due to gust on the wing, $Q_{4m}(s)$; gust on the tail, $Q_{5m}(s)$; and gust on the wing, $Q_{6m}(s)$.

$$Q_m^G(s) = \sum_{r=4}^{6} Q_{rm}(s) \tag{57}$$

Expression for evaluating the generalized force arising from downwash on the tail due to gust on the wing (r=4) is given by equation (D22) and is reproduced below.

$$Q_{4m}(s) = C_V D_m^G \Delta_1^G(s) \tag{58}$$

where $C_V = (V^2/b_R^2 g)$, and the coefficient $D_m^G$ depends on the tail geometry and aerodynamics and is evaluated by equation (D23). The generalized force variation, $\Delta_1^G(s)$, is evaluated for the first mode only, because the assumption of a rigid tail makes the unsteady aerodynamic functions due to gust and downwash nearly independent of the mode shape for the six normal modes considered in this problem. The expression for evaluating the generalized force variation is given by equation (D24) as

$$\Delta_1^G(s) = \sum_{k=0}^{3} \Delta_{1k}^G(s) \tag{59}$$

The component parts of the generalized force variations as given by equations (D25) to (D27) are reproduced below.

$$\Delta_{10}^{G}(s) = -\left|\partial\varepsilon/\partial\alpha\right|\delta_{G}(0)\chi(s-s_{G}) \tag{60}$$

$$\left.\begin{aligned} &\dot{\Delta}_{11}^{G}(s) + Q_1\Delta_{11}^{G}(s) = Q_2\chi(s-s_{G}),\ k = 1 \\ &\dot{\Delta}_{12}^{G}(s) + Q_3\Delta_{12}^{G}(s) = Q_4\chi(s-s_{G}),\ k = 2 \\ &\dot{\Delta}_{13}^{G}(s) + Q_5\Delta_{13}^{G}(s) + Q_6\int_0^s[\Delta_{13}^{G}(\sigma) + Q_7\chi(\sigma-s_{G})]d\sigma = \\ &\qquad Q_8\chi(s-s_{G}),\ k = 3 \end{aligned}\right\} \tag{61}$$

where $s_G$ is the time delay between the airplane zero time reference point and the assumed start of tail lift build up due to downwash resulting from gust on the wing. The coefficients appearing in equations (61) are defined as

$$\left.\begin{aligned} Q_1 &= \alpha_{11}^{G} \\ Q_2 &= -a_{11}^{G}\alpha_{11}^{G}\left|\partial\varepsilon/\partial\alpha\right| \end{aligned}\right\} \quad k = 1$$

$$\left.\begin{aligned} Q_3 &= \alpha_{12}^{G} \\ Q_4 &= -a_{12}^{G}\alpha_{12}^{G}\left|\partial\varepsilon/\partial\alpha\right| \end{aligned}\right\} \quad k = 2$$

$$\left.\begin{aligned} Q_5 &= 2\alpha_{13}^{G} \\ Q_6 &= (\alpha_{13}^{G})^2 + (\omega_{13}^{G})^2 \\ Q_7 &= +a_{13}^{G}\left|\partial\varepsilon/\partial\alpha\right| \\ Q_8 &= -[a_{13}^{G}\alpha_{13}^{G} - b_{13}^{G}\omega_{13}^{G}]\left|\partial\varepsilon/\partial\alpha\right| \end{aligned}\right\} \quad k = 3 \tag{62}$$

where the constant $|\partial\varepsilon/\partial\alpha|$ is the absolute value of an assumed negative downwash slope due to gust on the wing (also wing motion).

The form of the expressions describing the generalized forces for gust on the wing and tail is similar to the expressions for downwash on the tail due to gust on the wing. These relationships are found in Appendix D, Sections I and II, and they are reproduced below.

The generalized force due to gust on the tail (r = 5) is given by

$$Q_{5m}(s) = C_V D_m^T \Psi_1^T(s) \tag{63}$$

where $D_m^T$ is evaluated using equation (D7). The generalized force variation is

$$\Psi_1^T(s) = \sum_{k=0}^{3} \Psi_{1k}^T(s) \tag{64}$$

where the component parts of the generalized force are given by

$$\Psi_{10}^T(s) = \psi_T(0)\chi(s-s_T) \tag{65}$$

$$\left.\begin{aligned}
&\dot{\Psi}_{11}^T(s) + O_1\Psi_{11}^T(s) = O_2\chi(s-s_T), \quad k = 1 \\
&\dot{\Psi}_{12}^T(s) + O_3\Psi_{12}^T(s) = O_4\chi(s-s_T), \quad k = 2 \\
&\dot{\Psi}_{13}^T(s) + O_5\Psi_{13}^T(s) + O_6\int_0^s[\Psi_{13}^T(\sigma) + O_7\chi(\sigma-s_T)]d\sigma = \\
&\qquad O_8\chi(s-s_T), \qquad k = 3
\end{aligned}\right\} \tag{66}$$

and $s_T$ is the time delay between the airplane zero time reference point and the start of tail lift build up due to gust on the tail. The coefficients appearing in equation (66) are defined by

$$
\left.\begin{aligned}
O_1 &= \alpha_{11}^T \\
O_2 &= a_{11}^T \alpha_{11}^T
\end{aligned}\right\} \quad k = 1
$$

$$
\left.\begin{aligned}
O_3 &= \alpha_{12}^T \\
O_4 &= a_{12}^T \alpha_{12}^T
\end{aligned}\right\} \quad k = 2
$$

$$
\left.\begin{aligned}
O_5 &= 2\alpha_{13}^T \\
O_6 &= (\alpha_{13}^T)^2 + (\omega_{13}^T)^2 \\
O_7 &= -a_{13}^T \\
O_8 &= a_{13}^T \alpha_{13}^T - b_{13}^T \omega_{13}^T
\end{aligned}\right\} \quad k = 3 \qquad (67)
$$

Finally the generalized force due to gust on the wing (r = 6) is

$$Q_{6m}(s) = C_V D_m^W \Psi_m^W(s) \qquad (68)$$

where $D_m^W$ is evaluated using equation (D7). The generalized force variation and its component parts are dependent on the mode shapes (including rigid and flexible airplane modes), and are given by

$$\Psi_m^W(s) = \sum_{k=0}^{3} \Psi_{mk}^W(s) \qquad (69)$$

where

$$\Psi_{m0}^W(s) = \Psi_{10}^W(s) = \psi_W(0)\chi(s-s_W) \qquad (70)$$

$$
\left.\begin{aligned}
&\overset{\circ}{\Psi}_{m1}^W(s) + N_{m1}\Psi_{m1}^W(s) = N_{m2}\chi(s-s_W), && k = 1 \\
&\overset{\circ}{\Psi}_{m2}^W(s) + N_{m3}\Psi_{m2}^W(s) = N_{m4}\chi(s-s_W), && k = 2 \\
&\overset{\circ}{\Psi}_{m3}^W(s) + N_{m5}\Psi_{m3}^W(s) + N_{m6}\int_0^s [\Psi_{m3}^W(\sigma) + N_{m7}\chi(\sigma-s_W)]d\sigma = \\
&\qquad N_{m8}\chi(s-s_W), && k = 3
\end{aligned}\right\} \qquad (71)
$$

The coefficients in equation (71) are

$$\left.\begin{aligned} N_{m1} &= \alpha^W_{m1} \\ N_{m2} &= a^W_{m1}\alpha^W_{m1} \end{aligned}\right\} \quad k = 1$$

$$\left.\begin{aligned} N_{m3} &= \alpha^W_{m2} \\ N_{m4} &= a^W_{m2}\alpha^W_{m2} \end{aligned}\right\} \quad k = 2$$

$$\left.\begin{aligned} N_{m5} &= 2\alpha^W_{m3} \\ N_{m6} &= (\alpha^W_{m3})^2 + (\omega^W_{m3})^2 \\ N_{m7} &= -a^W_{m3} \\ N_{m8} &= a^W_{m3}\alpha^W_{m3} - b^W_{m3}\omega^W_{m3} \end{aligned}\right\} \quad k = 3 \qquad (72)$$

The final form of the equations of motion, equation (33), may now be obtained by evaluating the contributions of the kinetic and potential energies using equations (34) and (35) and substituting for the generalized forces due to motion and gust using equations (36) and (57).

$$\begin{aligned} &\sum_{n=1}^{N} [A_{mn}\overset{\infty}{\xi}_n(s) + B_{mn}\overset{\circ}{\xi}_n(s) + C_{mn}\xi_n(s)] \\ &\quad + A_{m\gamma}\overset{\circ\circ}{\gamma}(s) + B_{m\gamma}\overset{\circ}{\gamma}(s) + C_{m\gamma}\gamma(s) \\ &\quad + \sum_{k=1}^{2}[\Phi^W_{mk}(s) + \Phi^T_{mk}(s)] + D^M_m \sum_{k=0}^{3} \Delta^M_{1k}(s) \\ &\quad - \sum_{k=0}^{3} [D^G_m \Delta^G_{1k}(s) + D^T_m \Psi^T_{1k}(s) + D^W_m \Psi^W_{mk}(s)] \qquad (73) \end{aligned}$$

$$\text{for } m = 1, 2, \ldots, N$$

The constants in equation (73) are defined as follows:

$$\left.\begin{aligned} A_{mn} &= A_{mn}^{WN} + A_{mn}^{TN} + M_{mn} \\ B_{mn} &= B_{mn}^{WN} + B_{mn}^{TN} + \phi_W(0)B_{mn}^{WC} + \phi_T(0)B_{mn}^{TC} \\ C_{mn} &= \phi_W(0)C_{mn}^{WC} + \phi_T(0)C_{mn}^{TC} + (b_R/V)^2\omega_m^2 M_{mn} \end{aligned}\right\} \quad (74)$$

$$\left.\begin{aligned} A_{m\gamma} &= A_{m\gamma}^{TN} + M_{m\gamma} \\ B_{m\gamma} &= B_{m\gamma}^{TN} + \phi_T(0)B_{m\gamma}^{TC} \\ C_{m\gamma} &= \phi_T(0)C_{m\gamma}^{TC} \end{aligned}\right\} \quad (75)$$

In equation (73) the unsteady aerodynamics associated with gust on the wing, gust on the tail, downwash due to gust on the wing, and downwash due to wing motion are summed from k = 0 to k = 3. The component parts represented by the k = 0 contribution are included in order to be able to introduce the simplification of instantaneous aerodynamics in the equations of motion. This simplification is introduced in the equations by setting the constant terms in equations(53), (60), (65) and (70) equal to unity, that is, $\delta_M(0) = \delta_G(0) = \psi_T(0) = \psi_W(0) = 1.0$. Associated with this change, the unsteady aerodynamic terms as defined by equations (54), (61), (66) and (71) are made equal to zero through appropriate use of equations (56), (62), (67) and (72). In the case where unsteady aerodynamic terms are included, the constants $\delta_M(0)$, $\delta_G(0)$, $\psi_T(0)$ and $\psi_W(0)$ are set equal to zero.

Before simple harmonic motion is introduced into equation (73), the expressions for solving the unsteady circulatory generalized forces due to motion are rearranged, that is, equations (42) and (49) become,

<u>for wing motion</u>:

$$\left.\begin{aligned} \dot{\Phi}_{m1}^W(s) + F_1\Phi_{m1}^W(s) &= \sum_{n=1}^{N}[E_{mn}\dot{\xi}_n(s) + F_{mn}\xi_n(s)] \\ \dot{\Phi}_{m2}^W(s) + F_2\Phi_{m2}^W(s) &= F_3[\dot{\Phi}_{m1}^W(s) + F_1\Phi_{m1}^W(s)] \end{aligned}\right\} \quad (76)$$

where

$$\left.\begin{aligned} F_1 &= \beta_1^W \\ F_2 &= \beta_2^W \\ F_3 &= b_2^W\beta_2^W/b_1^W\beta_1^W \\ E_{mn} &= b_1^W\beta_1^W B_{mn}^{WC} \\ F_{mn} &= b_1^W\beta_1^W C_{mn}^{WC} \end{aligned}\right\} \quad (77)$$

and for tail motion:

$$\left.\begin{aligned} \dot{\Phi}_{m1}^T(s) + J_1\Phi_{m1}^T(s) &= \sum_{n=1}^{N}[I_{mn}\dot{\xi}_n(s) + J_{mn}\xi_n(s)] \\ &\quad + I_{m\gamma}\dot{\gamma}(s) + J_{m\gamma}\gamma(s) \\ \dot{\Phi}_{m2}^T(s) + J_2\Phi_{m2}^T(s) &= J_3[\dot{\Phi}_{m1}^T(s) + J_1\Phi_{m1}^T(s)] \end{aligned}\right\} \quad (78)$$

where

$$\left.\begin{aligned} J_1 &= \beta_1^T \\ J_2 &= \beta_2^T \\ J_3 &= b_2^T\beta_2^T/b_1^T\beta_1^T \\ I_{mn} &= b_1^T\beta_1^T B_{mn}^{TC} \\ J_{mn} &= b_1^T\beta_1^T C_{mn}^{TC} \\ I_{m\gamma} &= b_1^T\beta_1^T B_{m\gamma}^{TC} \\ J_{m\gamma} &= b_1^T\beta_1^T C_{m\gamma}^{TC} \end{aligned}\right\} \quad (79)$$

Introduction of simple harmonic motion in equation (73) as discussed in Section I yields, for the equations of motion,

$$\sum_{n=1}^{N} [(C_{mn} - \kappa^2 A_{mn}) + i\kappa B_{mn}]\xi_n(\omega)$$

$$+ [(C_{m\gamma} - \kappa^2 A_{m\gamma}) + i\kappa B_{m\gamma}]\gamma(\omega)$$

$$+ \sum_{k=1}^{2} [\Phi^W_{mk}(\omega) + \Phi^T_{mk}(\omega)] + D^M_m \sum_{k=0}^{3} \Delta^M_{1k}(\omega)$$

$$= \sum_{k=0}^{3} [D^G_m \Delta^G_{1k}(\omega) + D^T_m \Psi^T_{1k}(\omega) + D^W_m \Psi^W_{mk}(\omega)] \qquad (80)$$

The expressions for the aerodynamic lag equations in their order of appearance in equation (80) are summarized below.

$$\left.\begin{aligned} \Phi^W_{m1}(\omega) &= [(F_1 - i\kappa)/(F_1^2 + \kappa^2)] \sum_{n=1}^{N} [F_{mn} + i\kappa E_{mn}]\xi_n(\omega) \\ \Phi^W_{m2}(\omega) &= [(F_2 - i\kappa)/(F_2^2 + \kappa^2)]\ F_3[F_1 + i\kappa]\Phi^W_{m1}(\omega) \end{aligned}\right\} \qquad (81)$$

$$\left.\begin{aligned} \Phi^T_{m1}(\omega) &= [(J_1 - i\kappa)/(J_1^2 + \kappa^2)] \left\{ \sum_{n=1}^{N} [J_{mn} + i\kappa I_{mn}]\xi_n(\omega) \right. \\ &\qquad \left. + [J_{m\gamma} + i\kappa I_{m\gamma}]\gamma(\omega) \right\} \\ \Phi^T_{m2}(\omega) &= [(J_2 - i\kappa)/(J_2^2 + \kappa^2)]\ J_3[J_1 + i\kappa]\ \Phi^T_{m1}(\omega) \end{aligned}\right\} \qquad (82)$$

$$\Delta^M_{10}(\omega) = \delta_M(0)\ f_M(\omega)$$

$$\Delta^M_{11}(\omega) = [(R_1 - i\kappa)/(R_1^2+\kappa^2)]R_2 f_M(\omega)$$

$$\Delta^M_{12}(\omega) = [(R_3 - i\kappa)/(R_3^2+\kappa^2)]R_4 f_M(\omega)$$

$$\Delta^M_{13}(\omega) = [N_M/D_M] f_M(\omega)$$

where

$$N_M = (R_5R_8 + R_6R_7)\kappa^2 - R_6^2R_7 + i[R_5R_6R_7 + R_8(R_6-\kappa^2)]\kappa$$

$$D_M = R_6^2 - (2R_6 - R_5^2)\kappa^2 + \kappa^4$$

and

$$f_M(\omega) = \left\{ \sum_{n=1}^{2} [C_n^M + i\kappa B_n^M]\xi_n(\omega) \right\} [\cos \kappa s_M - i \sin \kappa s_M] \qquad (83)$$

$$\Delta^G_{10}(\omega) = -\left|\partial\varepsilon/\partial\alpha\right| \delta_G(0) f_G(\omega)$$

$$\Delta^G_{11}(\omega) = [(Q_1 - i\kappa)/(Q_1^2+\kappa^2)]\ Q_2 f_G(\omega)$$

$$\Delta^G_{12}(\omega) = [(Q_3 - i\kappa)/(Q_3^2+\kappa^2)]\ Q_4 f_G(\omega)$$

$$\Delta^G_{13}(\omega) = [N_G/D_G] f_G(\omega)$$

where

$$N_G = (Q_5Q_8 + Q_6Q_7)\kappa^2 - Q_6^2Q_7 + i[Q_5Q_6Q_7 + Q_8(Q_6-\kappa^2)]\kappa$$

$$D_G = Q_6^2 - (2Q_6 - Q_5^2)\kappa^2 + \kappa^4$$

and

$$f_G(\omega) = \cos \kappa s_G - i \sin \kappa s_G \qquad (84)$$

$$\left.\begin{aligned}
\Psi^T_{10}(\omega) &= \psi_T(0) f_T(\omega) \\
\Psi^T_{11}(\omega) &= [(O_1 - i\kappa)/(O_1^2 + \kappa^2)]\, O_2 f_T(\omega) \\
\Psi^T_{12}(\omega) &= [(O_3 - i\kappa)/(O_3^2 + \kappa^2)]\, O_4 f_T(\omega) \\
\Psi^T_{13}(\omega) &= [N_T/D_T] f_T(\omega)
\end{aligned}\right\} \quad (85)$$

where

$$N_T = (O_5 O_8 + O_6 O_7)\kappa^2 - O_6^2 O_7 + i[O_5 O_6 O_7 + O_8(O_6 - \kappa^2)]\kappa$$

$$D_T = O_6^2 - (2O_6 - O_5^2)\kappa^2 + \kappa^4$$

and

$$f_T(\omega) = \cos \kappa s_T - i \sin \kappa s_T$$

$$\left.\begin{aligned}
\Psi^W_{m0}(\omega) &= \psi_W(0) f_W(\omega) \\
\Psi^W_{m1}(\omega) &= [(N_{m1} - i\kappa)/(N_{m1}^2 + \kappa^2)]\, N_{m2} f_W(\omega) \\
\Psi^W_{m2}(\omega) &= [(N_{m3} - i\kappa)/(N_{m3}^2 + \kappa^2)]\, N_{m4} f_W(\omega) \\
\Psi^W_{m3}(\omega) &= [N_{Wm}/D_{Wm}] f_W(\omega)
\end{aligned}\right\} \quad (86)$$

where

$$N_{Wm} = (N_{m5} N_{m8} + N_{m6} N_{m7})\kappa^2 - N_{m6}^2 N_{m7} + i[N_{m5} N_{m6} N_{m7} + N_{m8}(N_{m6} - \kappa^2)]\kappa$$

$$D_{Wm} = N_{m6}^2 - (2N_{m6} - N_{m5}^2)\kappa^2 + \kappa^4$$

and

$$f_W(\omega) = \cos \kappa s_W - i \sin \kappa s_W$$

## V. Airplane Structural Loads

The wing incremental structural loads are derived herein using the mode acceleration method, with the aerodynamic forces being approximated by the rigid-body airload distribution which would produce the previously calculated rigid-body vertical acceleration. The incremental shear at the tail root is based on the force summation method, with the unsteady aerodynamic forces due to motion, gust, and downwash being summed over the tail panels. The associated tail torque and bending moment are obtained by multiplying the lift by appropriate moment arms.

The final equations for the wing total shear, $S_i^W(s)$, bending moment, $M_i^W(s)$, and torque about an axis perpendicular to the airplane center line at the intersection of the elastic axis and the $i^{th}$ spanwise load station, $T_i^W(s)$, are summarized below, from equations (F66 ), in terms of the aerodynamic and inertial contributions.

$$S_i^W(s) = C_V \sum_{n=1}^{N} A_{in}^{W\bar{S}} \ddot{\xi}_n(s) + (g/g_a) A_{ia}^{W\bar{S}} \ddot{\xi}_{1W}(s) \tag{87}$$

$$M_i^W(s) = C_V \sum_{n=1}^{N} A_{in}^{W\bar{M}} \ddot{\xi}_n(s) + (g/g_a) A_{ia}^{W\bar{M}} \ddot{\xi}_{1W}(s) \tag{88}$$

$$T_i^W(s) = C_V \sum_{n=1}^{N} A_{in}^{W\bar{T}} \ddot{\xi}_n(s) + (g/g_a) A_{ia}^{W\bar{T}} \ddot{\xi}_{1W}(s) \tag{89}$$

where

$$(g/g_a) = 1 \frac{\text{pounds (mass)}}{\text{pounds (force)}}$$

The coefficients, $A_{ia}^{W\bar{S}}$, $A_{ia}^{W\bar{M}}$, and $A_{ia}^{W\bar{T}}$, used in the mode-acceleration method are evaluated from the rigid-body aerodynamic loading distribution associated with an incremental one "g" vertical acceleration. The acceleration term, $\ddot{\xi}_{1W}(s)$, is defined as the effective airplane rigid-body acceleration with the tail aerodynamic force removed.

This variable is evaluated by equation (F34).

$$\overset{\infty}{\xi}_{1W}(s) = \overset{\infty}{\xi}_1(s) + V_0 \ell_T(s)/M_{11} \tag{90}$$

where, from equation (F 12 ),

$$\ell_T(s) = \sum_{n=1}^{N} [A_n^T \overset{\infty}{\xi}_n(s) + B_n^T \overset{\circ}{\xi}_n(s) + C_n^T \xi_n(s)]$$

$$+ A_\gamma^T \overset{\infty}{\gamma}(s) + B_\gamma^T \overset{\circ}{\gamma}(s) + C_\gamma^T \gamma(s)$$

$$+ V_1 \sum_{k=1}^{2} \Phi_{1k}^T(s) + V_2 \sum_{k=0}^{3} [\Delta_{1k}^M(s) + \Delta_{1k}^G(s)$$

$$+ \Psi_{1k}^T(s)] \tag{91}$$

The equations for the tail shear, bending moment, and torque at the intersection of the fuselage side and torque tube (stabilizer station 14) also are expressed in terms of aerodynamic and inertial contributions. These equations, reproduced from equation (F 67 ), are

$$S_1^T(s) = C_V[\ell_T(s) + \sum_{n=1}^{N} A_{1n}^{T\overline{S}} \overset{\infty}{\xi}_n(s) + A_{1\gamma}^{T\overline{S}} \overset{\infty}{\gamma}(s)] \tag{92}$$

$$M_1^T(s) = C_V[y_0 \ell_T(s) + \sum_{n=1}^{N} A_{1n}^{T\overline{M}} \overset{\infty}{\xi}_n(s) + A_{1\gamma}^{T\overline{M}} \overset{\infty}{\gamma}(s)] \tag{93}$$

$$T_1^T(s) = C_V[x_0 \ell_T(s) + \sum_{n=1}^{N} A_{1n}^{T\overline{T}} \overset{\infty}{\xi}_n(s) + A_{1\gamma}^{T\overline{T}} \overset{\infty}{\gamma}(s)] \tag{94}$$

Introduction of simple harmonic motion into the wing and tail load equations reduces equations (87) to (94) to the following:

$$S_i^W(\omega) = -\kappa^2 [C_V \sum_{n=1}^{N} A_{in}^{W\overline{S}} \xi_n(\omega) + (g/g_a) A_{ia}^{W\overline{S}} \xi_{1W}(\omega)] \tag{95}$$

$$M_i^W(\omega) = -\kappa^2[C_V \sum_{n=1}^{N} A_{in}^{W\overline{M}}\xi_n(\omega) + (g/g_a)A_{ia}^{W\overline{M}}\xi_{1W}(\omega)] \quad (96)$$

$$T_i^W(\omega) = -\kappa^2[C_V \sum_{n=1}^{N} A_{in}^{W\overline{T}}\xi_n(\omega) + (g/g_a)A_{ia}^{W\overline{T}}\xi_{1W}(\omega)] \quad (97)$$

$$\xi_{1W}(\omega) = \xi_1(\omega) - [V_0 \ell_T(\omega)]/\kappa^2 M_{11} \quad (98)$$

$$\begin{aligned}\ell_T(\omega) = &\sum_{n=1}^{N}[(C_n^T - \kappa^2 A_n^T) + i\kappa B_n^T]\xi_n(\omega) \\ &+ [(C_\gamma^T - \kappa^2 A_\gamma^T) + i\kappa B_\gamma^T]\gamma(\omega) + V_1 \sum_{k=1}^{2} \Phi_{1k}^T(\omega) \\ &+ V_2 \sum_{k=0}^{3}[\Delta_{1k}^M(\omega) + \Delta_{1k}^G(\omega) + \Psi_{1k}^T(\omega)]\end{aligned} \quad (99)$$

$$S_1^T(\omega) = C_V[\ell_T(\omega) - \kappa^2 \sum_{n=1}^{N} A_{1n}^{T\overline{S}}\xi_n(\omega) - \kappa^2 A_{1\gamma}^{T\overline{S}}\gamma(\omega)] \quad (100)$$

$$M_1^T(\omega) = C_V[y_0 \ell_T(\omega) - \kappa^2 \sum_{n=1}^{N} A_{1n}^{T\overline{M}}\xi_n(\omega) - \kappa^2 A_{1\gamma}^{T\overline{M}}\gamma(\omega)] \quad (101)$$

$$T_1^T(\omega) = C_V[x_0 \ell_T(\omega) - \kappa^2 \sum_{n=1}^{N} A_{1n}^{T\overline{T}}\xi_n(\omega) - \kappa^2 A_{1\gamma}^{T\overline{T}}\gamma(\omega)] \quad (102)$$

## VI. Airplane Response Equations

The equations for the normal and pitching accelerations and velocities at any point on the airplane are expressed in units of real time although they are dependent upon and presented as functions of non-dimensional time. These and the displacement equations are given by

$$\left.\begin{aligned}
\ddot{h}_i(s) &= (V/b_R)^2 \sum_{n=1}^{N} f_{h_n}(\nu_i)\, \ddot{\xi}_n(s) \\
\ddot{\alpha}_i(s) &= (V/b_R)^2 \sum_{n=1}^{N} f_{\alpha_n}(\nu_i)\, \ddot{\xi}_n(s) \\
\dot{h}_i(s) &= (V/b_R) \sum_{n=1}^{N} f_{h_n}(\nu_i)\, \dot{\xi}_n(s) \\
\dot{\alpha}_i(s) &= (V/b_R) \sum_{n=1}^{N} f_{\alpha_n}(\nu_i)\, \dot{\xi}_n(s) \\
h_i(s) &= \sum_{n=1}^{N} f_{h_n}(\nu_i)\xi_n(s) \\
\alpha_i(s) &= \sum_{n=1}^{N} f_{\alpha_n}(\nu_i)\xi_n(s)
\end{aligned}\right\} \qquad (103)$$

where the subscript i is assigned integer values which are associated with particular points on the aircraft. For example, i=1 represents the cockpit in the present study. The parameter $\nu_i$ denotes the location of the $i^{th}$ response point. For simple harmonic motion, equations (103) reduce to the following relationships:

$$\left.\begin{aligned}
\ddot{h}_i(\omega) &= -(V/b_R)^2 \kappa^2 \sum_{n=1}^{N} f_{h_n}(\nu_i)\xi_n(\omega) \\
\ddot{\alpha}_i(\omega) &= -(V/b_R)^2 \kappa^2 \sum_{n=1}^{N} f_{\alpha_n}(\nu_i)\xi_n(\omega)
\end{aligned}\right\} \qquad (104)$$

$$
\left.
\begin{aligned}
\dot{h}_i(\omega) &= i\kappa(V/b_R) \sum_{n=1}^{N} f_{h_n}(\nu_i)\xi_n(\omega) \\
\dot{\alpha}_i(\omega) &= i\kappa(V/b_R) \sum_{n=1}^{N} f_{\alpha_n}(\nu_i)\xi_n(\omega) \\
h_i(\omega) &= \sum_{n=1}^{N} f_{h_n}(\nu_i)\xi_n(\omega) \\
\alpha_i(\omega) &= \sum_{n=1}^{N} f_{\alpha_n}(\nu_i)\xi_n(\omega)
\end{aligned}
\right\} \quad (104)
$$

## VII. Power Spectral Techniques

The basic expressions required for the application of power-spectral techniques in the present analysis are developed and discussed in References 2 through 6 . In this section, these expressions are summarized in the notation of this report, and the numerical evaluation of an integral which occurs is discussed. Two sets of the basic expressions are given, one in terms of the frequency, $\omega$, in radians per second, and the second in terms of the reduced frequency, $\Omega$, in radians per foot, where

$$\Omega = \omega/V \tag{105}$$

The power spectrum of the vertical gust velocity, not including any spanwise variation, is given by equation (1) of Reference 3 .

$$\tilde{\Phi}_{w_G}(\Omega) = \sigma_{w_G}^2 \frac{L}{\pi} \frac{1 + 3\Omega^2 L^2}{[1 + \Omega^2 L^2]^2} \tag{106}$$

where L is the scale of turbulence in feet. The relationship between the power spectra as a function of the independent variables $\Omega$ and $\omega$ is given by equation (15), Reference 2 , which is reproduced below.

$$\bar{\Phi}_{w_G}(\omega) = \tilde{\Phi}_{w_G}(\Omega)/V \tag{107}$$

Combining equations (105) to (107),

$$\bar{\Phi}_{w_G}(\omega) = \sigma_{w_G}^2 \frac{L}{\pi V} \frac{1 + 3\omega^2 L^2/V^2}{[1 + \omega^2 L^2/V^2]^2} \tag{108}$$

Representing the transfer function of the response variable under consideration by $\tilde{T}_y(\Omega)$ and the output power spectrum by $\tilde{\Phi}_y(\Omega)$, the expression relating these two quantities and the gust power spectrum is given by equation (18), Reference 2 , as

$$\tilde{\Phi}_y(\Omega) = \tilde{\Phi}_{w_G}(\Omega) \left|\tilde{T}_y(\Omega)\right|^2 \tag{109}$$

or in terms of the frequency, $\omega$,

$$\overline{\Phi}_y(\omega) = \overline{\Phi}_{w_G}(\omega) \left|\overline{T}_y(\omega)\right|^2 \tag{110}$$

The response power-spectral-density function may now be used to define the characteristic frequency, $N_{0_y}$, and root-mean-square value, $\sigma_y$, of the particular variable in question. These are given in Reference 3 as

$$N_{0_y}^2 = \frac{1}{4\pi^2} \frac{\int_0^\infty \omega^2 \overline{\Phi}_y(\omega)\, d\omega}{\int_0^\infty \overline{\Phi}_y(\omega)\, d\omega} \tag{111}$$

$$\sigma_y^2 = \int_0^\infty \overline{\Phi}_y(\omega)\, d\omega \tag{112}$$

The constant $N_{0_y}$ gives the expected number of times per second that the variable y crosses the value zero with a positive slope.

A more general parameter, N(y), which is dependent on $N_{0_y}$, is defined as the expected number of times per second that the variable crosses some finite value of y with a positive slope. This parameter is also an approximation for the average number of peaks per second exceeding a given value of y, and will be used in this sense throughout this report. An analytical representation of N(y) is given by equation (21) in Reference 6. This expression contains two terms to account for both storm and non-storm turbulence. For the present study, which is restricted to low-altitude flight, the second term associated with storm turbulence is neglected. The expression for N(y) then becomes:

$$N(y) = P_1 N_{0_y} e^{-\frac{y}{B(\sigma_y/\sigma_{w_G})}} \tag{113}$$

where $P_1$ is the proportion of total flight time in non-storm turbulence, and B is a scale parameter in the probability distribution of root-mean-square gust velocity.

Note that for $y = 0$ and $P_1 = 1.0$, equation (113) reduces to $N(0) = N_{0_y}$.

At this point, it is noted that, since equations (111) and (112) require integration from zero to infinity, the values of the integrals may become infinite if the response power spectrum does not decay fast enough. In order to investigate these integrals further, equation (110) is introduced and the integrals are written in general form as

$$I_{y_k}^2 = \int_0^\infty \omega^{2k} \bar{\Phi}_{w_G}(\omega) \left| \bar{T}_y(\omega) \right|^2 d\omega \tag{114}$$

Also, the expression for the gust power spectrum (equation (108)), is approximated as follows:

$$\bar{\Phi}_{w_G}(\omega) \simeq \frac{\sigma_{w_G}^2}{\pi} \frac{L}{V}, \text{ for } \omega \text{ small} \tag{115}$$

$$\bar{\Phi}_{w_G}(\omega) \simeq \frac{\sigma_{w_G}^2}{\pi} \frac{3V}{L\omega^2}, \text{ for } \omega \text{ large} \tag{116}$$

Equating the above two expressions results in a "breakpoint" frequency,

$$\omega_b(L) = \frac{V\sqrt{3}}{L} = \omega_b \tag{117}$$

A typical gust power spectrum, as given by equation (108), and its approximation, as given by equations (115) to (117), are shown in Figure 1.

Combining equations (114) to (117),

$$I_{y_k}^2 = \frac{\sigma_{w_G}^2}{\pi} \left[ \frac{L}{V} \int_0^{\omega_b} \omega^{2k} \left| \bar{T}_y(\omega) \right|^2 d\omega + \frac{3V}{L} \int_{\omega_b}^\infty \omega^{2(k-1)} \left| \bar{T}_y(\omega) \right|^2 d\omega \right] \tag{118}$$

For some reasonable value of the scale of turbulence, the first integral of equation (118) always possesses a finite value if the transfer function $\bar{T}_y(\omega)$ is bounded. For the

second integral of equation (118), a stronger restriction must be associated with the function $\bar{T}_y(\omega)$; that is, it must have a certain rate of decay at the high frequencies. The assumption is now made that at the high frequencies the transfer function depends upon the frequency in the following manner:

$$\left|\bar{T}_y(\omega)\right| = \omega^{\varepsilon} \tag{119}$$

Introducing equation (119) into the second integral of equation (118) yields

$$\int_{\omega_b}^{\infty} \omega^{2(k-1)} \left|\bar{T}_y(\omega)\right|^2 d\omega = \int_{\omega_b}^{\infty} \omega^{[2(k-1)+2\varepsilon]} d\omega$$

$$= \left.\frac{\omega^{[2k-1+2\varepsilon]}}{2k-1+2\varepsilon}\right|_{\omega_b}^{\infty} \tag{120}$$

Therefore, in order for the integral in equation (114) to have a finite value, the following restriction must be imposed:

$$2k-1+2\varepsilon < 0 \tag{121}$$

For the response parameters considered in the present study, i.e., displacements, velocities, accelerations, and structural loads, an upper bound to the value of the exponent in equation (119) is $\varepsilon = 0$. For certain other response parameters, such as the rate of change of acceleration (jerk), $\varepsilon$ could be positive, but these will not be considered herein. For $\varepsilon = 0$ then, equation (120) becomes

$$\int_{\omega_b}^{\infty} \omega^{2(k-1)} \left|\bar{T}_y(\omega)\right|^2 d\omega = \left.\omega^{2k-1}/(2k-1)\right|_{\omega_b}^{\infty} \tag{122}$$

Thus, equation (121) reduces to

$$2k-1 < 0 \tag{123}$$

which, since k is an integer, becomes

$$k \leq 0 \tag{124}$$

Introducing the requirement of equation (124) into equation (114) and then comparing this equation with equations (111) and (112), it is seen that the integration for the root-mean-square response, $\sigma_y$, is bounded whereas that for the characteristic frequency, $N_{0_y}$, may become infinite. This last conclusion is of course inconsistent with realistic considerations, and to eliminate this condition it has been proposed in Reference 4 that the expression for the gust power spectrum as given by equation (108) be modified so that theoretical response peak calculations become consistent with flight test data. This modified gust power spectrum is

$$\bar{\Phi}^*_{w_G}(\omega) = \frac{\sigma^2_{w_G} L}{\pi V}\left[\frac{1 + 3\omega^2L^2/V^2}{[1 + \omega^2L^2/V^2]^2} + \frac{C^4 + 6C^2\omega^2L^2/V^2 - 3\omega^4L^4/V^4}{[C^2 + \omega^2L^2/V^2]^3}\right] \tag{125}$$

A value of 50 for the parameter C in this equation has been proposed in the above reference.

With the aid of equation (125), an investigation was made to determine an acceptable upper limit of integration for the response power spectra being considered in this study. It was concluded that the use of an upper limit of 200 rad./sec. in conjunction with the gust power spectrum of equation (108) would yield characteristic frequencies which are in good agreement with those obtained by the use of an effectively infinite limit of integration in conjunction with the power spectrum of equation (125). Also, this upper limit of 200 rad./sec. was found to be more than sufficient for accurate calculation of root-mean-square response values.

Figure 1

GUST POWER-SPECTRAL-DENSITY FUNCTION

AND SIMPLIFIED APPROXIMATION FOR $\sigma_{w_G}$ = 1 FT./SEC.

L = 500 Ft., V = 1000 Ft./Sec.

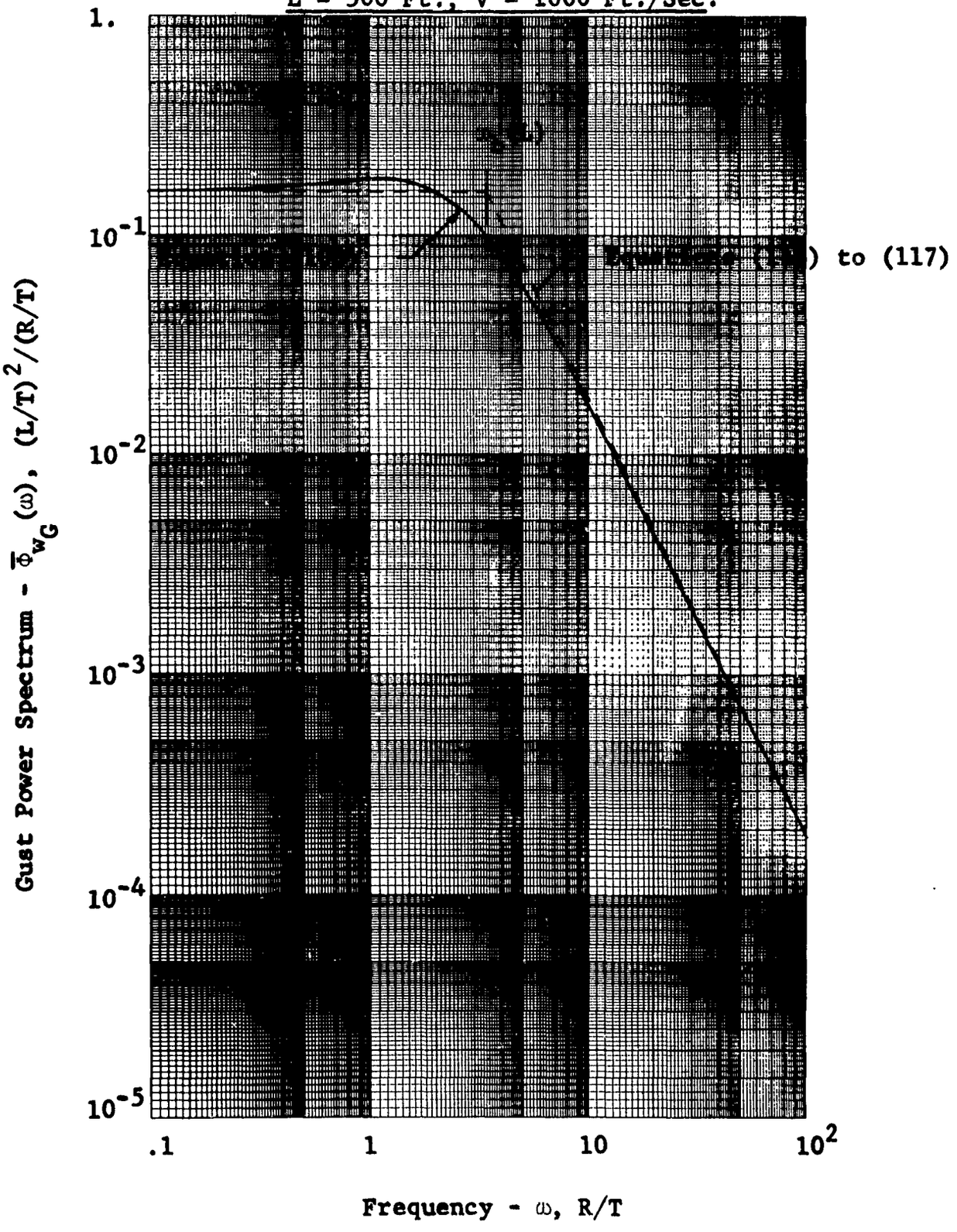


) to (117)

# APPENDIX A

## AUTOPILOT AND CONTROL SYSTEM EQUATIONS

### I. Autopilot Signal

A mathematical description of the A-6A (A2F-1) autopilot and its related systems is given in Reference 7 In particular, Figures 2 and 3 of Reference 7 provide block diagrams for the autopilot system in terms of the five following autopilot modes: stability augmentation, attitude hold, Mach hold, altitude hold, and G command. For the present gust response study, only two of these autopilot modes are included in the analysis, namely, stability augmentation and attitude hold. Considering only these two modes, the block diagrams in Reference 7 are translated into the following equation in terms of Laplace transform operators:

$$\bar{\mu}(p) = [2pk_7/(2p + 1)]\mathcal{L}[\dot{\alpha}(x_\mu^{\dot{\alpha}}, t)] + k_8\mathcal{L}[\alpha(x_\mu^{\alpha}, t)] \qquad \text{(A1)}$$

As written, equation (A1) is the transform equation of the autopilot system for the attitude hold mode. It may be reduced to the stability augmentation mode by simply equating $k_8$ to zero. The values of the constants obtained from the block diagram in Reference 7 are

$$\left.\begin{aligned} k_7 &= \frac{10g}{\frac{1}{2}\rho V^2} + 0.09,\ \frac{R}{R/T} \\ k_8 &= 1,\ R/R \end{aligned}\right\} \qquad \text{(A2)}$$

The autopilot input is now expressed in terms of the normal modes and mode shapes at the location of the various sensing devices as follows:

$$\left.\begin{aligned} \dot{\alpha}(x_\mu^{\dot{\alpha}}, t) &= \sum_n f_{\alpha_n}(x_\mu^{\dot{\alpha}})\dot{\xi}_n(t) \\ \alpha(x_\mu^{\alpha}, t) &= \sum_n f_{\alpha_n}(x_\mu^{\alpha})\xi_n(t) \end{aligned}\right\} \qquad \text{(A3)}$$

## APPENDIX A

Also, to be consistent with other equations to be developed subsequently, the real time, t, is replaced by the non-dimensional time, s, by use of the following relationships:

$$\left.\begin{aligned} s &= (V/b_R)t \\ d/dt &= (V/b_R)(d/ds) \\ d^2/dt^2 &= (V/b_R)^2(d^2/ds^2) \end{aligned}\right\} \qquad (A4)$$

Substituting equation (A3) into equation (A1), and then taking the inverse Laplace transform of this expression yields the autopilot equation as a function of real time, t. Conversion to non-dimensional time may now be accomplished through use of equations (A4). The final expression for the autopilot signal is

$$\dot{\mu}(s) + L_{10}\mu(s) = \sum_n [L_{1n}\ddot{\xi}_n(s) + L_{2n}\dot{\xi}_n(s) + L_{3n}\xi_n(s)] \qquad (A5)$$

where the coefficients in equation (A5) are given by

$$\left.\begin{aligned} L_{10} &= b_R/2V \\ L_{1n} &= (V/b_R)k_7 f_{\alpha_n}(x_\mu^{\dot{\alpha}}) \\ L_{2n} &= k_8 f_{\alpha_n}(x_\mu^{\alpha}) \\ L_{3n} &= (b_R/2V)k_8 f_{\alpha_n}(x_\mu^{\alpha}) \end{aligned}\right\} \qquad (A6)$$

# APPENDIX A

## II. Stick and Sprashpot Signals

A complete description of the A-6A manual control system, together with numerical values of the properties of the various components, is presented in Reference 8. Reference 9 summarizes the basic data presented in Reference 8 , and also presents equations of motion for the rigid-body airplane together with the expressions for the stick and sprashpot systems as a function of the rigid airplane vertical and angular accelerations. In the present analysis, airplane flexibility will also be considered. Therefore, the stick and sprashpot equations are rederived in this section in terms of the airplane normal modes. The basic derivation follows the procedure presented in Reference 10, pages 22 to 24, which applies to a rigid airplane.

A schematic diagram of the manual control system (stick and sprashpot) is shown in Figure A1, which is a modification of Figure 2.1 in Reference 8 . The control system without bobweights has a basic weight moment of inertia about the stick pivot point denoted by $I_{s0}$. The expression for the additional control system inertia due to bobweights, $I_{s1}$, is now obtained. The effective kinetic energy of the stick may be related to the kinetic energy of the bobweight system through the following expression:

$$\tfrac{1}{2}(I_{s1}/g)\dot{\tau}(t)^2 = \tfrac{1}{2}(I_a/g)(N_a\dot{\tau}(t))^2 + \tfrac{1}{2}(I_f/g)(N_f\dot{\tau}(t))^2 \qquad \text{(A7)}$$

where $N_a$ and $N_f$ are the ratios of the bobweight angular motions to control stick angular motion for the aft and forward bobweights, respectively. The bobweight inertias about their own pivot points, disregarding the contributions about their own centers of gravity, are given by

$$\left.\begin{aligned} I_a &= m_a R_a^2 \\ I_f &= m_f R_f^2 \end{aligned}\right\} \qquad \text{(A8)}$$

Combining equations (A7) and (A8) will provide the moment of inertia about the stick pivot point.

## APPENDIX A

$$I_{s1} = m_f N_f^2 R_f^2 + m_a N_a^2 R_a^2 \tag{A9}$$

The total control moment inertia referred to the stick pivot point is therefore given by

$$\left.\begin{aligned} I_s &= I_{s0} + I_{s1} \\ &= I_{s0} + m_f N_f^2 R_f^2 + m_a N_a^2 R_a^2 \end{aligned}\right\} \tag{A10}$$

It is assumed in the above derivation that the forward and aft bobweights are the only control system components sensing airplane acceleration. The further assumptions made are that normal (positive down) and pitch (positive nose-up) acceleration sensing are not dependent upon stick position, and that forces normal to the flight path are very nearly perpendicular to the airplane fuselage reference line.

The moment about the stick pivot point due to airplane and control system accelerations, $M_{1_\tau}(t)$, may now be written as follows:

$$\begin{aligned} M_{1_\tau}(t) = (I_s/g)[\ddot{\tau}(t) + \ddot{\alpha}(x_s,t)] \\ - (m_f R_f N_f/g)[\ddot{h}(x_f,t) - R_f \ddot{\alpha}(x_f,t)] \\ + (m_a R_a N_a/g)[\ddot{h}(x_a,t) + R_a \ddot{\alpha}(x_a,t)] \end{aligned} \tag{A11}$$

where the indicated normal and angular accelerations about the stick pivot point and the forward and aft bobweight pivot points are given in terms of the normal modes by

$$\left.\begin{aligned} \ddot{\alpha}(x_s,t) &= \Sigma_n f_{\alpha_n}(x_s)\ddot{\xi}_n(t) \\ \ddot{\alpha}(x_f,t) &= \Sigma_n f_{\alpha_n}(x_f)\ddot{\xi}_n(t) \\ \ddot{h}(x_f,t) &= \Sigma_n f_{h_n}(x_f)\ddot{\xi}_n(t) \\ \ddot{\alpha}(x_a,t) &= \Sigma_n f_{\alpha_n}(x_a)\ddot{\xi}_n(t) \\ \ddot{h}(x_a,t) &= \Sigma_n f_{h_n}(x_a)\ddot{\xi}_n(t) \end{aligned}\right\} \tag{A12}$$

## APPENDIX A

Additional moments about the stick pivot point resulting from sources other than the accelerations are due to the sprashpot and artificial feel spring. Under the assumption that the spring moment is proportional to the stick angular displacement, and the sprashpot contribution is proportional to the sprashpot angular velocity measured at a point between the spring and the damper, the additional moment on the stick is given by

$$M_{2\tau}(t) = K_\tau \tau(t) + C_\eta \dot{\eta}(t) \tag{A13}$$

where $K_\tau$ and $C_\eta$ are the angular spring constant and angular damping constant about the stick pivot point of the artificial feel spring and sprashpot, respectively. The total moment about the stick pivot point, without any external forces such as pilot input, is given by

$$M_{1\tau}(t) + M_{2\tau}(t) = 0 \tag{A14}$$

Combining equations (A11) and (A13),

$$(I_s/g)[\ddot{\tau}(t) + \ddot{\alpha}(x_s,t)] - (m_f R_f N_f/g)[\ddot{h}(x_f,t) - R_f \ddot{\alpha}(x_f,t)]$$

$$+ (m_a R_a N_a/g)[\ddot{h}(x_a,t) + R_a \ddot{\alpha}(x_a,t)]$$

$$+ K_\tau \tau(t) + C_\eta \dot{\eta}(t) = 0 \tag{A15}$$

The expression relating the stick angular displacement and the sprashpot equivalent angular motion is given by

$$C_\eta \dot{\eta}(t) + K_\eta[\eta(t) - \tau(t)] = 0 \tag{A16}$$

where $K_\eta$ is the angular spring constant of the sprashpot about the stick pivot point.

After introducing the non-dimensional time and making the appropriate substitutions into equations (A15) and (A16), the final expressions for the stick and sprashpot become

## APPENDIX A

$$\ddot{\tau}(s) + H_{30}\tau(s) = \sum_{n=1}^{6} H_{3n}\ddot{\xi}_n(s) + H_{3\eta}\dot{\eta}(s) \tag{A17}$$

and

$$\dot{\eta}(s) + H_{40}\eta(s) = H_{40}\tau(s) \tag{A18}$$

where the coefficients are given by

$$\left.\begin{aligned} H_{30} &= (K_\tau/I_s)(b_R/V)^2 g \\ H_{3\eta} &= -(C_\eta/I_s)(b_R/V) g \end{aligned}\right\} \tag{A19}$$

$$\begin{aligned} H_{3n} = -(1/I_s) \Big\{ & I_{s0} f_{\alpha_n}(x_s) \\ & + m_f R_f N_f [R_f (N_f f_{\alpha_n}(x_s) + f_{\alpha_n}(x_f)) - f_{h_n}(x_f)] \\ & + m_a R_a N_a [R_a (N_a f_{\alpha_n}(x_s) + f_{\alpha_n}(x_a)) + f_{h_n}(x_a)] \Big\} \end{aligned} \tag{A20}$$

$$H_{40} = (K_\eta/C_\eta)(b_R/V) \tag{A21}$$

# APPENDIX A

## III. Stabilizer Rotation

A block diagram of the A-6A (A2F-1) longitudinal power control system in the manual and series modes is shown in Figure 4.2 of Reference 11. For the frequency range of interest in the present gust response studies, it would have been sufficient, from the standpoint of the stabilizer response characteristics, to approximate the power control system by a first-order differential equation representing the linear factor of the power control actuator dynamics. For the calculation of inertia loads, however, it was required to include a second order or angular acceleration term. For this purpose, the power-control-system transfer function was represented by the expression

$$\bar{\gamma}(p)/\bar{\gamma}_s(p) = 1/(T_1p+1)(T_2p+1) \tag{A22}$$

In this expression, the dynamics of the secondary actuator shown in Figure 4.2 of Reference 11 are neglected. The first time constant, $T_1$, is the same as that inherent in the first factor of the original third-order power-control-actuator equation. The second time constant, $T_2$, is an approximation which reduces the third-order power-control-actuator equation to a second-order one.

The actual differential equation for stabilizer rotation used in the present study is given as

$$a_\gamma \ddot{\gamma}(t) + b_\gamma \dot{\gamma}(t) + \gamma(t) = \gamma_s(t) \tag{A23}$$

where

$$a_\gamma = T_1T_2 \tag{A24}$$

$$b_\gamma = T_1 + T_2 \tag{A25}$$

and $\gamma_s(t)$ is the total signal input to this equation. The input consists of two signals, one, due to the autopilot, $\mu(t)$, and the other due to the stick including the stabilizer-to-control-stick linkage ratio, $k_\tau\tau(t)$. The

## APPENDIX A

final form of the expression describing the stabilizer rotation is given in terms of non-dimensional time as

$$\overset{\circ\circ}{\gamma}(s) + H_{20}\overset{\circ}{\gamma}(s) + H_{21}\gamma(s) = H_{21}\mu(s) + H_{22}\tau(s) \qquad (A26)$$

where the coefficients are defined by

$$H_{20} = (b_\gamma/a_\gamma)(b_R/V) \qquad (A27)$$

$$H_{21} = (1/a_\gamma)(b_R/V)^2 \qquad (A28)$$

$$H_{22} = (k_\tau/a_\gamma)(b_R/V)^2 \qquad (A29)$$

Figure A1

SCHEMATIC DIAGRAM OF STICK AND SPRASHPOT SYSTEM

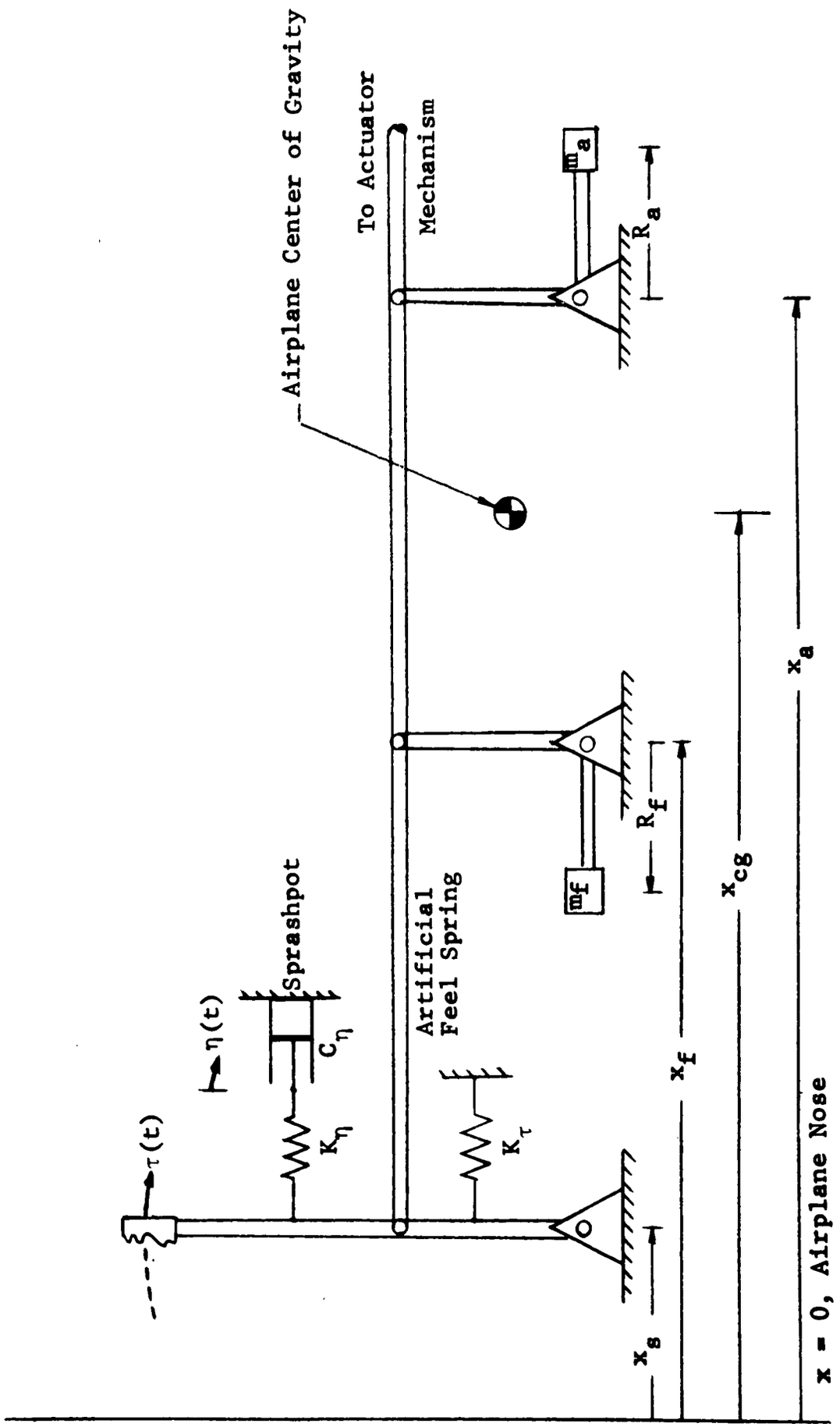

# APPENDIX B

## UNSTEADY AERODYNAMICS OF RECTANGULAR PLANFORMS DUE TO GUST, MOTION, AND DOWNWASH (Indicial Lift Functions)

### I. Indicial Lift Functions for Gust on a Planform (Küssner-Type Functions)

#### A. Planform Küssner-Type Function

The idealized model of a two-dimensional wing-tail combination flying at a constant subsonic Mach number, M, and encountering a stationary vertical gust with a vertical gust velocity $w_G$ ($w_G \ll V$) is represented in Figure B1. Tail position with respect to the wing (defined by the parameters $s_T^x$ and $s_T^z$) is important in evaluating lift build up on the tail due to wing downwash. Downwash effects, whether due to wing motion or gust on the wing, will be discussed in Section III of this appendix.

The Küssner-type function is defined herein as the time variation of lift for an airfoil of arbitrary aspect ratio and flying at an arbitrary subsonic Mach number, due to a step change in vertical gust velocity, normalized with respect to the steady-state lift at infinite time. (The Küssner function itself is restricted to apply only to the normalized lift build up due to a step gust on a two-dimensional airfoil (AR = ∞) in incompressible flow (M = 0). The Küssner-type function is dependent on a non-dimensional time, $\eta$, defined in terms of planform (wing or tail) reference semichords traveled.

$$\eta = Vt/b_\eta \qquad \text{(B1)}$$

where V is the airplane forward velocity and $b_\eta$ is a reference semichord for the planform under consideration. For an untapered planform, $b_\eta$ would be identically equal to half the geometric chord, whereas for a tapered planform it would be half the chord at a reference spanwise station such as the mean aerodynamic chord. The Küssner-type function increases from an initial value of zero to

## APPENDIX B

a steady-state value of unity at $\eta$ equal to infinity. As shown in Figure B2, the effect of Mach number on the basic Küssner function is to decrease the rate of build up, whereas finite aspect ratio has the opposite effect.

Küssner-type functions for two-dimensional airfoils at Mach numbers other than zero and for finite-aspect-ratio airfoils in incompressible flow have been derived in various technical reports. (See References 12, 13, 14.) By interpolation or extrapolation from these two groups, values of the Küssner-type functions for any Mach number and aspect ratio, other than the given curves, may be estimated. The method used in the present investigation is based on the following assumed formula:

$$\psi(M, AR, \eta) = \left[\frac{\psi(0, AR, \eta)}{\psi(0, \infty, \eta)}\right] \psi(M, \infty, \eta) \qquad (B2)$$

where $\psi(0, \infty, \eta)$ is the incompressible two-dimensional (Küssner) function (See Reference 15, page 288) and $\psi(0, AR, \eta)$ and $\psi(M, \infty, \eta)$ are incompressible three-dimensional, and compressible two-dimensional Küssner-type functions such as those evaluated in the references stated previously.

Equation (B2) as given provides a time relationship for the indicial lift function based upon a non-dimensional time measured in planform semichords. Subsequent to evaluating this function for the given conditions, it is desirable to approximate the results by simple analytical expressions to facilitate the use of indicial lift functions in the present study. A simple and useful approximation is an expression consisting of exponential terms, where the number of terms is dictated by the desired accuracy of the approximation. The assumed expression then is of the following general form:

$$\psi(\eta) = \psi(0) + \sum_{k=1}^{K_\psi} a_k (1 - e^{-\bar{\alpha}_k \eta}) \qquad (B3)$$

Note that, to obtain the correct steady-state lift, the following condition must be imposed upon the coefficients $a_k$:

$$\psi(0) + \sum_{k=1}^{K_\psi} a_k = 1.0 \qquad (B4)$$

## APPENDIX B

The function $\psi(\eta)$ provides the analytical approximation of the indicial lift as calculated from the expression $\psi(M, AR, \eta)$ given by equation (B2). The maximum index, $K_\psi$, appearing in equation (B3) designates the number of exponentials used in approximating the planform indicial lift function. The purpose of the constant, $\psi(0)$, is to permit the reduction of the equation to the limiting case for which the lift build up due to gust is assumed instantaneous, that is, no transient effects are present. The reduction of equation (B3) to instantaneous lift build up may be accomplished simply by letting $\psi(0) = 1.0$ and all $a_k = 0$.

Evaluation of the constants appearing in equation (B3) may be carried out by a graphical procedure as follows. First the variable $1 - \psi(M, AR, \eta)$ is plotted on semi-log paper versus the non-dimensional time for some finite value of $\eta$. Any straight line drawn on the semi-log paper represents one exponential term, as defined by $a_k e^{-\alpha_k \eta}$; therefore, the constants $a_k$ and $\bar{\alpha}_k$ are easily evaluated. A number of these straight lines whose sum is equal to $1 - \psi(M, AR, \eta)$ will represent the variable $(1 - \psi(\eta))$ with the desired accuracy.

The application of these exponential expressions to a given wing-tail combination is summarized below.

### B. Explicit Expressions for the Wing and Tail Küssner-Type Functions

For a specific wing-tail combination, the real time, t, is non-dimensional with respect to an arbitrary distance, $b_R$, through the relationship,

$$s = Vt/b_R \qquad \text{(B5)}$$

In the present analysis, the planform reference semichord, $b_\eta$, for the wing was chosen as half the wing mean aerodynamic chord, $b_W$, and similarly, $b_\eta$ for the tail was chosen as half the tail mean aerodynamic chord, $b_T$. Thus, for the purposes of evaluating the Küssner-type functions, the actual swept wing-tail combination was replaced by a rectangular wing-tail combination as shown in Figure B3.

## APPENDIX B

The arbitrary reference distance, $b_R$, used in non-dimensionalizing the time variable was chosen in the present analysis as $b_W$. The relationship between the non-dimensional time parameters defined by equations (B1) and (B5) is obtained by combining these equations.

$$\eta = (b_R/b_\eta)s \tag{B6}$$

For the gust on the wing, the expression for the Küssner-type function is given by an expression similar to equation (B3) where the time $\eta$ is replaced by s and the subscript and superscript, W, designates the wing.

$$\psi_W(s)^* = \psi_W(0) + \sum_{k=1}^{K_\psi^W} a_k^W(1-e^{-\alpha_k^W s}) \tag{B7}$$

This result is obtained by substituting equation (B6) into equation (B3), and, as discussed above, setting

$$\left.\begin{aligned} b_\eta &= b_W \\ b_R &= b_W \end{aligned}\right\} \tag{B8}$$

Therefore, the new exponent $\alpha_k^W$ is defined by the following expression,

$$\alpha_k^W = \frac{b_R}{b_\eta}\bar{\alpha}_k^W = \frac{b_W}{b_W}\bar{\alpha}_k^W = \bar{\alpha}_k^W \tag{B9}$$

---

* Note: In order to keep the number of symbols used to a minimum, the left hand side of equation (B3) will be represented by $\psi_W(s)$, after substitution of equation (B6) into equation (B3), rather than $\psi_W(\frac{b_R}{b_\eta}s)$. Note that this procedure in representing the functional relationships will be used throughout the analysis whenever it is necessary to switch from one independent variable to another.

## APPENDIX B

As noted earlier, the values for $\bar{\alpha}_k^W$ are evaluated based upon $\eta$, and are dependent on the wing aspect ratio and airplane Mach number.

For the gust on the tail, the Küssner-type function is similar to equation (B7) with the subscript or superscript, W, replaced by T.

$$\psi_T(s) = \psi_T(0) + \sum_{k=1}^{K_\psi^T} a_k^T(1-e^{-\alpha_k^T s}) \tag{B10}$$

In this case the semichord $b_\eta$ is defined by

$$b_\eta = b_T \tag{B11}$$

Once again, $b_R = b_W$, since the same nondimensionalizing reference distance must be used throughout the analysis. The new exponent for the tail is identified by the superscript, T, and is given by

$$\alpha_k^T = \frac{b_R}{b_\eta}\,\bar{\alpha}_k^T = \frac{b_W}{b_T}\,\bar{\alpha}_k^T \tag{B12}$$

As before, the values of $\bar{\alpha}_k^T$ in equation (B12) are defined in terms of the non-dimensional time, $\eta$, and depend on the tail aspect ratio and airplane Mach number.

# APPENDIX B

## II. Indicial Lift Functions Due to Planform Motion (Wagner-Type Functions)

### A. Planform Wagner-Type Function

The following discussion of the Wagner-type function is similar to that in the previous section on the Küssner-type function. The Wagner-type function is defined herein as the time variation of lift for an airfoil of arbitrary aspect ratio and flying at an arbitrary subsonic Mach number due to motion resulting in a step change in angle of attack, normalized with respect to the steady-state lift at infinite time. The term Wagner function as used here is restricted to the special case of the Wagner-type function in which a two dimensional airfoil is flying in incompressible flow.

In contrast to the Küssner-type function, the Wagner-type function exhibits an instantaneous partial lift and thereafter a build up to the steady-state value of unity. As shown in Figure B4, the Wagner-type function is greater than the Küssner-type function for all values of the non-dimensional time, $\eta$, but the functions approach each other asymptotically as $\eta$ approaches infinity.

The Wagner-type function will be evaluated by an expression similar to equation (B2).

$$\phi(M, AR, \eta) = \left[\frac{\phi(0, AR, \eta)}{\phi(0, \infty, \eta)}\right] \phi(M, \infty, \eta) \qquad (B13)$$

where $\phi(0, \infty, \eta)$ is the incompressible two-dimensional (Wagner) function and $\phi(0, AR, \eta)$ and $\phi(M, \infty, \eta)$ are special cases of the Wagner-type function such as those found in References 12, 13, and 14.

The assumed approximation for the Wagner-type function is similar to equation (B3).

$$\phi(\eta) = \phi(0) + \sum_{k=1}^{K_\phi} b_k (1 - e^{-\beta_k \eta}) \qquad (B14)$$

where now the constant $\phi(0)$ possesses a positive value less than one, and in the case of two-dimensional incompressible flow its value is 0.5.

# APPENDIX B

## B. Explicit Expressions for the Wing and Tail Wagner-Type Functions

For wing motion, the expression representing the wing Wagner-type function for any Mach number is given by a relationship similar to equation (B7).

$$\phi_W(s) = \phi_W(0) + \sum_{k=1}^{K_\phi^W} b_k^W(1 - e^{-\beta_k^W s}) \qquad \text{(B15)}$$

where the exponent, $\beta_k^W$, is defined in a manner similar to equation (B9).

$$\beta_k^W = \frac{b_R}{b_\eta}\,\bar{\beta}_k^W = \frac{b_W}{b_W}\,\bar{\beta}_k^W = \bar{\beta}_k^W \qquad \text{(B16)}$$

For tail motion, the expressions are similar to equations (B15) and (B16) with the letter W replaced by T.

$$\phi_T(s) = \phi_T(0) + \sum_{k=1}^{K_\phi^T} b_k^T(1 - e^{-\beta_k^T s}) \qquad \text{(B17)}$$

$$\beta_k^T = \frac{b_R}{b_\eta}\,\bar{\beta}_k^T = \frac{b_W}{b_T}\,\bar{\beta}_k^T \qquad \text{(B18)}$$

The exponent $\bar{\beta}_k$ is based upon the non-dimensional time, $\eta$, and is a function of the planform aspect ratio and Mach number. Since the wing and tail have different aspect ratios, the values of $\bar{\beta}_k$ differ for the two surfaces.

# APPENDIX B

## III. Indicial Lift Functions Due To Downwash on the Tail Caused By Wing Motion and Gust on the Wing (Hobbs-Type Functions)

### A. Indicial Downwash Functions

Hobbs in Reference 1 has developed expressions for calculating the downwash variation on the tail in incompressible flow due to a unit step vertical gust moving at various gust front velocities ranging from zero (for a stationary gust field acting on the wing) to infinity (which is equivalent to wing motion). For the purpose of easy reference to these functions, the descriptive statement indicial downwash functions will be used to describe the time variation of downwash on the tail normalized with respect to the steady-state value. Furthermore, the downwash effects may be divided into downwash caused by wing motion and downwash caused by gust on the wing, and hence, the indicial downwash functions will be referred to as indicial motion downwash functions and indicial gust downwash functions, respectively.

The indicial downwash functions are of the general form presented in Figure B5* where the variable $w(M_g, M, AR_W, s_T^x, s_T^z, s)$ represents the indicial downwash as a function of the gust front Mach number (either zero or infinity for most applications), airplane flight Mach number, wing aspect ratio, horizontal and vertical positions of the tail with respect to the wing, and non-dimensional time. The locations of the negative peak values in the indicial downwash functions depend upon the parameter, $s_T^x$, which defines the relative position of the stabilizer and the wing in the longitudinal direction (see Figure B6). For the downwash due to motion, this peak location will occur just prior to a time given by $(s_T^x - 1)$ whereas for the downwash due to gust, it occurs just prior to a time defined by $(s_T^x + 1)$.

---

*Note: For the present study, Hobbs' curves are normalized with respect to the steady-state downwash slope, $\partial\varepsilon/\partial\alpha$, and the actual value of $\partial\varepsilon/\partial\alpha$ is included in the final coefficients of the generalized forces which are the inputs to the equations of motion.

## APPENDIX B

The magnitude of the peak value depends on the height of the horizontal stabilizer above the wing, $s_T^z$, and its maximum value is obtained when both surfaces lie in the same plane ($s_T^z = 0$).

For the present study, unsteady downwash functions similar to those shown in Figure B5 are evaluated from either the expressions or the final curves which Hobbs has obtained. The effects of airplane Mach number on the indicial downwash functions and downwash variation across the tail span have been neglected in the present analysis.

### B. Explicit Expressions for the Hobbs-Type Functions

The unsteady downwash experienced at the tail has the characteristics of gust regardless of whether it arises from wing motion or gust on the wing. Therefore, lift build up on the tail due to downwash is evaluated through the use of Duhamel's integral and the tail Küssner type function. The variable, $\delta(M_g, M, AR_W, AR_T, s_T^x, s_T^z, s)$, will be used to represent the normalized lift build up on the tail associated with the unsteady downwash due to a step gust on the wing or a step change in wing angle of attack. This variable will be referred to as the Hobbs-type function, and the words motion or gust will be added as appropriate to designate downwash on the tail due to wing motion, or downwash on the tail due to gust on the wing, respectively. In terms of Duhamel's integral,

$$\delta(M_g, M, AR_W, AR_T, s_T^x, s_T^z, s) = \int_0^s w(M_g, 0, AR_W, s_T^x, s_T^z, \sigma)\psi_T'(s-\sigma)d\sigma \qquad (B19)$$

Note that the expression for $\psi_T(s)$, as given by equation (B10), is a function of airplane Mach number, M, and tail aspect ratio, $AR_T$. Therefore, in spite of the fact that the

## APPENDIX B

indicial downwash function as shown in equation (B19) is independent of airplane Mach number and tail aspect ratio, the Hobbs-type function is dependent on these parameters.

The effect of superimposing the unsteady lift build up on the indicial downwash is shown by the curves in Figure B7. When these curves are compared to the indicial downwash functions of Figure B5, it is seen that the unsteady lift build up has the effect of shifting the entire curves to the right (including their intersection with the horizontal axis), and also reducing the ordinates for the initial values of s.

The expression for the normalized lift build up on the tail due to a step gust on the wing (Hobbs-type gust function) will be obtained from equation (B19) with $M_g = 0$. If the functional variable, $\delta(0, M, AR_W, AR_T, s_T^x, s_T^z, s)$, is replaced by $\delta_G(s)$ where the subscript, G, designates gust on the wing, the result is

$$\delta_G(s) = \int_0^s w(0, 0, AR_W, s_T^x, s_T^z, \sigma)\psi_T'(s-\sigma)d\sigma \qquad (B20)$$

Note that downwash due to gust on the wing is assumed to commence when the gust reaches a reference point on the wing defined by the intersection of the wing leading edge and the spanwise location of the wing mean aerodynamic chord (see Figure B6).

The expression for the normalized lift build up on the tail due to a step change in wing angle of attack resulting from wing motion (Hobbs-type motion function) will be obtained from equation (B19) with $M_g = \infty$. Again the functional variable $\delta(\infty, M, AR_W, AR_T, s_T^x, s_T^z, s)$, is replaced by $\delta_M(s)$ where now the subscript, M, designates wing motion. The result is

$$\delta_M(s) = \int_0^s w(\infty, 0, AR_W, s_T^x, s_T^z, \sigma)\psi_T'(s-\sigma)d\sigma \qquad (B21)$$

where the downwash due to wing motion is assumed to originate from the trailing edge of the wing mean aerodynamic chord (see Figure B6).

Figure B1

IDEALIZED TWO-DIMENSIONAL WING-TAIL COMBINATION ENCOUNTERING A STATIONARY GUST FIELD

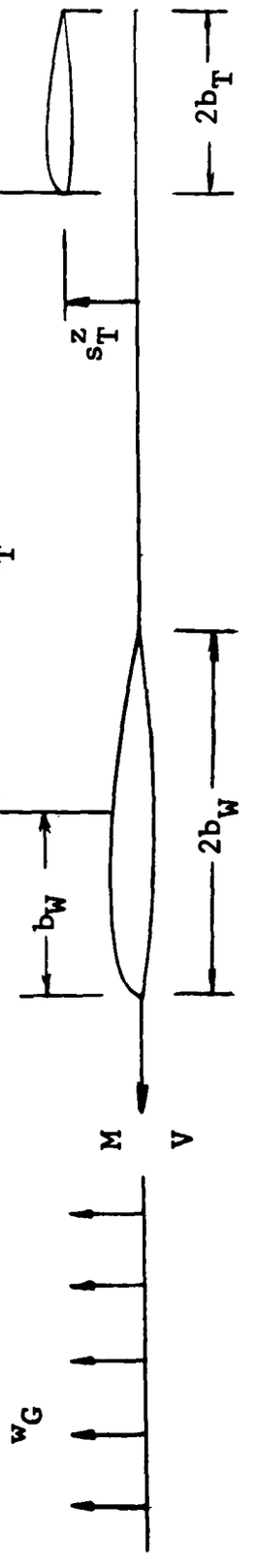

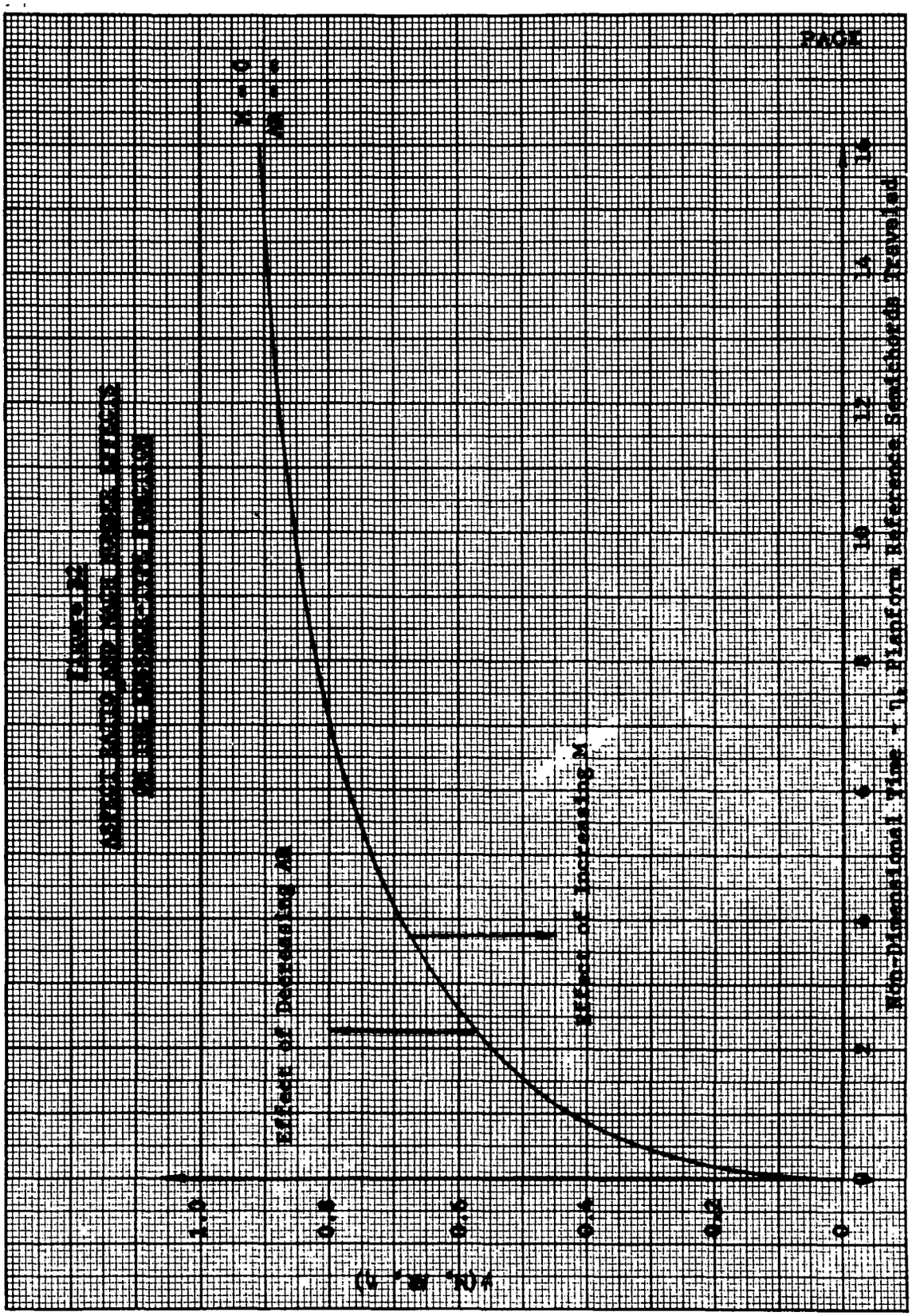
PAGE
Non-Orthogonal Line + U, Platform Reference Sandboard Traveled
Effect of Decreasing M
Effect of Increasing M
(M = 1.0)

Figure B3

DEFINITION OF REFERENCE SEMICHORDS

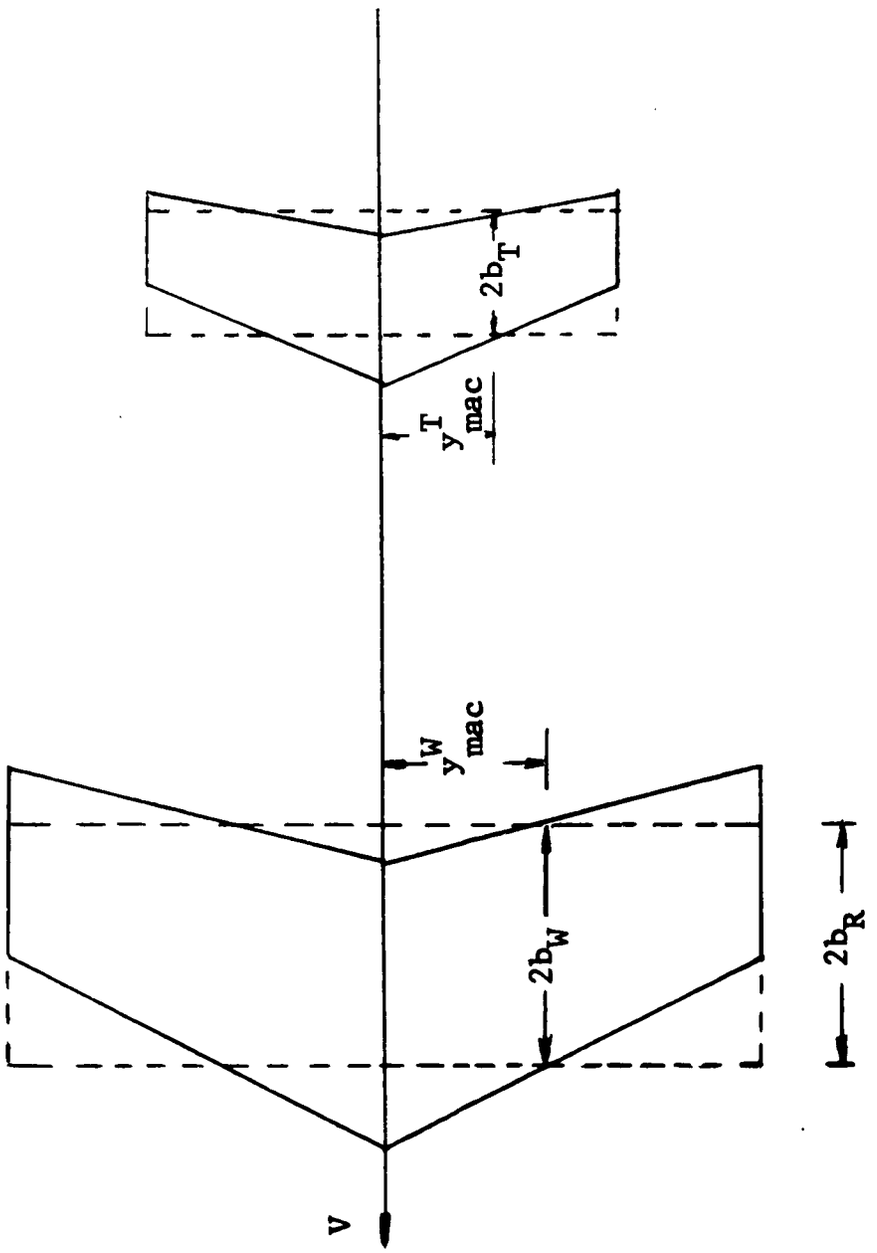

Figure B4

COMPARISON OF THE WAGNER AND THE KÜSSNER-TYPE FUNCTIONS FOR THE SAME AIRFOIL AT THE SAME MACH NUMBERS

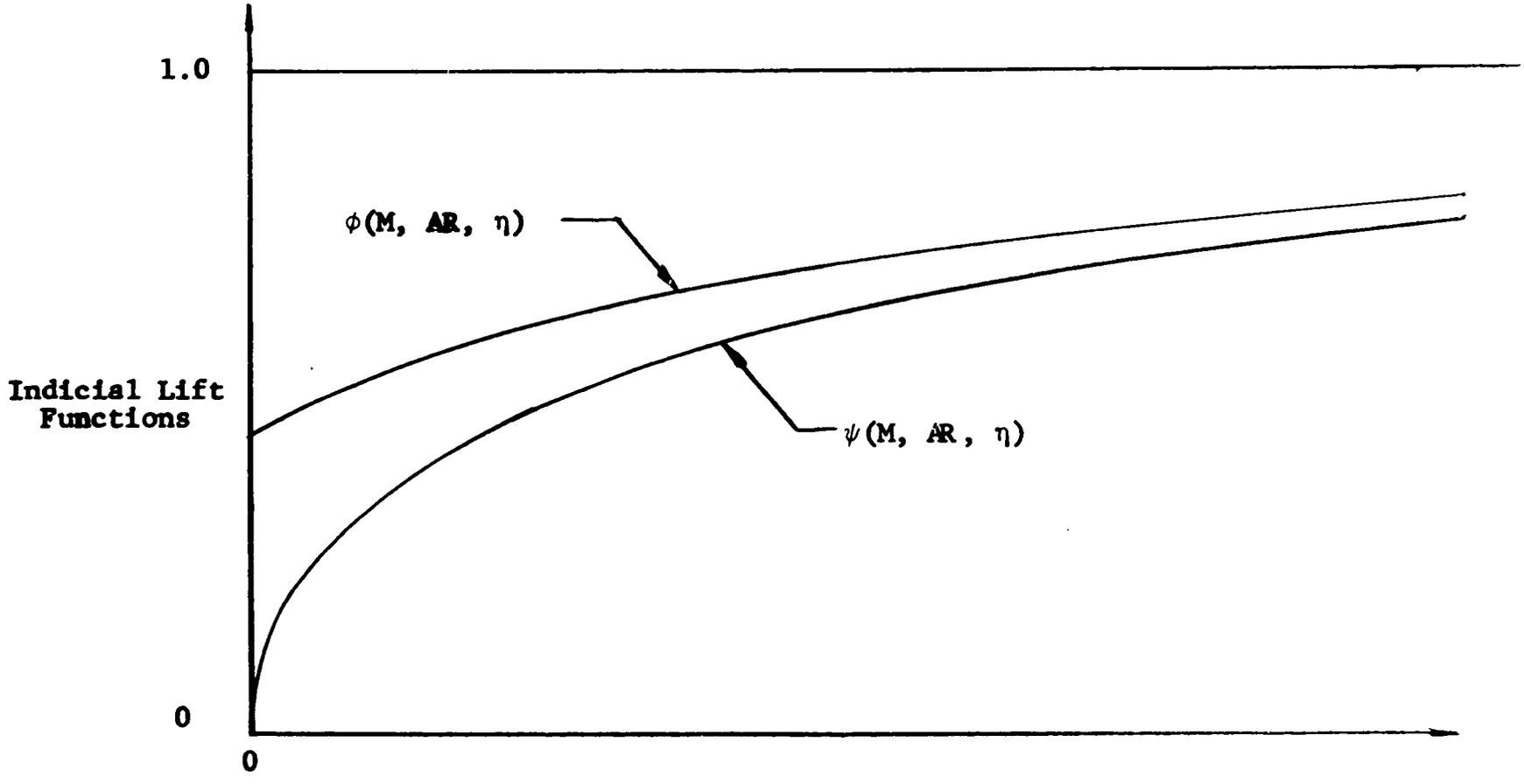

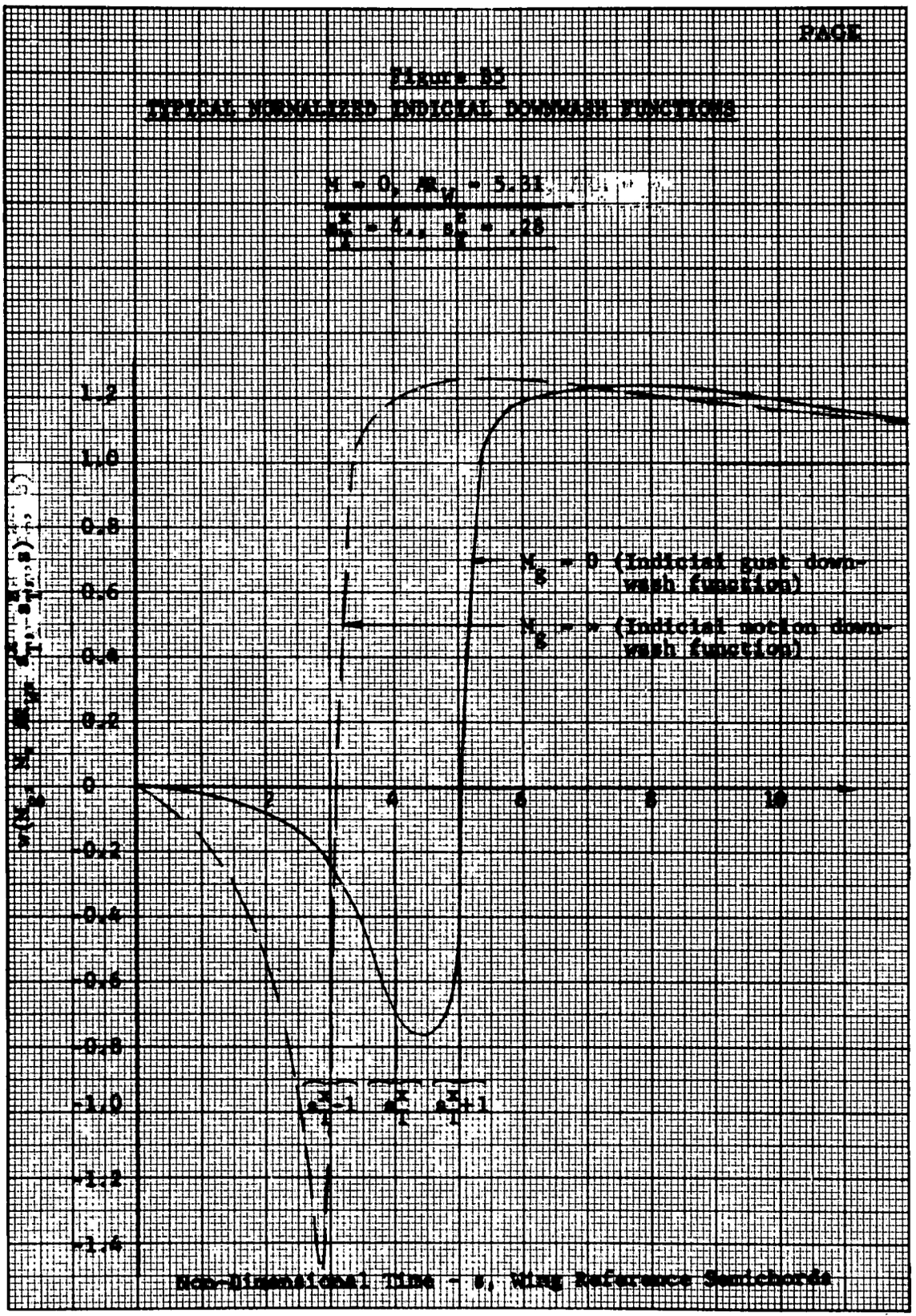
PAGE
Figure 35
TYPICAL NORMALIZED INDICIAL DOWNWASH FUNCTIONS
M = 0, AR_W = 5.31
a_0^x = 4., s_0^2 = .25
1.2
1.0
0.8
0.6
0.4
0.2
0
-0.2
-0.4
-0.6
-0.8
-1.0
-1.2
-1.4
2
4
6
8
10
K_g = 0 (Indicial gust downwash function)
K_g = ∞ (Indicial motion downwash function)
Non-Dimensional Time - s, Wing Reference Semichords

Figure B6
DEFINITION OF TIME DELAY ASSOCIATED
WITH THE INDICIAL DOWNWASH FUNCTIONS

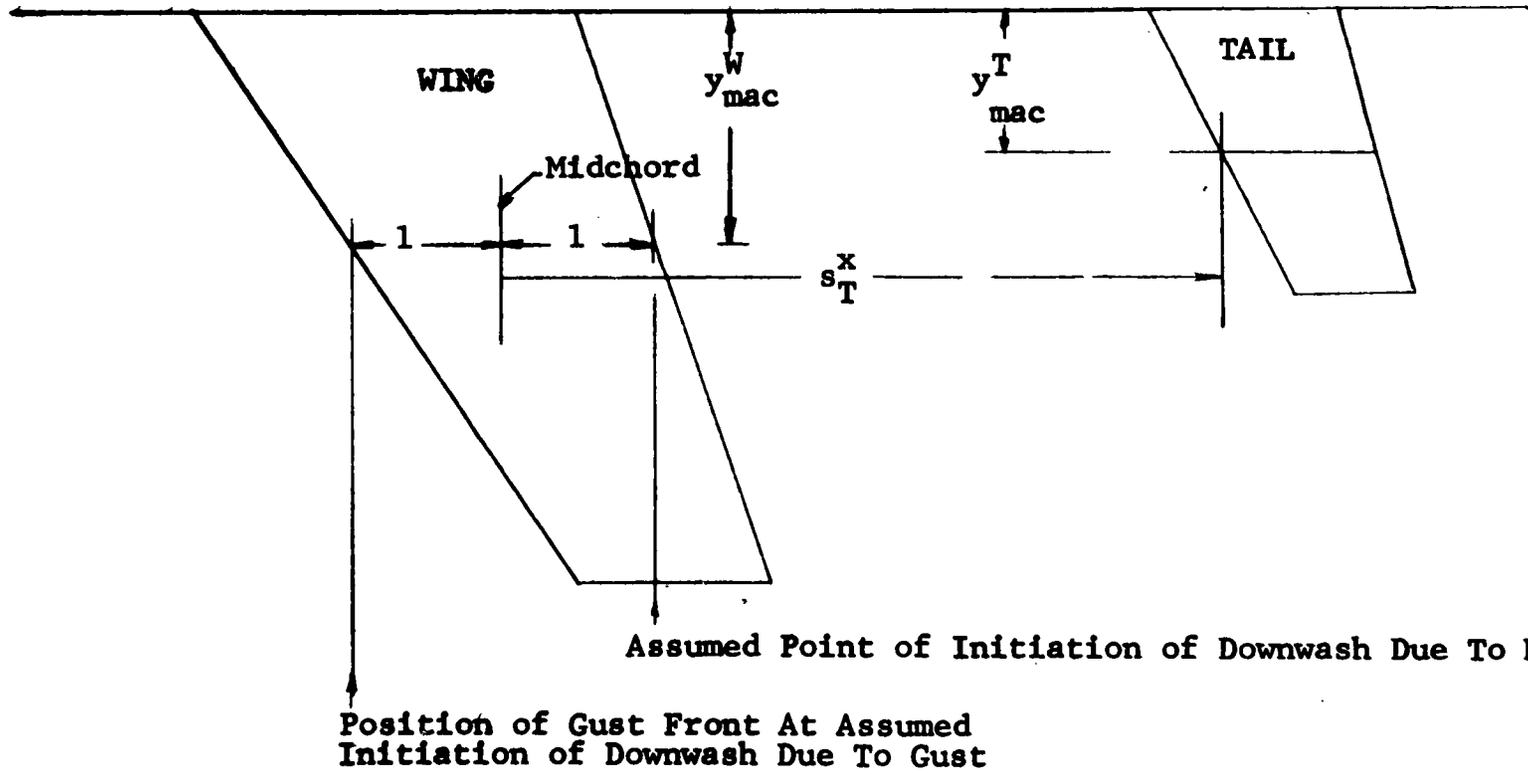

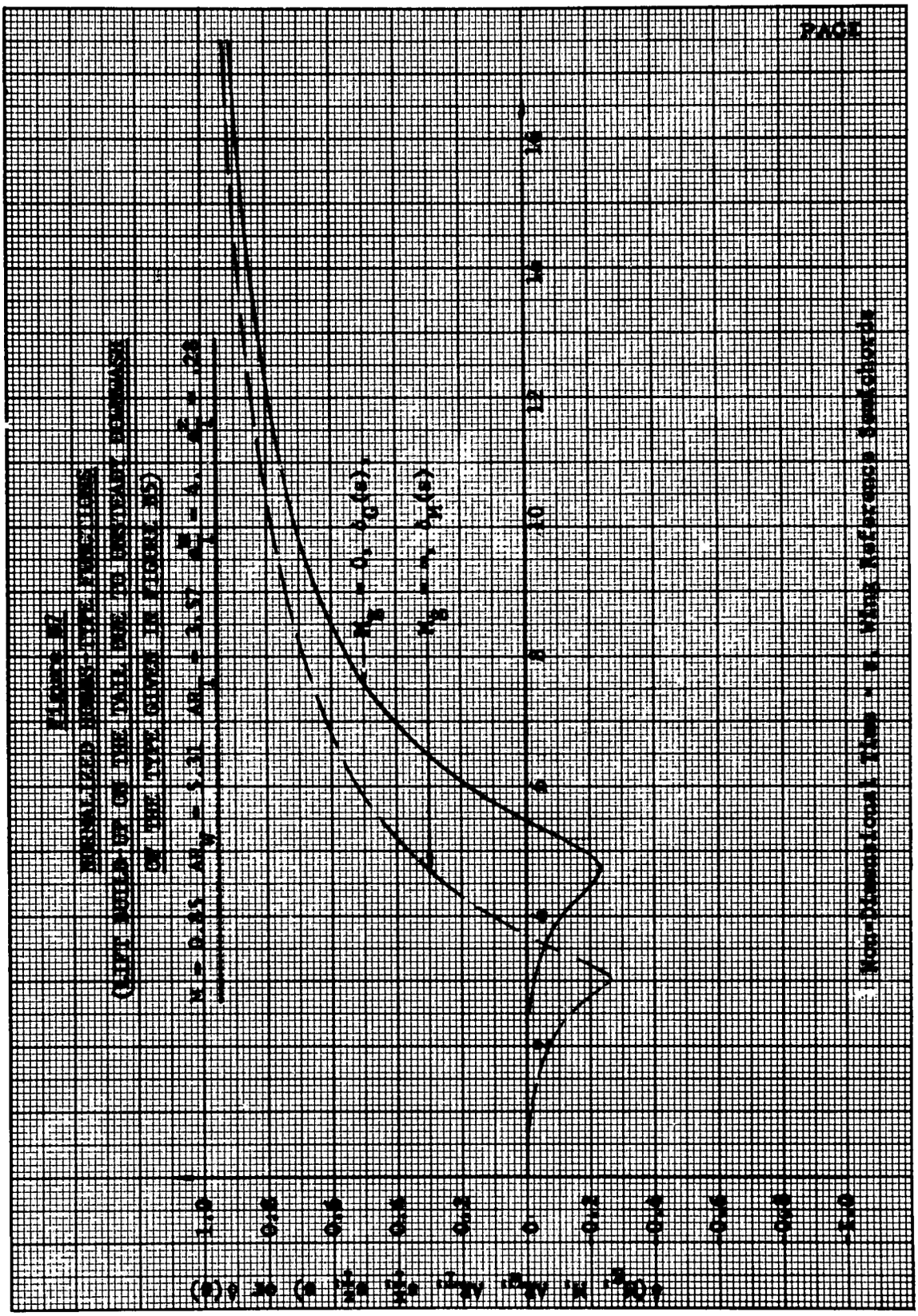

# APPENDIX C

## UNSTEADY AERODYNAMICS OF SWEPT PLANFORMS DUE TO GUST AND DOWNWASH (Indicial Generalized Force Functions)

### I. Calculation of the Wing and Tail Indicial Generalized Force Functions

#### A. Gust on an Arbitrary Planform

Consider a planform traveling at a constant horizontal velocity, V, and encountering a stationary vertical gust, $w_G$. For the representation shown in Figure C1 (assuming symmetrical conditions half the planform is shown) the planform apex enters the gust first, and the subsequent spanwise rate of immersion into the gust depends upon the forward velocity, V, and the leading edge sweep angle, $\Lambda_{LE}$. The planform is divided into a number of rectangular panels, and it is assumed that the lift build up on each of the panels is defined by the Küssner-type function evaluated for the aspect ratio of the entire planform in question. The incremental lift build up time history on the $i^{th}$ panel due to a step change in gust velocity is given by the following basic expression in terms of non-dimensional time in planform reference semichords traveled.

$$\left.\begin{aligned} \ell_\psi(y_i,\eta) &= \tfrac{1}{2}\left(\frac{\rho}{g}V^2\right)[\Delta y(y_i)2b(y_i)c_{\ell\alpha}(y_i)]\frac{w_G}{V}\,\psi(\eta-\bar{\sigma}(y_i)) \\ &\qquad \text{for } \bar{\sigma}(y_i) \leq \eta \leq \infty \\ \ell_\psi(y_i,\eta) &= 0, \text{ for } 0 \leq \eta < \bar{\sigma}(y_i) \end{aligned}\right\} \quad (C1)$$

where the transport time, $\bar{\sigma}(y_i)$, is related to the planform sweep through the following expression:

$$\bar{\sigma}(y_i) = \frac{\tan \Lambda_{LE}}{b_\eta} y_i = \frac{b_R}{b_\eta}\sigma(y_i) \quad (C2)$$

## APPENDIX C

and the gravitational constant, g, is introduced because the air density, $\rho$, is defined in this report in terms of pounds mass rather than slugs. For a unit gust, $w_G$ = 1 foot per second, equation (C1) becomes

$$\ell_\psi(y_i,\eta) = \frac{\rho}{g} V[\Delta y(y_i) b(y_i) c_{\ell\alpha}(y_i)]\psi(\eta-\bar{\sigma}(y_i)) \qquad (C3)$$

where the same conditions still hold as in equation (C1).

At the time the gust reaches the panel leading edge, lift build up commences according to the Küssner-type function, and associated with this lift build up there exists a pitching moment about the reference axis. Until the airfoil is completely enveloped by the gust, the local center of pressure is located at a point forward of the steady state value. For the present analysis, however, it is assumed to be situated at the steady-state location immediately upon gust contact. The pitching moment about the reference axis at any time is therefore obtained by multiplying the incremental lift given by equation (C3) by the moment arm $-b(y_i)[c(y_i) - a(y_i)]$.

$$t_\psi(y_i,\eta) = -b(y_i)[c(y_i) - a(y_i)]\ell_\psi(y_i,\eta) \qquad (C4)$$

Finally, the generalized force on the $i^{th}$ panel for the $m^{th}$ mode due to a unit gust is evaluated from the expression

$$q_{rm}(y_i,\eta) = -f_{h_m}(y_i)\ell_\psi(y_i,\eta) + f_{\alpha_m}(y_i)\, t_\psi(y_i,\eta) \qquad (C5)$$

where $f_{h_m}(y_i)$ and $f_{\alpha_m}(y_i)$ are the vertical and angular displacements, respectively, in the $m^{th}$ mode at the reference axis of the $i^{th}$ panel. The minus sign in the first term is due to the assumed opposite positive directions of the lift and vertical displacement vectors. The index, r, in the generalized force symbol is used to denote the origin of each of the various generalized force components as follows:

r = 1 Motion of the wing

r = 2 Motion of the tail

## APPENDIX C

| | |
|---|---|
| r = 3 | Downwash on the tail due to motion of the wing. |
| r = 4 | Downwash on the tail due to gust on the wing |
| r = 5 | Gust on the tail |
| r = 6 | Gust on the wing |

Note that equation (C5) as written applies only to r = 5 and r = 6. For example, for the evaluation of the downwash contributions to the generalized forces, the Küssner-type function, $\psi(\eta)$, in equation (C3) should be replaced by the Hobbs-type function, $\delta(\eta)$. Note also that when r is either 2, 3, 4 or 5 the airfoil parameters of the generalized force equation refer to the horizontal tail, and when r is either 1 or 6, the section parameters are those of the wing. Combining equations (C3) to (C5) and rearranging terms, the generalized force becomes

$$q_{rm}(y_i,\eta) = -\frac{\rho}{g} V\, p_m(y_i, \infty)\psi(\eta-\bar{\delta}(y_i)) \tag{C6}$$

where the constant $p_m(y_i,\infty)$ is defined by

$$p_m(y_i,\infty) = [\Delta y(y_i)b(y_i)c_{\ell_\alpha}(y_i)]\left\{ f_{h_m}(y_i) + b(y_i)[c(y_i) - a(y_i)]f_{\alpha_m}(y_i)\right\} \tag{C7}$$

The total generalized force is now obtained by summing over the panels.

$$Q_{rm}(\eta) = \sum_{i=1}^{I} q_{rm}(y_i,\eta) \tag{C8}$$

The final form of the total planform generalized force for a unit vertical gust, after equations (C6) and (C8) are combined, may be given in terms of a parameter proportional to the steady-state generalized force and the indicial

## APPENDIX C

generalized force function.

$$Q_{rm}(\eta) = -\frac{\rho}{g} V P_m(\infty)\psi_m(\eta) \tag{C9}$$

where the indicial generalized force function for the $m^{th}$ mode is defined in terms of the basic data and the Küssner-type function as follows:

$$\psi_m(\eta) = \frac{\sum_{i=1}^{I} [p_m(y_i,\infty)\psi(\eta-\bar{\sigma}(y_i))]}{P_m(\infty)} \tag{C10}$$

and the constant $P_m(\infty)$ is defined in terms of the basic data.

$$P_m(\infty) = \sum_{i=1}^{I} p_m(y_i,\infty) \tag{C11}$$

The specific steps necessary for evaluating and approximating the wing and tail indicial generalized force functions are indicated in the following sections.

### B. Gust on the Wing

In applying the above expressions to a specific wing-tail combination, the general non-dimensional time, $\eta$, which applies to an arbitrary planform considered alone, is replaced by the non-dimensional time, s, which is defined in terms of an airplane reference distance, $b_R$. Following the procedure discussed in Appendix B, and making use of equations (B6) and (B8), the wing indicial generalized force function referenced to zero time at the wing apex is obtained from equation (C10).

$$\psi_m^W(s) = \frac{\sum_{i=1}^{I_W} [p_m(y_i^W,\infty)\psi_W(s-\sigma(y_i^W))]}{P_m^W(\infty)} \tag{C12}$$

where the wing Küssner-type function $\psi_W(s)$ is the exponential approximation given by equation (B7), and the

letter W used as a subscript or superscript denotes that the planform parameters are those of the wing. The shape of the indicial generalized force function as calculated from equation (C12) depends primarily upon the particular mode for which $\psi_m^W(s)$ is calculated. In order to obtain a physical picture of these functions, Figure C2 has been prepared showing some possible shapes.

Analytical approximations to the type of functions represented by Figure C2 are assumed to be made up of a series of exponential and damped trigonometric terms as follows:

$$\psi_m^W(s) = \psi_W(0) + \sum_{k=1}^{2} a_{mk}^W (1-e^{-\alpha_{mk}^W s}) + [a_{m3}^W (1-e^{-\alpha_{m3}^W s}\cos \omega_{m3}^W s) - b_{m3}^W e^{-\alpha_{m3}^W s}\sin \omega_{m3}^W s] \tag{C13}$$

The constant, $\psi_m^W(0)$, is introduced to facilitate consideration of the quasi-steady case, for which it is set equal to one for an instantaneous lift build up and $a_{mk}$ and $b_{mk}$ are set equal to zero. In general, the constants appearing in equation (C13) are not all zero and their evaluation will be carried out according to the technique known as Prony's method which is discussed in a later section of this appendix.

## C. Gust on the Tail

The tail indicial generalized force function referred to zero time at the tail apex is calculated from an expression similar to equation (C12), where the letter W is replaced by T to represent the tail.

$$\psi_m^T(s) = \frac{\sum_{i=1}^{I_T} [p_m(y_i^T,\infty)\psi_T(s-\sigma_i(y_i^T))]}{p_m^T(\infty)} \tag{C14}$$

## APPENDIX C

This expression, like equation (C12), is derived from equation (C10) by introducing a change in the non-dimensional time with the aid of equations (B6) and (B11). The tail Küssner-type function, $\psi_T(s)$, is given by equation (B10), and the other quantities in equation (C14) are similar to equations (C7) and (C11).

If a flexible tail is considered, the indicial generalized force functions for the various modes will vary considerably as shown for the wing generalized forces in Figure C2. Under the assumption of rigid stabilizer, however, tail indicial generalized force functions become numerically very close, since the relative tail deflections in these modes are themselves very similar. Therefore, it is necessary to calculate the tail indicial generalized force function for the first mode only, and it can then be assumed that those for the remaining modes are equal to the curve calculated for the first mode. Under this assumption the analytical approximation to the tail indicial generalized force function is given by

$$\left.\begin{aligned} \psi_m^T(s) &= \psi_T(0) + \sum_{k=1}^{2} a_{mk}^T\left(1-e^{-\alpha_{mk}^T s}\right) \\ &\quad + \left[a_{m3}^T\left(1-e^{-\alpha_{m3}^T s}\cos\omega_{m3}^T s\right) - b_{m3}^T e^{-\alpha_{m3}^T s}\sin\omega_{m3}^T s\right] \\ &\text{for } m = 1 \\ \psi_m^T(s) &= \psi_1^T(s) \text{ for } 2 \le m \le N \end{aligned}\right\} \quad \text{(C15)}$$

Again, $\psi_T(0)$ is introduced to permit reduction of the equations to the case of instantaneous lift build up. Then $\psi_T(0)$ is set equal to one and the other constant coefficients are zero. In general, the initial values of the indicial generalized force functions are zero, and the other constants will be calculated by Prony's method.

# APPENDIX C

## D. Downwash on the Tail Due to Wing Motion and Gust on the Wing

The tail indicial generalized force function due to downwash caused by wing motion will be given by an expression similar to equation (C14), where the Kussner-type function, $\psi_T(s)$, is replaced by the Hobbs-type motion function given by equation (B21).

$$\delta_m^M(s) = \frac{\sum_{i=1}^{I_T} [p_m(y_i^T, \infty)\ \delta_M(s-\sigma(y_i^T))]}{P_m^T(\infty)} \tag{C16}$$

The analytical approximation is given by

$$\left.\begin{aligned} \delta_m^M(s) &= \delta_M(0) + \sum_{k=1}^{2} a_{mk}^M (1-e^{-\alpha_{mk}^M s}) \\ &\quad + [a_{m3}^M(1-e^{-\alpha_{m3}^M s}\cos\omega_{m3}^M s) - b_{m3}^M e^{-\alpha_{m3}^M s}\sin\omega_{m3}^M s] \\ &\text{for } m=1 \\ \delta_m^M(s) &= \delta_1^M(s),\ 2 \le m \le N \end{aligned}\right\} \tag{C17}$$

In the case of downwash due to gust, the necessary expressions are

$$\delta_m^G(s) = \frac{\sum_{i=1}^{I_T} p_m(y_i^T, \infty)\ \delta_G(s-\sigma(y_i^T))}{P_m^T(\infty)} \tag{C18}$$

## APPENDIX C

where $\delta_G(s)$ is given by equation (B20), and

$$\left.\begin{aligned} \delta_m^G(s) &= \delta_G(0) + \sum_{k=1}^{2} a_{mk}^G \left(1-e^{-\alpha_{mk}^G s}\right) \\ &\quad + \left[a_{m3}^G\left(1-e^{-\alpha_{m3}^G s}\cos \omega_{m3}^G s\right) - b_{m3}^G e^{-\alpha_{m3}^G s}\sin \omega_{m3}^G s\right] \\ &\text{for } m=1 \\ \delta_m^G(s) &= \delta_1^G(s) \quad \text{for } 2 \le m \le N \end{aligned}\right\} \quad \text{(C19)}$$

Figure C3 shows a typical calculated and approximated $\delta_m^G(s)$ function. Because the calculated indicial generalized force function has comparatively small amplitudes initially, it is extremely difficult to obtain an approximation based on Prony's method which is accurate throughout the complete time history. However, the introduction of an incremental time delay in the approximation ($\Delta s_A$ as indicated in Figure C3) improves the representation of the Hobbs-type functions considerably.

# APPENDIX C

## II. Application of Prony's Method of Analytical Approximation of the Indicial Generalized Force Functions

As stated previously the approximations to the indicial generalized force functions will be of the form given by equations (C13), (C15), (C17), and (C19). The method used in evaluating the constants in these expressions is a special case of Prony's method which is discussed in Section 9.4 of Reference 16 . The following presentation is more detailed than that given in Reference 16 in order to summarize the specific sets of equations that must be programmed on the digital computer. Some typical shapes of the curves that must be approximated are indicated in Figures C2 and C3.

Prony's method approximates a curve which approaches zero as the independent variable approaches infinity; therefore, the following new function is defined,

$$\left.\begin{aligned} f_m^*(s) &= 1-\psi_m(s), \qquad \text{for gust effects} \\ \text{or} & \\ f_m^*(s) &= 1-\delta_m(s), \qquad \text{for downwash effects} \end{aligned}\right\} \tag{C20}$$

where the boundary conditions associated with the above expression are

$$\left.\begin{aligned} f_m^*(0) &= 1.0 \\ f_m^*(\infty) &= 0. \end{aligned}\right\} \tag{C21}$$

A three term approximation to either one of equations (C20) which is equivalent to the form of equations (C13), (C15), (C17), and (C19) is as follows.

$$f^*(s) \cong F(s) = A_1 e^{\alpha_{A_1} s} + A_2 e^{\alpha_{A_2} s} + A_3 e^{\alpha_{A_3} s} \tag{C22}$$

where the subscript m is deleted for convenience,

## APPENDIX C

and the coefficients and exponents in the above expression may be either all real or contain a complex conjugate pair. An equivalent form of equation (C22) is

$$F(s) = A_1\Lambda_1^s + A_2\Lambda_2^s + A_3\Lambda_3^s \tag{C23}$$

where

$$\Lambda_k = e^{\alpha_{A_k}} \tag{C24}$$

To perform the actual numerical approximation, values of the curve f(s) must be specified for J equally spaced values of s where $J \geq 6$, since there are six constants to be evaluated in equation (C23). By introducing the transformation,

$$s_j = j\Delta s, \; j = 0, 1, 2, \ldots, J-1 \tag{C25}$$

or

$$j = \frac{s_j}{\Delta s} \tag{C26}$$

equations (C23) and (C24) are now rewritten as

$$F(j) \equiv F_j = A_1\lambda_1^j + A_2\lambda_2^j + A_3\lambda_3^j \tag{C27}$$

where

$$\lambda_k = \Lambda_k^{\Delta s} = e^{\alpha_{A_k}\Delta s} \tag{C28}$$

Equation (C27) is now expanded to form a set of equations for the solution of the coefficients, $A_k$, assuming for the moment that the $\lambda_k$ are known.

## APPENDIX C

$$
\left.
\begin{aligned}
F_0 &= A_1 + A_2 + A_3 \\
F_1 &= A_1\lambda_1^1 + A_2\lambda_2^1 + A_3\lambda_3^1 \\
&\vdots \quad\quad \vdots \quad\quad \vdots \quad\quad \vdots \\
F_j &= A_1\lambda_1^j + A_2\lambda_2^j + A_3\lambda_3^j \\
&\vdots \quad\quad \vdots \quad\quad \vdots \quad\quad \vdots \\
F_{J-1} &= A_1\lambda_1^{J-1} + A_2\lambda_2^{J-1} + A_3\lambda_3^{J-1}
\end{aligned}
\right\} \qquad (C29)
$$

This set of J linear equations in the unknowns, $A_1$, $A_2$, and $A_3$ may be solved exactly if $J = 3$, or approximately by the method of least squares if $J > 3$.

Since the $\lambda_k$ are actually not known, it is now assumed that $\lambda_1$, $\lambda_2$, and $\lambda_3$ are the three roots of the equation,

$$\lambda^3 - \varepsilon_1\lambda^2 - \varepsilon_2\lambda - \varepsilon_3 = (\lambda-\lambda_1)(\lambda-\lambda_2)(\lambda-\lambda_3) = 0 \qquad (C30)$$

where the coefficients $\varepsilon_1$, $\varepsilon_2$, and $\varepsilon_3$ in the above expression are real and are determined according to the following procedure. The first of equations (C29) is multiplied by $\varepsilon_3$, the second by $\varepsilon_2$, the third by $\varepsilon_1$, and the fourth by -1.

$$
\left.
\begin{aligned}
\varepsilon_3 F_0 &= \varepsilon_3(A_1 + A_2 + A_3) \\
\varepsilon_2 F_1 &= \varepsilon_2(A_1\lambda_1 + A_2\lambda_2 + A_3\lambda_3) \\
\varepsilon_1 F_2 &= \varepsilon_1(A_1\lambda_1^2 + A_2\lambda_2^2 + A_3\lambda_3^2) \\
-F_3 &= -(A_1\lambda_1^3 + A_2\lambda_2^3 + A_3\lambda_3^3)
\end{aligned}
\right\} \qquad (C31)
$$

## APPENDIX C

Since the $\lambda_k$ satisfy equation (C30), the result of adding the expressions in equation (C31) will be of the form,

$$F_3 - \varepsilon_1 F_2 - \varepsilon_2 F_1 - \varepsilon_3 F_0 = 0 \qquad \text{(C32)}$$

A set of J-3 similar equations is obtained by starting successively with the second, third, ..., and (J-3)$^{th}$ expression of equation (C29). Thus, equations (C29) and (C30) imply the J-3 linear equations,

$$\left.\begin{aligned} F_3 &= \varepsilon_1 F_2 + \varepsilon_2 F_1 + \varepsilon_3 F_0 \\ F_4 &= \varepsilon_1 F_3 + \varepsilon_2 F_2 + \varepsilon_3 F_1 \\ &\vdots \\ F_j &= \varepsilon_1 F_{j-1} + \varepsilon_2 F_{j-2} + \varepsilon_3 F_{j-3} \\ &\vdots \\ F_{J-1} &= \varepsilon_1 F_{J-2} + \varepsilon_2 F_{J-3} + \varepsilon_2 F_{J-4} \end{aligned}\right\} \qquad \text{(C33)}$$

Since the ordinates $F_j$ are known, equations (C33) can be solved directly for $\varepsilon_k$ if $J = 6$, or approximately by the method of least squares if $J > 6$.

Subsequent to evaluating the $\varepsilon_k$'s, the $\lambda_k$ are found as roots of equation (C30). The roots may be either all real or contain a complex conjugate pair. With the $\lambda_k$ known, the $A_k$ are now determined by applying the least squares technique to the set of linear equations (C29).

As stated previously the type of curve to be approximated is such that $F(s) \to 0$ as $s \to \infty$; therefore, the real

## APPENDIX C

parts of the exponents, $\alpha_k$, should be negative. If the $\lambda_k$ are all real,

$$\lambda_k = \lambda_{k\rho}, \quad 1 \leq k \leq 3 \tag{C34}$$

then the approximation will be of the form,

$$F_m(s) = \sum_{k=1}^{3} a_{mk} e^{-\alpha_{mk} s} \tag{C35}$$

where the modal index m is now reintroduced to indicate the dependence of the indicial generalized force function on the mode. The coefficients $a_{mk}$ are given by

$$a_{mk} = A_k, \quad 1 \leq k \leq 3 \tag{C36}$$

where the $A_k$ are obtained from equations (C29) for the $m^{th}$ mode. The exponents $\alpha_{mk}$ are given by

$$-\alpha_{mk} = \alpha_{A_k} = \frac{1}{\Delta s} \ell n \lambda_k, \quad 0 < \lambda_k < 1.0 \tag{C37}$$

where the $\lambda_k$ are given by equation (C34).

The exponential approximation of the indicial generalized force function, as given by equation (C35) will approximate a curve of the type (a) in Figure C2. In the case of curves (b) and (c), it appears that the approximation will include damped trigonometric terms. For this condition, the solution of equation (C30) will consist of complex roots, or more specifically, two roots must be a complex conjugate pair (since the $\epsilon_k$ are real)

## APPENDIX C

and one of the roots must be real. That is

$$\lambda_1 = \lambda_{1\rho} \tag{C38}$$

and

$$\left.\begin{aligned} \lambda_3 &= \lambda_{3\rho} + i\lambda_{3\iota} \\ \lambda_2 &= \lambda_{3\rho} - i\lambda_{3\iota} \end{aligned}\right\} \tag{C39}$$

These roots are now converted into the exponents in equation (C22) with the aid of equation (C28).

$$\left.\begin{aligned} \alpha_{A_1} &= \frac{1}{\Delta s} \ln \lambda_{1\rho} \\ \alpha_{A_2} &= \frac{1}{\Delta s} \ln(\lambda_{3\rho} - i\lambda_{3\iota}) \\ &= \frac{1}{\Delta s}\left[\tfrac{1}{2}\ln(\lambda_{3\rho}^2 + \lambda_{3\iota}^2) - i \tan^{-1}\frac{\lambda_{3\iota}}{\lambda_{3\rho}}\right] \\ \alpha_{A_3} &= \frac{1}{\Delta s} \ln(\lambda_{3\rho} + i\lambda_{3\iota}) \\ &= \frac{1}{\Delta s}\left[\tfrac{1}{2}\ln(\lambda_{3\rho}^2 + \lambda_{3\iota}^2) + i \tan^{-1}\frac{\lambda_{3\iota}}{\lambda_{3\rho}}\right] \end{aligned}\right\} \tag{C40}$$

The corresponding coefficients in equation (C22), which are obtained as solutions to equation (C29), are of the form,

$$\left.\begin{aligned} A_1 &= A_{1\rho} \\ A_2 &= A_{3\rho} - i\,A_{3\iota} \\ A_3 &= A_{3\rho} + i\,A_{3\iota} \end{aligned}\right\} \tag{C41}$$

## APPENDIX C

Equation (C22) therefore becomes

$$F(s) = A_{1\rho} e^{\alpha_{A_{1\rho}} s} + (A_{3\rho} - iA_{3\iota}) e^{(\alpha_{A_{3\rho}} - i\alpha_{A_{3\iota}})s} + (A_{3\rho} + iA_{3\iota}) e^{(\alpha_{A_{3\rho}} - i\alpha_{A_{3\iota}})s} \quad \text{(C42)}$$

where

$$\left.\begin{aligned} \alpha_{A_{1\rho}} &= \frac{1}{\Delta s} \ln \lambda_{1\rho} \\ \alpha_{A_{3\rho}} &= \frac{1}{2\Delta s} \ln(\lambda_{3\rho}^2 + \lambda_{3\iota}^2) \\ \alpha_{A_{3\iota}} &= \frac{1}{\Delta s} \tan^{-1} \frac{\lambda_{3\iota}}{\lambda_{3\rho}} \end{aligned}\right\} \quad \text{(C43)}$$

Finally, rearranging terms in equation (C42) yields the final form of the approximation used for indicial generalized force functions of the type illustrated by curves (b) and (c) of Figure C2.

$$F_m(s) = a_{m1} e^{-\alpha_{m1} s} + e^{-\alpha_{m3} s} [a_{m3} \cos(\omega_{m3} s) + b_{m3} \sin(\omega_{m3} s)] \quad \text{(C44)}$$

where

$$\left.\begin{aligned} a_{m1} &= A_{1\rho} \\ a_{m3} &= 2A_{3\rho} \\ b_{m3} &= -2A_{3\iota} \end{aligned}\right\} \quad \text{(C45)}$$

## APPENDIX C

$$\left.\begin{aligned} \alpha_{m1} &= -\alpha_{A_{1\rho}} \\ \alpha_{m3} &= -\alpha_{A_{3\rho}} \\ \omega_{m3} &= \alpha_{A_{3\iota}} \end{aligned}\right\} \quad (C45)$$

An alternate approach to solving for combined exponential damped-trigonometric approximations is as follows. The $\lambda_k$ are obtained as before, and, after having established that $\lambda_2$ and $\lambda_3$ are complex conjugates, use is made of the representation.

$$\left.\begin{aligned} \lambda_1 &= e^{\alpha_{A_{1\rho}}\Delta s} \\ \lambda_2 &= e^{(\alpha_{A_{3\rho}} - i\alpha_{A_{3\iota}})\Delta s} \\ \lambda_3 &= e^{(\alpha_{A_{3\rho}} + i\alpha_{A_{3\iota}})\Delta s} \end{aligned}\right\} \quad (C46)$$

Equation (C42) is now rewritten in the form,

$$F_j = A_{1\rho}e^{j\alpha_{A_{1\rho}}\Delta s} + 2A_{3\rho}e^{j\alpha_{A_{3\rho}}\Delta s} \cos j\alpha_{A_{3\iota}}\Delta s$$
$$-2A_{3\iota}e^{j\alpha_{A_{3\rho}}\Delta s} \sin j\alpha_{A_{3\iota}}\Delta s \quad (C47)$$

This result is now used to obtain a system of equations similar to equation (C29).

## APPENDIX C

$$
\begin{aligned}
F_0^* &= B_1 + B_2 \\
F_1 &= B_1 v_1^1 + B_2 v_2^1 + B_3 v_3^1 \\
&\vdots \\
F_j &= B_1 v_1^j + B_2 v_2^j + B_3 v_3^j \\
&\vdots \\
F_{J-1} &= B_1 v_1^{J-1} + B_2 v_2^{J-1} + B_3 v_3^{J-1}
\end{aligned}
\qquad \text{(C48)}
$$

where

$$
\begin{aligned}
B_1 &= A_{1\rho} \\
B_2 &= 2A_{3\rho} \\
B_3 &= -2A_{3\iota}
\end{aligned}
\qquad \text{(C49)}
$$

and

$$
\begin{aligned}
v_1^j &= e^{j\alpha_{A_{1\rho}}\Delta s} \\
v_2^j &= e^{j\alpha_{A_{3\rho}}\Delta s} \cos j\alpha_{A_{3\iota}}\Delta s \\
v_3^j &= e^{j\alpha_{A_{3\rho}}\Delta s} \sin j\alpha_{A_{3\iota}}\Delta s
\end{aligned}
\qquad \text{(C50)}
$$

The solution of equations (C48) for the unknowns, $B_k$, where the $v_k^j$ are given by equation (C50) and $\alpha_{A_{1\rho}}$, $\alpha_{A_{3\rho}}$,

---

* $F_0 = B_1 v_1^0 + B_2 v_2^0 + B_3 v_3^0$ where $v_1^0 = v_2^0 = 1$ and $v_3^0 = 0$

## APPENDIX C

and $\alpha_{A_{3\iota}}$ are given by equation (C43), constitutes the second step in this alternate approximation procedure. The final form of the approximation for each mode,

$$F_m(s) = a_{m1} e^{-\alpha_{m1} s} + e^{-\alpha_{m3} s} [a_{m3} \cos(\omega_{m3} s) + b_{m3} \sin(\omega_{m3} s)] \quad (C51)$$

is now developed by means of the relationships,

$$\left.\begin{aligned} a_{m1} &= B_1 \\ a_{m3} &= B_2 \\ b_{m3} &= B_3 \\ \alpha_{m1} &= -\alpha_{A_{1\rho}} \\ \alpha_{m3} &= -\alpha_{A_{3\rho}} \\ \omega_{m3} &= \alpha_{A_{3\iota}} \end{aligned}\right\} \quad (C52)$$

At this point it is noted that the parameter $\alpha_{A_{3\iota}}$ in equation (C47) may be replaced by the somewhat simpler expression,

$$\alpha_{A_{3\iota}} = \frac{1}{\Delta s} \tan^{-1} \left| \frac{\lambda_{3\iota}}{\lambda_{3\rho}} \right| \quad (C53)$$

with no loss in generality for the present application. From equation (C28), it is seen that for a complex root of equation (C39),

## APPENDIX C

$$\lambda_3 = e^{(\alpha_{A_{3\rho}} + i\alpha_{A_{3\iota}})\Delta s}$$

$$= e^{\alpha_{A_{3\rho}}\Delta s}\left[\cos(\alpha_{A_{3\iota}}\Delta s) + i\,\sin(\alpha_{A_{3\iota}}\Delta s)\right] \qquad \text{(C54)}$$

For the adequate numerical representation of a curve having a frequency component, $\alpha_{A_{3\iota}}$, the points $F_j$ should be chosen with a spacing $\Delta s$ of less than approximately $1.5/\alpha_{A_{3\iota}}$. Under these circumstances,

$$\left| \alpha_{A_{3\iota}}\Delta s \right| < \frac{\pi}{2} \qquad \text{(C55)}$$

and therefore, the problem of choosing between multiple arguments in equation (C43) will not occur.

Consider now the sign of $\alpha_{A_{3\iota}}$. If equation (C53) rather than equation (C43) is used in the evaluation of the $\nu_3^j$ by equations (C50), the sign of $\nu_3^j$ may be reversed. However, the use of $-(\nu_3^j)$ rather than the actual $\nu_3^j$ in equations (C48) will merely result in a corresponding change in sign of the unknown $B_3$. The net result, therefore, is that the product $B_3\nu_3^j$ remains unaffected, and hence, the $F_j$ given by equation (C47), as well as the corresponding final form of the approximation given by equation (C53), will remain correct in spite of a change in sign of $\alpha_{A_{3\iota}}$.

Finally, a general form of the approximation to the gust functions is established by combining equations (C20), (C35), and (C44) as follows,

## APPENDIX C

$$\psi_m(s) = a_{m1}(1-e^{-\alpha_{m1}s}) + a_{m2}(1-e^{-\alpha_{m2}s})$$

$$+ a_{m3}[1-e^{-\alpha_{m3}s}\cos(\omega_{m3}s)]-b_{m3}e^{-\alpha_{m3}s}\sin(\omega_{m3}s) \quad (C56)$$

The corresponding approximations for the downwash indicial generalized force functions will also be of this form, with the variable $\psi_m(s)$ replaced by $\delta_m(s)$. For an approximation to consist of <u>three exponential terms</u>,

$$b_{m3} = \omega_{m3} = 0 \quad (C57)$$

In the case of <u>one exponential and one damped trigonometric term</u>, the second exponential term is deleted, that is

$$a_{m2} = 0 \quad (C58)$$

In conclusion it is noted that, while Prony's method will determine $a_{mk}$'s whose sum is approximately 1, the $a_{mk}$'s should be modified so that their sum is exactly 1. These corrections will yield indicial generalized force functions which are consistent with steady-state values of unity.

Figure C1

DEFINITION OF PLANFORM PARAMETERS

USED IN GENERALIZED FORCE CALCULATIONS

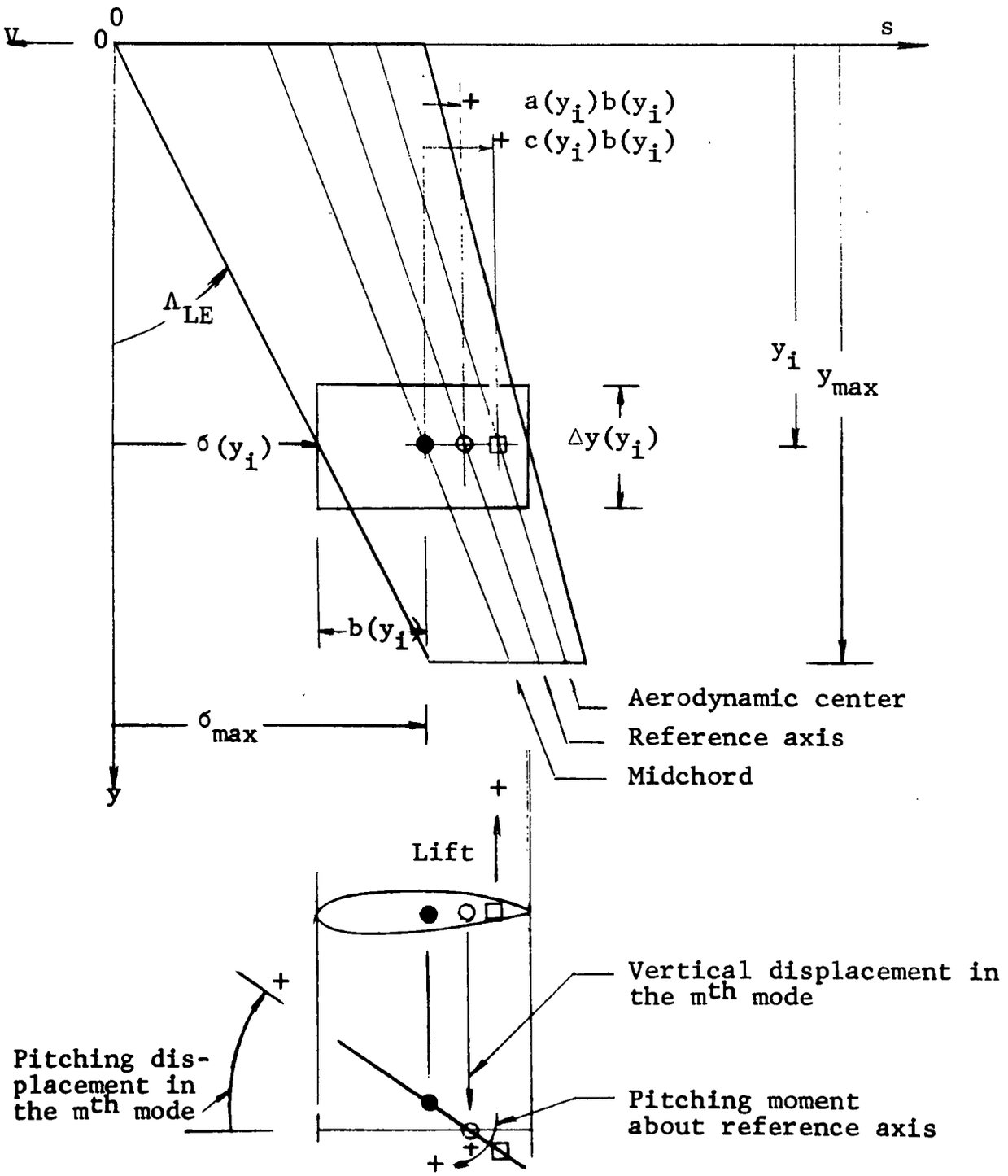

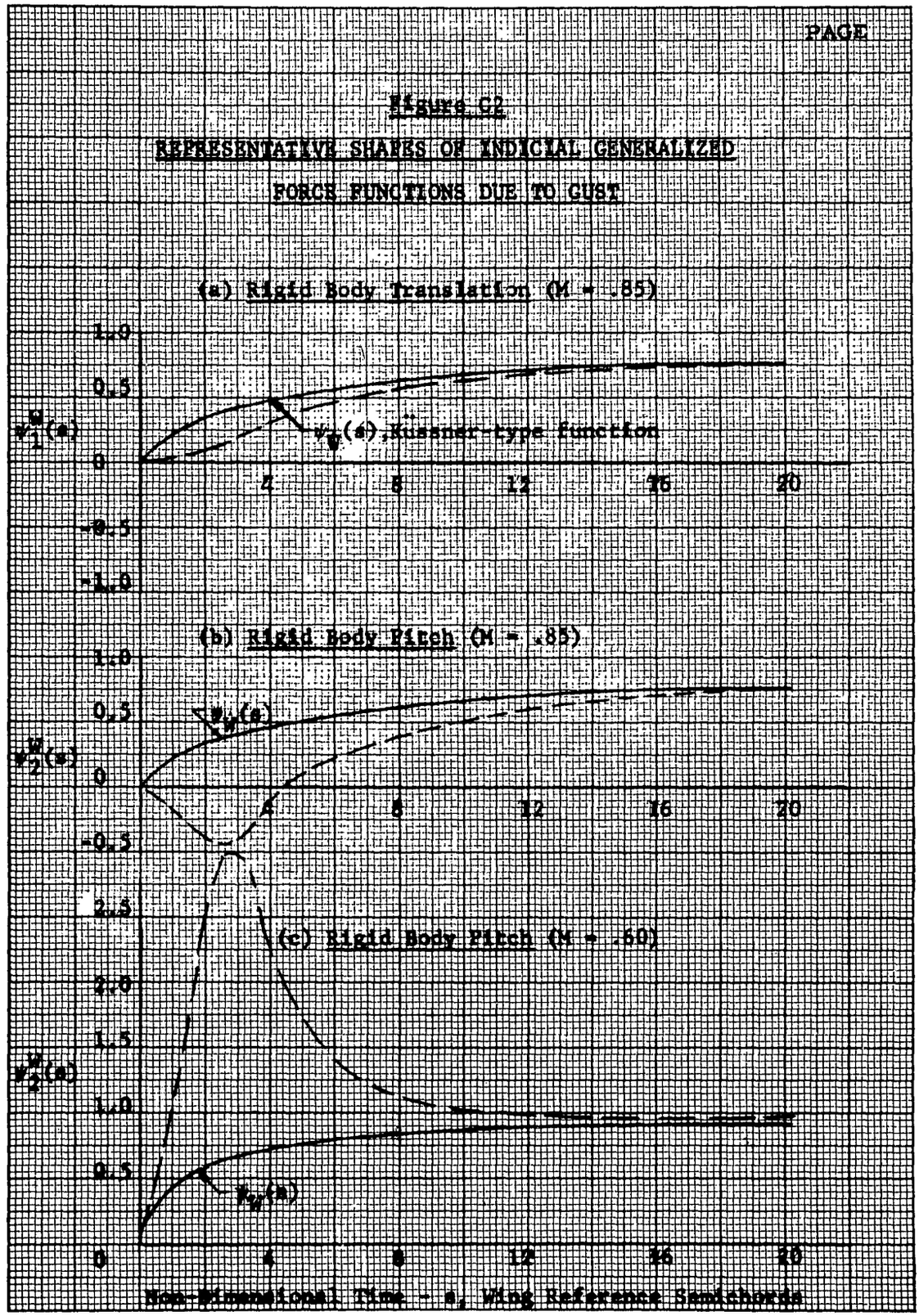
PAGE
Figure G2
REPRESENTATIVE SHAPES OF INDICIAL GENERALIZED
FORCE FUNCTIONS DUE TO GUST
(a) Rigid Body Translation (M = .85)
(b) Rigid Body Pitch (M = .85)
(c) Rigid Body Pitch (M = .60)
Kussner-type function
Non-Dimensional Time - s, Wing Reference Semichords

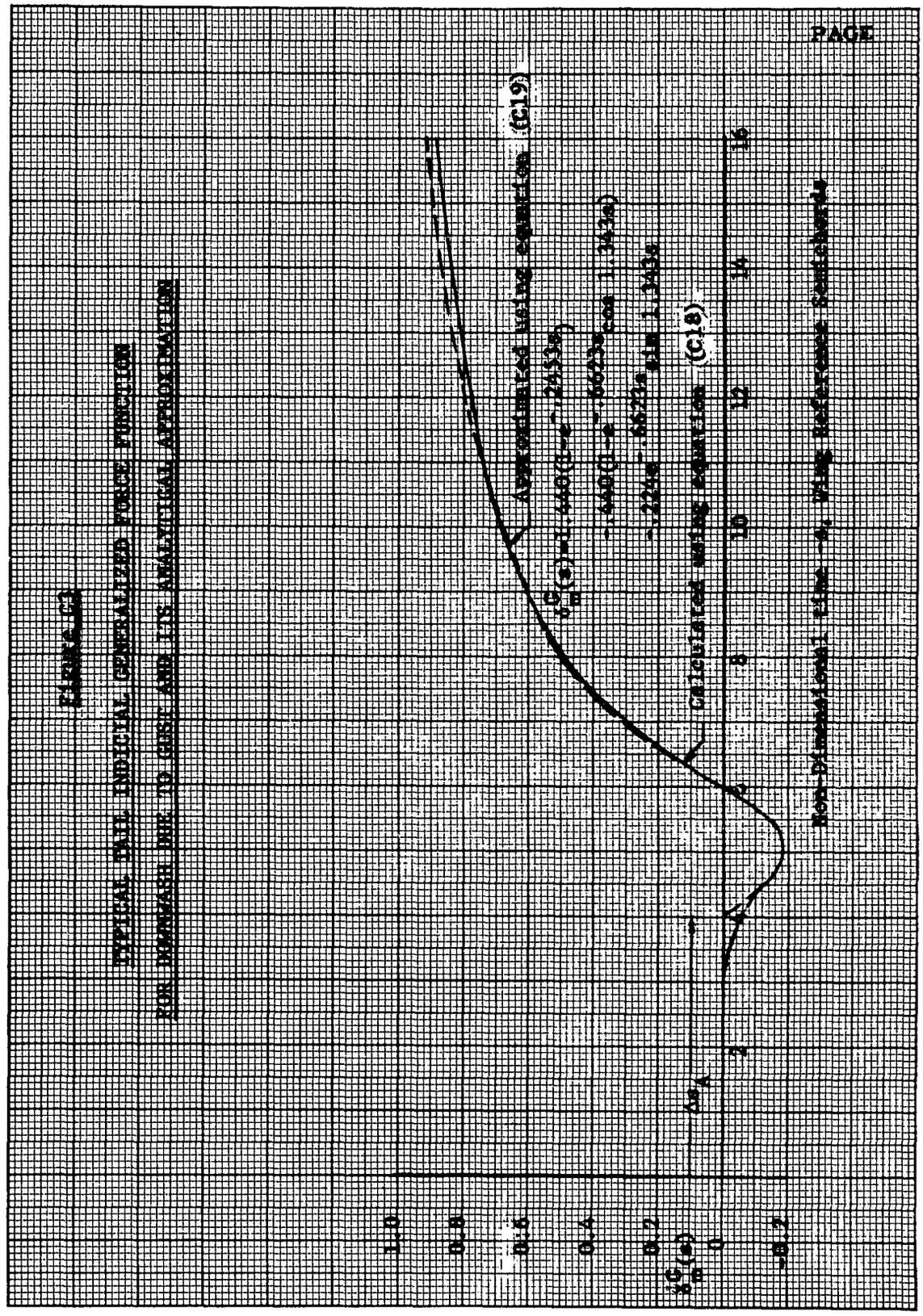
PAGE
FIGURE C3
TYPICAL PAIR INDICIAL GENERALIZED FORCE FUNCTION
FOR NONPLANAR MOTION OF (NACA 0012) AIRFOIL AND ITS ANALYTICAL APPROXIMATION
Approximated using equation (C19)
$\phi_{\theta\theta}(s) = 1 - .440e^{-.2655s} - .440e^{-.6623s}\cos 1.3439s$
$+ .440e^{-.6623s}\sin 1.3439s$
Calculated using equation (C18)
Non-dimensional time, s, semi-chords traveled
$\phi_{\theta\theta}(s)$
1.0
0.8
0.6
0.4
0.2
0
-0.2
2
4
6
8
10
12
14
16

# APPENDIX D

## GENERALIZED FORCE DUE TO GUST AND ASSOCIATED DOWNWASH

### I. Gust on the Wing

Planform (wing or tail) generalized forces due to gust, which are part of the inputs to the equations of motion, are evaluated through Duhamel's integral in conjunction with indicial generalized force functions developed in Appendix C and the forcing function, $\chi(s)$, which represents an arbitrary gust. The development of the generalized force begins by considering the incremental lift and moment existing on the $i^{th}$ panel, and these quantities are then converted to a generalized force by making use of the mode shapes. The incremental lift on the $i^{th}$ panel is given in terms of the non-dimensional time s as follows:

$$\ell_{\psi}(y_i, s) = \frac{1}{2} \frac{\rho}{g} V^2 \left[\Delta y(y_i)\ 2b(y_i)\ c_{\ell_\alpha}(y_i)\right] f_{\psi}(s-\sigma(y_i)) \qquad (D1)$$

In general, the forcing function, $f_{\psi}(s-\sigma(y_i))$, on each panel is given by Duhamel's integral in terms of the Küssner-type function, $\psi(s)$, and the change in angle of attack due to gust, $\chi(s)/V$,

$$f_{\psi}(s) = \int_0^s \left[\chi(\sigma)/V\right] \psi'(s-\sigma)\, d\sigma \qquad (D2)$$

Note that when $\chi(s) = 1.0$ (unit step gust input) equation (D1) reduces to equation (C3).

The generalized force for the $m^{th}$ mode and $i^{th}$ panel due to an incremental lift given by equation (D1) is similar to equation (C6).

$$q_{rm}(y_i, s) = -C_V \left[\rho b_R^{\,2} p_m(y_i, \infty)\right] f_{\psi}(s-\sigma(y_i)) \qquad (D3)$$

where the constant $C_V$ is defined as follows:

$$C_V = (V/b_R)^2\ (1/g) \qquad (D4)$$

## APPENDIX D

and $p_m(y_i,\infty)$ is defined by equation (C7). The subscript r is assigned the value of 5 to denote gust on the tail and 6 to denote gust on the wing.

The total generalized force may now be obtained by summing over the panels and rearranging equation (D3) as follows:

$$Q_{rm}(s) = C_V \left[-\rho b_R^2 P_m(\infty)\right] \sum_i \left[ \frac{P_m(y_i,\infty)}{P_m(\infty)} f_\psi(s-\sigma(y_i)) \right] \quad (D5)$$

where the constant $P_m(\infty)$ is given by equation (C11). After substituting equation (D2) into equation (D5), the generalized force may be written as

$$Q_{rm}(s) = C_V D_m \Psi_m(s) \quad (D6)$$

where the constant, $D_m$, is given by

$$D_m = -(\rho/V) b_R^2 P_m(\infty) \quad (D7)$$

The generalized force variation, $\Psi_m(s)$, is given by Duhamel's integral in terms of the gust input, $\chi(s)$, and the indicial generalized force function, $\psi_m(s)$.

$$\Psi_m(s) = \int_0^s \chi(\sigma)\, \psi_m'(s-\sigma)\, d\sigma \quad (D8)$$

where the indicial generalized force function is given by the following basic expression, which is the same as equation (C12).

$$\psi_m(s) = \sum_{i=1}^{I} \left[ \frac{P_m(y_i,\infty)}{P_m(\infty)} \psi(s-\sigma(y_i)) \right] \quad (D9)$$

Note that thus far in the development the letter W used as a subscript or superscript to designate gust on the wing has been omitted since the expressions are general and equally applicable to both the wing and the tail. It is understood that the expressions may be applied in other parts of the report by the use of the appropriate subscript.

## APPENDIX D

The solution of equation (D8), and hence also equation (D6), may be obtained by combining it with the analytical approximation for the indicial generalized force function given by equation (C56). The procedure that is followed here is to obtain the Laplace transform of equations (D8) and (C56) as follows:

$$\bar{\Psi}_m(p) = \bar{\chi}(p)\ p\ \bar{\psi}_m(p) \tag{D10}$$

$$\bar{\psi}_m(p) = \frac{\psi(0)}{p} + \sum_{k=1}^{2} \frac{a_{mk}\alpha_{mk}}{p(p+\alpha_{mk})}$$

$$+ \frac{[a_{m3}\ \alpha_{m3} - b_{m3}\omega_{m3}]\ p + a_{m3}\ [\alpha_{m3}^2 + \omega_{m3}^2]}{p\ [p^2 + 2\alpha_{m3}p + (\alpha_{m3}^2 + \omega_{m3}^2)]} \tag{D11}$$

Equation (D10) is now redefined in terms of the component parts of the Laplace transform given in equation (D11).

$$\bar{\Psi}_m(p) = \sum_{k=0}^{3} \bar{\Psi}_{mk}(p) \tag{D12}$$

where the component parts of the Laplace transform are given by

$$\bar{\Psi}_{m0}(p) = \psi(0)\ \bar{\chi}(p) \tag{D13}$$

$$\bar{\Psi}_{mk}(p) = \left[\frac{a_{mk}\alpha_{mk}}{p+\alpha_{mk}}\right]\ \bar{\chi}(p), \text{ for } k=1,2 \tag{D14}$$

$$\bar{\Psi}_{mk}(p) = \left\{\frac{[a_{mk}\alpha_{mk} - b_{mk}\omega_{mk}]\ p + a_{mk}\ [\alpha_{mk}^2 + \omega_{mk}^2]}{p^2 + 2\alpha_{mk}p + (\alpha_{mk}^2 + \omega_{mk}^2)}\right\}\bar{\chi}(p), \tag{D15}$$

for k=3

## APPENDIX D

Finally, the generalized force, $Q_{rm}(s)$, for the $m^{th}$ mode due to the gust on the wing is obtained from equation (D6) and (D12) through (D15). Also, the r is assigned the value of 6 and the letter W is used as superscript to indicate gust on the wing.

$$Q_{6m}(s) = C_V \, D_m^W \, \Psi_m^W(s) \tag{D16}$$

The generalized force variation, $\Psi_m^W(s)$, is evaluated by taking the inverse Laplace transform of equations (D12) through (D15).

$$\Psi_m^W(s) = \sum_{k=0}^{3} \Psi_{mk}^W(s) \tag{D17}$$

The component parts of the generalized force variation, $\Psi_{mk}^W(s)$, are given by the solutions to the following set of differential equations, which are obtained by taking the inverse of equations (D13) to (D15).

$$\Psi_{m0}^W(s) = \psi_W(0) \, \chi(s-s_W) \tag{D18}$$

$$\dot{\Psi}_{mk}^W(s) + \alpha_{mk}^W \, \Psi_{mk}^W(s) = a_{mk}^W \, \alpha_{mk}^W \, \chi \, (s-s_W), \text{ for } k=1,2 \tag{D19}$$

$$\ddot{\Psi}_{mk}^W(s) + 2\alpha_{mk}^W \dot{\Psi}_{mk}^W(s) + [(\alpha_{mk}^W)^2 + (\omega_{mk}^W)^2] \, \Psi_{mk}^W(s) =$$

$$[\, a_{mk}^W \alpha_{mk}^W - b_{mk}^W \omega_{mk}^W] \, \dot{\chi}(s-s_W) + a_{mk}^W \, [(\alpha_{mk}^W)^2 + (\omega_{mk}^W)^2] \, \chi(s-s_W)$$

$$\text{for } k=3 \tag{D20}$$

It is noted that the transport time delay introduced here accounts for the time the gust requires to travel from an arbitrary zero reference point located ahead of the wing to the wing apex as defined by the intersection of the airplane centerline and the wing leading edge.

# APPENDIX D

## II. Gust on the Tail

The development of the generalized forces for gust on the tail will be similar to that for gust on the wing. In fact, the final expressions for the tail generalized force will be the same as equations (D16) to (D20) except that the subscript r now has the value of 5 and the letter W is replaced by T to represent gust on the tail.

Since the indicial generalized force function for gust on the tail is assumed independent of the mode as indicated by equation (C15), the generalized force for gust on the tail reduces to

$$Q_{5m}(s) = C_V \, D_m^T \, \Psi_1^T(s) \qquad \text{(D21)}$$

where the tail generalized force variation, $\Psi_1^T(s)$, is obtained by solving equations similar to (D17) through (D20) for the first mode only (m=1).

## APPENDIX D

### III. Downwash on the Tail Due to Gust on the Wing

The expressions for the generalized forces on the tail due to downwash as a result of gust on the wing are similar in form to equation (D16), with the variable $\Psi_m^W(s)$ being replaced by $\Delta_m^G(s)$, the downwash slope $-\left|\partial\varepsilon/\partial\alpha\right|$ being introduced on the right side to account for the strength and direction of downwash, and the index r in $Q_{rm}(s)$ being assigned the value of 4.

$$Q_{4m}(s) = C_V \, D_m^G \, \Delta_1^G(s) \tag{D22}$$

$$D_m^G = D_m^T \tag{D23}$$

and that, as in the previous section, the generalized force variation due to downwash on the tail caused by gust on the wing, $\Delta_m^G(s)$, is independent of the mode (see equation (C19.))

The expression for calculating $\Delta_m^G(s)$ (for m=1) will be similar to equations (D17) to (D20).

$$\Delta_1^G(s) = \sum_{k=0}^{3} \Delta_{1k}^G(s) \tag{D24}$$

where

$$\Delta_{10}^G(s) = - \left|\frac{\partial\varepsilon}{\partial\alpha}\right| \delta_G(0) \quad \chi(s-s_G) \tag{D25}$$

$$\dot{\Delta}_{1k}^G(s) + \alpha_{1k}^G \, \Delta_{1k}^G(s) = - \left|\frac{\partial\varepsilon}{\partial\alpha}\right| a_{1k}^G \, \alpha_{1k}^G \, \chi(s-s_G)$$

$$\text{for } k=1,2 \tag{D26}$$

## APPENDIX D

$$\overset{\infty}{\Delta}{}^{G}_{1k}(s) + 2\alpha^{G}_{1k}\,\overset{\circ}{\Delta}{}^{G}_{1k}(s) + [(\alpha^{G}_{1k})^2 + (\omega^{G}_{1k})^2]\,\Delta^{G}_{1k}(s) =$$

$$-\left|\frac{\partial \varepsilon}{\partial \alpha}\right|\left\{[a^{G}_{1k}\,\alpha^{G}_{1k} - b^{G}_{1k}\,\omega^{G}_{1k}]\,\overset{\circ}{\chi}(s-s_G) + a^{G}_{1k}\,[(\alpha^{G}_{1k})^2 + (\omega^{G}_{1k})^2]\,\chi(s-s_G)\right\}$$

for $k=3$ (D27)

The time delay $s_G$ is introduced to account for the elapsed time between the passing of the gust over the zero reference point and the approximated start of tail lift build up resulting from the wing downwash due to that gust. More specifically, $s_G$, is the sum of the quantity $\Delta s_A$ shown in Figure C3 and the distance in semichords between the zero reference point and the longitudinal location of the point of intersection of the wing leading edge and its mean aerodynamic chord.

# APPENDIX E

## GENERALIZED FORCE DUE TO MOTION AND ASSOCIATED DOWNWASH

### I. Wing Motion

For a two dimensional airfoil section in incompressible flow, the incremental lift and pitching moment about the reference axis due to oscillatory airfoil motion is given by Reference15, page 272, equations (5-311) and (5-312), respectively. These expressions are reproduced below in a slightly modified form; most of the symbols used are defined in Figure C1.

$$\ell_\phi(t) = \pi \frac{\rho}{g} b^2 [\ddot{h}(t) + V\dot{\alpha}(t) - ba\ddot{\alpha}(t)] + 2\pi \frac{\rho}{g} Vbf_\phi(t) \qquad (E1)$$

$$t_\phi(t) = \pi \frac{\rho}{g} b^2 [ba\ddot{h}(t) - Vb(\tfrac{1}{2}-a)\dot{\alpha}(t) - b^2(a^2+1/8)\ddot{\alpha}(t)] + 2\pi \frac{\rho}{g} Vb^2(a+\tfrac{1}{2})f_\phi(t) \qquad (E2)$$

where

$$f_\phi(t) = - C(\kappa)w_\phi(t) \qquad (E3)$$

$C(\kappa)$ is Theodorsen's function, and the downwash at the three-quarter chord, $w_\phi(t)$, is given by

$$w_\phi(t) = - [\dot{h}(t)+V\alpha(t)+b(\tfrac{1}{2}-a)\dot{\alpha}(t)] \qquad (E4)$$

Note that the density, $\rho$, is defined in units of pounds-mass rather than slugs, and is therefore divided by the gravitational constant, g. The subscript, $\phi$, is used to denote lift and moment due to motion.

# APPENDIX E

Since the circulatory contribution to the lift and pitching moment given by equations (E1) and (E2) is defined in terms of Theodorsen's function, $C(\kappa)$, these equations are applicable to arbitrary motion, as is required for an arbitrary gust, equation (E3) is redefined in terms of Duhamel's integral and the Wagner-type function. In order to carry out this change, use is made of equation (5-370), page 285, and equations (8) through (10), page 815, of Reference 15. Equation (E3) is now presented in terms of Duhamel's integral as follows:

$$f_{\phi}(t) = -\int_0^t w_{\phi}(\tau)\phi'(t-\tau)d\tau \qquad \text{(E5)}$$

Note that in the subsequent development, where the independent variable is changed from t to s, the function $\phi(t)$ is replaced by the more familiar form, $\phi(s)$.

The above equations for section lift and pitching moment are now utilized to describe the unsteady aerodynamic forces due to motion of the $i^{th}$ panel of a three dimensional wing in compressible flow. Under the following assumptions, the equations are re-written below in terms of the section properties and airfoil motion at the spanwise position corresponding to the center of the $i^{th}$ panel, $y_i$.

(1). The circulatory lift and moment on the $i^{th}$ panel is determined by the downwash at the three-quarter chord point of that panel (equation (E4)).

(2). The magnitude of the circulatory lift and moment on each panel is based on the local lift curve slope ($2\pi$ is replaced by $c_{\ell_\alpha}(y_i)$), and local aerodynamic center (the factor $(a+\frac{1}{2})$ in the last term of equation (E2) is replaced by $(a(y_i)-c(y_i))$.

(3). The rate of circulatory lift build up on a three-dimensional airfoil is constant across the span, and is taken as the build up on a rectangular airfoil having the same aspect ratio as the actual airfoil being considered. The expression for the circulatory lift due to motion is that given by the Wagner-type function, whose analytical approximation is of the form given by equations (B15) and (B17) for the wing and tail, respectively.

## APPENDIX E

(4). Non-circulatory lift per unit span on a given panel is assumed to be identical to the lift on a two-dimensional section in incompressible flow.

The modified lift and moment equations are

$$\ell_\phi(y_i,t) = \frac{\rho}{2g} C(y_i)\Big\{ b(y_i)\,[\ddot{h}(y_i,t) + V\dot{\alpha}(y_i,t) - b(y_i)a(y_i)\,\ddot{\alpha}(y_i,t)] + 2Vf_\phi(y_i,t)\Big\} \tag{E6}$$

$$t_\phi(y_i,t) = \frac{\rho}{2g} C(y_i)b(y_i)\Big\{ b(y_i)\,\big[a(y_i)\ddot{h}(y_i,t) + V\,[a(y_i)-\tfrac{1}{2}]\dot{\alpha}(y_i,t) - b(y_i)\,[a^2(y_i)+1/8]\,\ddot{\alpha}(y_i,t)\big] - 2V\,[c(y_i)-a(y_i)]\,f_\phi(y_i,t)\Big\} \tag{E7}$$

where

$$C(y_i) = \Delta y(y_i)b(y_i)c_{\ell_\alpha}(y_i) \tag{E8}$$

$$f_\phi(y_i,t) = -\int_0^t w_\phi(y_i,\tau)\,\phi'(t-\tau)\,d\tau \tag{E9}$$

and the downwash at the three-quarter-chord point becomes

$$w_\phi(y_i,t) = -\,[\dot{h}(y_i,t)+V\alpha(y_i,t)-b(y_i)\,[a(y_i)-\tfrac{1}{2}]\,\dot{\alpha}(y_i,t)] \tag{E10}$$

The development of the present analysis is based upon the non-dimensional time, s, rather than the real time, t. The conversion of the time variable is given by the following relationships,

## APPENDIX E

$$\left.\begin{aligned} s &= \left(\frac{V}{b_R}\right)t \\ \frac{d}{dt} &= \left(\frac{V}{b_R}\right)\frac{d}{ds} \\ \frac{d^2}{dt^2} &= \left(\frac{V}{b_R}\right)^2\frac{d^2}{ds^2} \end{aligned}\right\} \qquad \text{(E11)}$$

Next, the vertical and angular deflections of the $i^{th}$ panel are expressed as the product of time dependent coordinates (normal modes) and space dependent coordinates (mode shapes).

$$\left.\begin{aligned} h(y_i,s) &= \sum_n f_{h_n}(y_i)\,\xi_n(s) \\ \alpha(y_i,s) &= \sum_n f_{\alpha_n}(y_i)\,\xi_n(s) \end{aligned}\right\} \qquad \text{(E12)}$$

Substitution of equations (E11) and (E12) into equations (E6) to (E10) yields the expressions for the lift and pitching moment on the $i^{th}$ panel in terms of the non-dimensional time, s, and the normal coordinates, $\xi_n(s)$. The expression for the lift on the $i^{th}$ panel is

$$\ell_\phi(y_i,s) = C_{V^2}\rho\left\{\sum_n \left[A^N_{\ell n}(y_i)\,\ddot{\xi}_n(s)+B^N_{\ell n}(y_i)\,\dot{\xi}_n(s)\right] + \int_0^s f_{\ell\phi}(y_i,\sigma)\,\phi'(s-\sigma)\,d\sigma\right\} \qquad \text{(E13)}$$

where the function $f_{\ell\phi}(y_i,s)$ is

$$f_{\ell\phi}(y_i,s) = \sum_n \left[B^C_{\ell n}(y_i)\,\dot{\xi}_n(s) + C^C_{\ell n}(y_i)\,\xi_n(s)\right] \qquad \text{(E14)}$$

## APPENDIX E

The coefficients are defined in terms of the basic data as follows:

$$\left.\begin{aligned} A^N_{\ell n}(y_i) &= \tfrac{1}{2}C(y_i)b(y_i)\,[f_{h_n}(y_i)-b(y_i)a(y_i)f_{\alpha_n}(y_i)] \\ B^N_{\ell n}(y_i) &= \tfrac{1}{2}b_R C(y_i)b(y_i)\,f_{\alpha_n}(y_i) \\ B^C_{\ell n}(y_i) &= b_R C(y_i)\,[f_{h_n}(y_i)-b(y_i)\,[a(y_i)-\tfrac{1}{2}]\,f_{\alpha_n}(y_i)] \\ C^C_{\ell n}(y_i) &= b_R^2\,C(y_i)\,f_{\alpha_n}(y_i) \end{aligned}\right\} \quad \text{(E15)}$$

In a similar manner the pitching moment on the $i^{th}$ panel is

$$t_\phi(y_i,s) = C_V\rho\left\{\sum_n [A^N_{tn}(y_i)\ddot{\xi}_n(s)+B^N_{tn}(y_i)\dot{\xi}_n(s)] + \int_0^s f_{t\phi}(y_i,\sigma)\,\phi'(s-\sigma)\,d\sigma\right\} \quad \text{(E16)}$$

where the function $f_{t\phi}(y_i,s)$ is

$$f_{t\phi}(y_i,s) = \sum_n [B^C_{tn}(y_i)\,\dot{\xi}_n(s) + C^C_{tn}(y_i)\,\xi_n(s)] \quad \text{(E17)}$$

and the coefficients are defined as follows:

$$A^N_{tn}(y_i) = \tfrac{1}{2}\,C(y_i)b^2(y_i)[a(y_i)f_{h_n}(y_i)-b(y_i)\,[a^2(y_i)+1/8]f_{\alpha_n}(y_i)]$$

## APPENDIX E

$$\left.\begin{aligned} B^N_{tn}(y_i) &= \tfrac{1}{2} b_R \, C(y_i) b^2(y_i) \, [a(y_i) - \tfrac{1}{2}] \, f_{\alpha_n}(y_i) \\ B^C_{tn}(y_i) &= - \, b(y_i) \, [c(y_i) - a(y_i)] \, B^C_{\ell n}(y_i) \\ C^C_{tn}(y_i) &= - \, b(y_i) \, [c(y_i) - a(y_i)] C^C_{\ell n}(y_i) \end{aligned}\right\} \quad \text{(E18)}$$

The constant $C_V$ appearing in equations (E13) and (E16) is given by

$$C_V = (V/b_R)^2 (1/g) \quad \text{(E19)}$$

The generalized force in the $m^{th}$ mode due to the $i^{th}$ panel is now defined as

$$q_{rm}(y_i, s) = - \, [\ell_\phi(y_i, s) f_{h_m}(y_i) - t_\phi(y_i, s) f_{\alpha_m}(y_i)] \quad \text{(E20)}$$

The total generalized force may be obtained by summing over the panels,

$$Q_{rm}(s) = \sum_i q_{rm}(y_i, s) \quad \text{(E21)}$$

Note that the index r is assigned the values of 1 and 2 to denote that the generalized force occurs due to wing motion and tail motion, respectively.

The equations developed thus far in this section may be used, if desired, to compute the total generalized forces due to motion. Specifically, equations (E13), (E16), (E20), and (E21) may be combined, and then used to evaluate the

## APPENDIX E

contributions of both the wing and the tail. A more convenient form of these equations, however, may be derived by interchanging the order of summation used thus far, that is, by summing over the panels first and then summing over the modes, rather than vice versa. The wing (r=1) total generalized force may now be expressed in terms of a non-circulatory component, $\Phi_m^{WN}(s)$, and a circulatory component, $\Phi_m^{WC}(s)$, as follows:

$$Q_{1m}(s) = -C_V[\Phi_m^{WN}(s) + \Phi_m^{WC}(s)] \tag{E22}$$

where the non-circulatory contribution to the generalized force is expressed in terms of the first and second derivatives of the normal modes,

$$\Phi_m^{WN}(s) = \sum_n [A_{mn}^{WN} \ddot{\xi}_n(s) + B_{mn}^{WN} \dot{\xi}_n(s)] \tag{E23}$$

and the coefficients $A_{mn}^{WN}$ and $B_{mn}^{WN}$ of the non-circulatory contribution to the generalized force are defined below.

$$A_{mn}^{WN} = \rho \sum_i [A_{\ell n}^N(y_i^W) f_{h_m}(y_i^W) - A_{tn}^N(y_i^W) f_{\alpha_m}(y_i^W)] \tag{E24}$$

$$B_{mn}^{WN} = \rho \sum_i [B_{\ell n}^N(y_i^W) f_{h_m}(y_i^W) - B_{tn}^N(y_i^W) f_{\alpha_m}(y_i^W)] \tag{E25}$$

where the coefficient appearing within the brackets in equations (E24) and (E25) are evaluated from the expressions given by equations (E15) and (E18) based upon the wing properties. The contribution of the circulatory part to the generalized force is given by

$$\Phi_m^{WC}(s) = \int_0^s F_m^W(\sigma)\, \phi_W'(s-\sigma)\, d\sigma \tag{E26}$$

where the forcing function $F_m^W(s)$ is defined in terms of $\dot{\xi}_n(s)$ and $\xi_n(s)$ as follows:

## APPENDIX E

$$F_m^W(s) = \sum_n [B_{mn}^{WC} \dot{\xi}_n(s) + C_{mn}^{WC} \xi_n(s)] \tag{E27}$$

and the coefficients in equation (E27) are given by

$$B_{mn}^{WC} = \rho \sum_i [B_{\ell n}^C(y_i^W) f_{h_m}(y_i^W) - B_{tn}^C(y_i^W) f_{\alpha_m}(y_i^W)] \tag{E28}$$

$$C_{mn}^{WC} = \rho \sum_i [C_{\ell n}^C(y_i^W) f_{h_m}(y_i^W) - C_{tn}^C(y_i^W) f_{\alpha_m}(y_i^W)] \tag{E29}$$

where once again the coefficients appearing on the right hand side of equations (E28) and (E29) are evaluated using equations (E15) and (E18). At this point, use is made of the exponential approximation to the Wagner-type function, given by equation (B15), which is reproduced below.

$$\phi_W(s) = \phi_W(0) + \sum_{k=1}^{K_1} b_k^W (1 - e^{-\beta_k^W s}) \tag{E30}$$

where

$$K_1 \equiv K_\phi^W \tag{E31}$$

The Laplace transform of equations (E26) and (E30) are

$$\bar{\Phi}_m^{WC}(p) = \bar{F}_m^W(p)\ p\ \bar{\phi}_W(p) \tag{E32}$$

$$\bar{\phi}_W(p) = \frac{\phi_W(0)}{p} + \sum_{k=1}^{K_1} \frac{b_k^W \beta_k^W}{p(p+\beta_k^W)} \tag{E33}$$

Now, redefine the Laplace transform given by equation (E32) as follows:

## APPENDIX E

$$\bar{\Phi}_m^{WC}(p) = \bar{\Phi}_{m0}^{W}(p) + \bar{\Phi}_m^{W}(p) \tag{E34}$$

where

$$\bar{\Phi}_m^{W}(p) = \sum_{k=1}^{2} \bar{\Phi}_{mk}^{W}(p) \tag{E35}$$

and the component parts of the Laplace transform in equations (E34) and (E35) are defined by combining equations (E32) and (E33).

$$\bar{\Phi}_{m0}^{W}(p) = \phi_W(0)\ \bar{F}_m^{W}(p) \tag{E36}$$

$$\bar{\Phi}_{mk}^{W}(p) = \frac{b_k^W \beta_k^W}{p+\beta_k^W}\ \bar{F}_m^{W}(p), \qquad k=1,2 \tag{E37}$$

The circulatory contribution to the generalized force is now obtained by taking the inverse Laplace transform of equations (E34) through (E37).

$$\Phi_m^{WC}(s) = \Phi_{m0}^{W}(s) + \Phi_m^{W}(s) \tag{E38}$$

where

$$\Phi_m^{W}(s) = \sum_{k=1}^{2} \Phi_{mk}^{W}(s) \tag{E39}$$

## APPENDIX E

and the component generalized forces on the right side of equations (E38) and (E39) are obtained from the following set of differential equations,

$$\Phi^W_{m0}(s) = \phi_W(0)\ F^W_m(s) \tag{E40}$$

$$\ddot{\Phi}^W_{mk}(s) + \beta^W_k\ \Phi^W_{mk}(s) = b^W_k \beta^W_k F^W_m(s),\ k=1,2 \tag{E41}$$

## APPENDIX E

### II. Tail Motion and Stabilizer Rotation

The generalized forces on an all-movable horizontal tail depend upon tail motion and stabilizer rotation. The expressions for the generalized force contribution due to tail motion will be exactly the same as those for the wing which were developed in section I. Development of the generalized force due to stabilizer rotation may be carried through by following the procedure in section I with certain modifications.

Basic expressions required for evaluating the generalized force due to stabilizer rotation are the panel lift and pitching moment, which in the case of wing motion, are given by equations (E6) and (E7) together with the auxiliary equations (E8) to (E10). These equations may be changed to apply to stabilizer rotation by replacing the vertical and angular displacements and their associated derivatives ($h(y_i,t)$, $\alpha(y_i,t),\ldots$)with the variable representing stabilizer rotation, $\gamma(t)$. If the horizontal tail reference axis, which is the torque tube, is chosen as the stabilizer pivot axis, these changes are equivalent to setting

$$\left.\begin{aligned} h(y_i,t) &\equiv 0 \\ \alpha(y_i,t) &\equiv \gamma(t) \end{aligned}\right\} \qquad \text{(E42)}$$

Introduction of equations (E42) into equations (E6) and (E7) will provide the panel lift and pitching moment due to stabilizer rotation.

$$\ell_\theta(y_i^T,t) = \frac{\rho}{2g}C(y_i^T)\Big\{\, b(y_i^T)\,[V\dot{\gamma}(t)-b(y_i^T)a(y_i^T)\dot{\gamma}(t)] + 2Vf_\theta(y_i^T,t)\Big\} \qquad \text{(E43)}$$

## APPENDIX E

$$t_\theta(y_i^T,t) = \frac{\rho}{2g}C(y_i^T)b(y_i^T)\Big\{\, b(y_i^T)\Big[V[a(y_i^T)-\tfrac{1}{2}]\dot{\gamma}(t)$$

$$-b(y_i^T)\,[\,a^2(y_i^T) + 1/8\,]\ddot{\gamma}(t)\Big]$$

$$-2V\,[\,c(y_i^T)-a(y_i^T)]\;\; f_\theta(y_i^T,t)]\Big\} \qquad \text{(E44)}$$

where

$$C(y_i^T) = \Delta y(y_i^T)b(y_i^T)c_{\ell_\alpha}(y_i^T) \qquad \text{(E45)}$$

$$f_{\dot\theta}(y_i^T,t) = -\int_0^t w_\theta(y_i,\tau)\phi_T'(t-\tau)\,d\tau \qquad \text{(E46)}$$

and the downwash due to stabilizer rotation becomes

$$w_\theta(y_i^T,t) = -\,[\,V\;\gamma(t)-b(y_i^T)\,[\,a(y_i^T)-\tfrac{1}{2}\,]\,\dot{\gamma}(t)] \qquad \text{(E47)}$$

Conversion of the panel lift and pitching moment to non-dimensional time may be accomplished by introducing equations (E11) into equations (E43) to (E47). The panel lift and pitching moment equations, then become, after re-arranging,

$$\ell_\theta(y_i^T,s) = C_V\rho\Big\{\, C(y_i^T)\,\frac{b(y_i^T)}{2}[b_R\dot{\gamma}(s)-b(y_i^T)a(y_i^T)\ddot{\gamma}(s)]$$

$$+\int_0^s f_{\ell\theta}(y_i^T,\sigma)\phi_T'(s-\sigma)\,d\sigma\Big\} \qquad \text{(E48)}$$

## APPENDIX E

$$t_\theta(y_i^T,s) = C_V\rho\left\{ C(y_i^T)\frac{b^2(y_i^T)}{2}\left[b_R\left[a(y_i^T)-\tfrac{1}{2}\right]\dot{\gamma}(s)\right.\right.$$

$$-b(y_i^T)\left[a^2(y_i^T)+1/8\right]\ddot{\gamma}(s)\Big]$$

$$\left.\left.+\int_0^s f_{t\theta}(y_i^T,\sigma)\,\phi_T'(s-\sigma)\,d\sigma\right\}\right. \qquad \text{(E49)}$$

where

$$f_{\ell\theta}(y_i^T,s) = b_R C(y_i^T)\left[b_R\gamma(s)-b(y_i^T)\left[a(y_i^T)-\tfrac{1}{2}\right]\dot{\gamma}(s)\right] \qquad \text{(E50)}$$

and

$$f_{t\theta}(y_i^T,s) = -b_R C(y_i^T)b(y_i^T)\left[c(y_i^T)-a(y_i^T)\right]\left[b_R\gamma(s)\right.$$

$$\left.-b(y_i^T)\left[a(y_i^T)-\tfrac{1}{2}\right]\dot{\gamma}(s)\right] \qquad \text{(E51)}$$

The generalized force due to tail motion and stabilizer rotation (r=2) in the $m^{th}$ mode due to the $i^{th}$ panel is now defined as

$$q_{2m}(y_i^T,\ s) = -\left[\ell_\phi^T(y_i^T,s)f_{h_m}(y_i^T)-t_\phi^T(y_i^T,s)f_{\alpha_m}(y_i^T)\right]$$

$$-\left[\ell_\theta(y_i^T,s)f_{h_m}(y_i^T)-t_\theta(y_i^T,s)f_{\alpha_m}(y_i^T)\right] \qquad \text{(E52)}$$

where the first bracket on the right side of equation (E52) is similar to equation (E20), based on the tail properties, and the second bracket is the contribution of the stabilizer rotation. The variables, $\ell_\phi^T(y_i^T,s)$ and $t_\phi^T(y_i^T,s)$, are given in equations (E13) and (E16).

## APPENDIX E

The total generalized force due to tail motion and stabilizer rotation is obtained by summing over the panels.

$$Q_{2m}(s) = \sum_i q_{2m}(y_i^T, s) \tag{E53}$$

Following the procedure of section I the tail total generalized force may now be expressed in terms of a non-circulatory component, $\Phi_m^{TN}(s)$, and a circulatory component, $\Phi_m^{TC}(s)$, in a manner similar to equation (E22).

$$Q_{2m}(s) = -C_V[\Phi_m^{TN}(s) + \Phi_m^{TC}(s)] \tag{E54}$$

The non-circulatory contribution to the generalized force is given by

$$\Phi_m^{TN}(s) = \sum_n [A_{mn}^{TN} \overset{\circ\circ}{\xi}_n(s) + B_{mn}^{TN} \overset{\circ}{\xi}_n(s)]$$

$$+ A_{m\gamma}^{TN} \overset{\circ\circ}{\gamma}(s) + B_{m\gamma}^{TN} \overset{\circ}{\gamma}(s) \tag{E55}$$

The circulatory contribution to the generalized force is

$$\Phi_m^{TC}(s) = \Phi_{m0}^T(s) + \Phi_m^T(s) \tag{E56}$$

where

$$\Phi_m^T(s) = \sum_{k=1}^{2} \Phi_{mk}^T(s) \tag{E57}$$

The component parts of the generalized forces in equations (E56) and (E57) are

$$\Phi_{m0}^T(s) = \phi_T(0)\, F_m^T(s) \tag{E58}$$

$$\overset{\circ}{\Phi}_{mk}^T(s) + \beta_k^T \Phi_{mk}^T(s) = b_k^T \beta_k^T F_m^T(s), \quad k = 1, 2 \tag{E59}$$

where the input to the above equation is

$$F_m^T(s) = \sum_n \left[ B_{mn}^{TC} \dot{\xi}_n(s) + C_{mn}^{TC} \xi_n(s) \right]$$

$$+ B_{m\gamma}^{TC} \dot{\gamma}(s) + C_{m\gamma}^{TC} \gamma(s) \qquad \text{(E60)}$$

The coefficients of $\ddot{\xi}_n(s)$, $\dot{\xi}_n(s)$, and $\xi_n(s)$ in equations (E55) and (E60) are given by expressions similar to equations (E24), (E25), (E28), and (E29) evaluated for the tail.

$$A_{mn}^{TN} = \rho \sum_i \left[ A_{\ell n}^N(y_i^T) f_{h_m}(y_i^T) - A_{tn}^N(y_i^T) f_{\alpha_m}(y_i^T) \right] \qquad \text{(E61)}$$

$$B_{mn}^{TN} = \rho \sum_i \left[ B_{\ell n}^N(y_i^T) f_{h_m}(y_i^T) - B_{tn}^N(y_i^T) f_{\alpha_m}(y_i^T) \right] \qquad \text{(E62)}$$

$$B_{mn}^{TC} = \rho \sum_i \left[ B_{\ell n}^C(y_i^T) f_{h_m}(y_i^T) - B_{tn}^C(y_i^T) f_{\alpha_m}(y_i^T) \right] \qquad \text{(E63)}$$

$$C_{mn}^{TC} = \rho \sum_i \left[ C_{\ell n}^C(y_i^T) f_{h_m}(y_i^T) - C_{tn}^C(y_i^T) f_{\alpha_m}(y_i^T) \right] \qquad \text{(E64)}$$

Finally, the coefficients of $\ddot{\gamma}(s)$, $\dot{\gamma}(s)$, and $\gamma(s)$ are given by

$$A_{m\gamma}^{TN} = \frac{\rho}{2} \sum_i \Big\{ C(y_i^T) b^2(y_i^T) \Big[ -a(y_i^T) f_{h_m}(y_i^T)$$

$$+ b(y_i^T) \left[ a^2(y_i^T) + 1/8 \right] f_{\alpha_m}(y_i^T) \Big] \Big\} \qquad \text{(E65)}$$

$$B_{m\gamma}^{TN} = \rho \frac{b_R}{2} \sum_i \Big\{ C(y_i^T) b(y_i^T) \Big[ f_{h_m}(y_i^T) - b(y_i^T) \left[ a(y_i^T) - \tfrac{1}{2} \right] f_{\alpha_m}(y_i^T) \Big] \Big\} \qquad \text{(E66)}$$

## APPENDIX E

$$B^{TC}_{m\gamma} = -\rho b_R \sum_i \left\{ C(y_i^T) b(y_i^T) [a(y_i^T) - \tfrac{1}{2}] \left[ f_{h_m}(y_i^T) + b(y_i^T) [c(y_i^T) - a(y_i^T)] f_{\alpha_m}(y_i^T) \right] \right\} \quad \text{(E67)}$$

$$C^{TC}_{m\gamma} = \rho b_R^2 \sum_i \left\{ C(y_i^T) \left[ f_{h_m}(y_i^T) + b(y_i^T) [c(y_i^T) - a(y_i^T)] f_{\alpha_m}(y_i^T) \right] \right\} \quad \text{(E68)}$$

Note that equations (E65) to (E68) may be obtained directly from equations (E61) to (E64) by changing the mode index n to $\gamma$ on the left hand side of these equations and substituting equations (E15) and (E18) together with the following equivalent of equation (E42).

$$\left.\begin{aligned} f_{h_n}(y_i^T) &\equiv 0 \\ f_{\alpha_n}(y_i^T) &\equiv 1 \end{aligned}\right\} \quad \text{(E69)}$$

## APPENDIX E

### III. Downwash on the Tail Due to Wing Motion

For a two dimensional wing executing plunging and pitching motion, the angle of attack governing the circulatory lift on the wing, and hence the strength of the vortices shed from the trailing edge, is determined by the planform downwash at the three-quarter-chord point given by equation (E4) and repeated below.

$$w_{\phi}^{W}(t) = -[\dot{h}(t) + V\alpha(t) + b(\tfrac{1}{2} - a)\dot{\alpha}(t)] \tag{E70}$$

In calculating the downwash at the tail due to wing motion, a spanwise station is chosen as a reference, and the downwash at this station is assumed to apply across the entire span of the tail. If the tail mean aerodynamic chord, $y_{mac}^{T}$, is chosen as the reference spanwise station for calculating downwash, equation (E70) when applied to this particular station becomes

$$w_{\phi}^{W}(y_{mac}^{T},t) = -\Big[\dot{h}_{W}(y_{mac}^{T},t) + V\alpha_{W}(y_{mac}^{T},t) - b_{W}(y_{mac}^{T})[a_{W}(y_{mac}^{T})-\tfrac{1}{2}]\dot{\alpha}_{W}(y_{mac}^{T},t)\Big] \tag{E71}$$

The downwash at the tail due to wing motion, assuming instantaneous downwash build up, is given by

$$w_{\delta}(t) = \left|\frac{\partial\varepsilon}{\partial\alpha}\right| w_{\phi}^{W}(y_{mac}^{T}, t-t_{M}) \tag{E72}$$

where $t_{M}$ accounts for the time delay between the wing motion and the assumed start of lift build up on the tail.

Vortices due to flexible motion are assumed to be dissipated by viscous effects before reaching the tail; therefore, only rigid-body wing motion is considered in

## APPENDIX E

evaluating the downwash at the tail as given by equation (E71). The vertical and angular deflections at the wing reference axis are expressed in terms of the mode shapes and normal coordinates in a manner similar to equations (E12), where the summation is carried out for the rigid-body modes only.

$$\left.\begin{aligned} h_W(y^T_{mac},s) &= \sum_{n=1}^{2} f^W_{h_n}(y^T_{mac})\xi_n(s) \\ \alpha_W(y^T_{mac},s) &= \sum_{n=1}^{2} f^W_{\alpha_n}(y^T_{mac})\xi_n(s) \end{aligned}\right\} \qquad \text{(E73)}$$

Substitution of equations (E73) into equation (E71) and introduction of the non-dimensional time, s, into equations (E71) and (E72) results in the following relationships.

$$w^W_\phi(y^T_{mac},s) = -\frac{V}{b_R}\sum_{n=1}^{2}\Big\{\Big[f^W_{h_n}(y^T_{mac}) - b_W(y^T_{mac})[a_W(y^T_{mac})-\tfrac{1}{2}]f^W_{\alpha_n}(y^T_{mac})\Big]\dot{\xi}_n(s) + b_R f^W_{\alpha_n}(y^T_{mac})\xi_n(s)\Big\} \qquad \text{(E74)}$$

$$w_\delta(s) = \left|\frac{\partial\varepsilon}{\partial\alpha}\right| w^W_\phi(y^T_{mac}, s-s_M) \qquad \text{(E75)}$$

The lift build up on the tail is evaluated based on strip theory, where it is assumed that the lift build up on each tail panel is given by the tail Küssner-type function with $\psi_T(0) = 0$ (see equation (B10)). The lift on each

## APPENDIX E

panel is given in terms of Duhamel's integral by the following expressions.

$$\ell_\delta(y_i^T, s) = \frac{\rho}{2g} V^2 [2C(y_i^T)] f_\delta(s-\sigma(y_i^T)) \tag{E76}$$

where

$$C(y_i^T) = \Delta y(y_i^T) b(y_i^T) c_{\ell_\alpha}(y_i^T) \tag{E77}$$

$$f_\delta(s) = \int_0^s \frac{w_\delta(\sigma)}{V} \psi_T'(s-\sigma)\, d\sigma \tag{E78}$$

The panel pitching moment about the reference axis of the $i^{th}$ panel is given in terms of the $i^{th}$ panel lift as follows:

$$t_\delta(y_i^T, s) = -b(y_i^T)[c(y_i^T) - a(y_i^T)] \ell_\delta(y_i^T, s) \tag{E79}$$

The $i^{th}$ panel generalized force due to downwash on the tail caused by wing motion (r = 3) is given by

$$q_{3m}(y_i^T, s) = -[\ell_\delta(y_i^T, s) f_{h_m}(y_i^T) - t_\delta(y_i^T, s) f_{\alpha_m}(y_i^T)] \tag{E80}$$

and the total generalized force may now be evaluated from equation (E80) by summing over the panels according to the following relationship,

$$Q_{3m}(s) = \sum_i q_{3m}(y_i^T, s) \tag{E81}$$

A more useful form of the generalized force is obtained by combining equations (E76) and (E78) to (E81).

## APPENDIX E

$$Q_{3m}(s) = -C_V[\rho b_R^2 \, P_m^T(\infty)]\Sigma_i[\frac{p_m(y_i^T,\infty)}{P_m^T(\infty)} \, f_\delta(s-\sigma(y_i^T))] \quad \text{(E82)}$$

where the constants $p_m(y_i^T,\infty)$ and $P_m^T(\infty)$ are evaluated using equations (C7) and (C11), and $f_\delta(s)$ is given by equation (E78). Now, combining equations (E78) and (E82) and rearranging the terms results in the following expressions.

$$Q_{3m}(s) = -C_V D_m^M \Delta_m^M(s) \quad \text{(E83)}$$

where the constant $D_m^M$ is given by

$$D_m^M = \frac{\rho}{V} \, b_R^2 \, P_m^T(\infty) = -D_m^T \quad \text{(E84)}$$

and the generalized force variation, $\Delta_m^M(s)$, is given by Duhamel's integral in terms of the downwash due to wing motion, $w_\delta(s)$, and the indicial generalized force function, $\delta_m^M(s)$.

$$\Delta_m^M(s) = \int_0^s w_\delta(\sigma)\delta_m^{M'}(s-\sigma)\,d\sigma \quad \text{(E85)}$$

where the function $\delta_m^M(s)$ is given by the following basic expression,

$$\delta_m^M(s) = \sum_{i=1}^{I_T} \left[ \frac{p_m(y_i^T,\infty)}{P_m^T(\infty)} \; \delta_M(s-\sigma(y_i^T)) \right] \quad \text{(E86)}$$

Note that $\delta_M(s)$ is given by equation (B21).
Use of the analytical approximation to equation (E86) as given by equation (C17) permits an evaluation of the integral

## APPENDIX E

given by equation (E85) along the same lines as the evaluation of equation (D8). Therefore, the final form of the generalized force variation due to downwash on the tail caused by wing motion will be given by an expression similar to equation (D17).

$$\left.\begin{aligned} \Delta^M_m(s) &= \sum_{k=0}^{3} \Delta^M_{mk}(s) \qquad \text{for } m = 1 \\ \Delta^M_m(s) &= \Delta^M_1(s) \qquad 2 \le m \le N \end{aligned}\right\} \tag{E87}$$

Note, however, that since the tail is assumed rigid, and hence the tail indicial generalized force functions are nearly independent of mode (as discussed in Appendix C), it only is necessary to evaluate the generalized force for the first mode. The component parts of the first mode generalized force are evaluated using the following set of differential equations.

$$\Delta^M_{10}(s) = \delta_M(0) F_M(s-s_M), \qquad \text{for } k = 0 \tag{E88}$$

$$\dot{\Delta}^M_{1k}(s) + \alpha^M_{1k}\Delta_{1k}(s) = a^M_{1k}\alpha^M_{1k}F_M(s-s_M), \qquad \text{for } k = 1, 2 \tag{E89}$$

$$\ddot{\Delta}^M_{1k}(s) + 2\alpha^M_{1k}\dot{\Delta}^M_{1k}(s) + [(\alpha^M_{1k})^2 + (\omega^M_{1k})^2]\Delta^M_{1k}(s) = [a^M_{1k}\alpha^M_{1k} - b^M_{1k}\omega^M_{1k}]\dot{F}_M(s-s_M) + a^M_{1k}[(\alpha^M_{1k})^2 + (\omega^M_{1k})^2]F_M(s-s_M) \tag{E90}$$

The expression for the input to equations (E88) to (E90) is given by

$$F_M(s) = \sum_{n=1}^{2} [B^M_n \xi_n(s) + C^M_n \dot{\xi}_n(s)] \tag{E91}$$

## APPENDIX E

where the coefficients in equation (E91) are given by

$$B_n^M = - \left| \frac{\partial \dot{\varepsilon}}{\partial \alpha} \right| \frac{V}{b_R} \left[ f_{h_n}^W(y_{mac}^T) - b_W(y_{mac}^T)[a_W(y_{mac}^T) - \tfrac{1}{2}] f_{\alpha_n}^W(y_{mac}^T) \right] \tag{E92}$$

$$C_n^M = - \left| \frac{\partial \varepsilon}{\partial \alpha} \right| V f_{\alpha_n}^W(y_{mac}^T) \tag{E93}$$

# APPENDIX F

## STRUCTURAL LOADS

### I. Aerodynamic Contributions to the Wing and Tail Structural Loads

#### A. Tail Loads Due to Tail Motion, Stabilizer Rotation, Gust on the Tail, and Downwash

Expressions are developed herein for the aerodynamic contribution to the structural loads at the pivot axis of an all-movable stabilizer at the intersection of the stabilizer and the fuselage side. The lift outboard of the fuselage (tail root chord) is evaluated by the force summation method. The bending moment and torque on the torque tube are then obtained by multiplying this lift by a bending moment arm, $y_0$, and a torque arm, $x_0$, defined in Figure F1.

$$\left.\begin{aligned} S_1^{TA*}(s) &= L_T(s) \\ M_1^{TA}(s) &= y_0 L_T(s) \\ T_1^{TA}(s) &= x_0 L_T(s) \end{aligned}\right\} \qquad (F1)$$

where the function $L_T(s)$ is the tail lift per side based on the surface outboard of the fuselage juncture with the stabilizer pivot axis. This lift consists of the following component parts: lift due to gust on the tail, motion of the tail, stabilizer rotation, and downwash on the tail due to gust on the wing and motion of the wing. In evaluating these components, use is made of the expressions developed in Appendices D and E. Note that the generalized

---

* Note that the subscript 1 used with these functions represents the loads at the tail root and is not to be associated with any panel point index. Also, the letter T represents loads on the tail, and the letter A designates the aerodynamic contributions to the structural loads.

## APPENDIX F

forces in these appendices are based upon a tail area defined between the airplane centerline and tail tip. To evaluate the tail loads, the area outboard of the fuselage is to be utilized. Therefore, the final expression for the tail lift as developed from the generalized forces will be modified to conform to this requirement.

The total tail lift is the negative of the tail contributions to the generalized force for the first mode, that is

$$L_T(s) = -\sum_{r=2}^{5} Q_{r1}(s) \tag{F2}$$

The lift on the tail due to motion of the tail and stabilizer rotation (r=2) is given by equation (E54), which is reproduced below for m = 1.

$$Q_{21}(s) = -C_V \left[\Phi_1^{TN}(s) + \Phi_1^{TC}(s)\right] \tag{F3}$$

where the non-circulatory contribution to the lift is given by equation (E55) and the circulatory contribution is given by equation (E56). The lift on the tail due to downwash as a result of wing motion (r=3) is given by equation (E83), also reproduced here for m = 1.

$$Q_{31}(s) = -C_V D_1^M \Delta_1^M(s) \tag{F4}$$

where the constant $D_1^M$ is the first mode value of $D_m^M$ as given by equation (E84), and the generalized force variation, $\Delta_1^M(s)$, is given by equations (E87) to (E90). The lift on the tail due to downwash as a result of gust on the wing (r=4) is given by equation (D22) for m = 1.

$$Q_{41}(s) = C_V D_1^G \Delta_1^G(s) \tag{F5}$$

where $D_1^G$ is obtained from equations (D23) and (D7) and

## APPENDIX F

$\Delta_1^G(s)$ is given by equations (D24) to (D27). Finally, the lift on the tail due to gust on the tail (r=5) is given by equation (D21) for m = 1.

$$Q_{51}(s) = C_V \, D_1^T \, \Psi_1^T(s) \tag{F6}$$

Note that in equations (F4) to (F6) the following equalities are true between the constants $D_1$.

$$\left.\begin{aligned} D_1^G &= D_1^T \\ D_1^M &= -D_1^T \end{aligned}\right\} \tag{F7}$$

Equations (F2) to (F7) are now combined to provide the final expression for the lift on the tail based on an area between the airplane centerline and tail tip.

$$L_A(s) = C_V \left\{ [\Phi_1^{TN}(s) + \Phi_1^{TC}(s)] - D_1^T[\Delta_1^M(s) + \Delta_1^G(s) + \Psi_1^T(s)] \right\} \tag{F8}$$

Expression (F8) may now be modified to represent the tail lift outboard of the fuselage as follows. First, the constant $(-D_1^T)$ is replaced by the symbol $V_2$ which is defined by an expression similar to equation (D7) but for which $P_1(\infty)$ as given by equation (C11) is defined by a summation over only the area outboard of the fuselage. If the panel bounded by the airplane centerline and fuselage side (see Figure F1) is designated as the first panel in the development of the tail generalized forces, the evaluation of $V_2$ will be obtained by a summation starting from the second panel and ending with the maximum tail panel, $I_T$, as follows:

$$V_2 = \frac{\rho}{V} b_R^2 \sum_{i=2}^{I_T} p_1(y_i^T, \infty) \tag{F9}$$

## APPENDIX F

where the constant $p_1(y_i^T, \infty)$ is given by equation (C7) for the first mode (m=1), in which case $f_{h_1}(y_i^T) = 1$ and $f_{\alpha_1}(y_i^T) = 0$. Next, the generalized force variations $\Delta_1^M(s)$, $\Delta_1^G(s)$, and $\Psi_1^T(s)$, which actually are based upon a tail area extending from the airplane centerline to the tail tip, are assumed to also be applicable to the tail area outboard of the fuselage side. Finally, the non-circulatory, $\Phi_1^{TN}(s)$, and circulatory, $\Phi_1^{TC}(s)$, functions due to tail motion and stabilizer rotation, as given by equations (E55) to (E68), are modified to include only the area from the fuselage side to the tail tip. The procedure will be to express the non-circulatory contributions $\Phi_1^{TN}(s)$, and $\Phi_{10}^T(s)$ components of the circulatory contributions in terms of the normal coordinates, $\xi_n(s)$, and the coefficients which will now be based upon a tail area outboard of the fuselage. The $\Phi_{1k}^T(s)$ components will be evaluated as before, but will be multiplied by the constant,

$$V_1 = \left[\sum_{i=2}^{I_T} p_1(y_i^T, \infty)\right] / \left[\sum_{i=1}^{I_T} p_1(y_i^T, \infty)\right] \qquad \text{(F10)}$$

The final expression for the tail lift based on an area outboard of the fuselage is

$$L_T(s) = C_V \, \ell_T(s) \qquad \text{(F11)}$$

where

$$\begin{aligned} \ell_T(s) = & \sum_{n=1}^{N} \left[A_n^{T\infty} \xi_n(s) + B_n^{T\bullet} \xi_n(s) + C_n^T \xi_n(s)\right] \\ & + A_\gamma^T \, \ddot{\gamma}^\circ(s) + B_\gamma^T \, \dot{\gamma}(s) + C_\gamma^T \, \gamma(s) \\ & + V_1 \sum_{k=1}^{2} \Phi_{1k}^T(s) + V_2 \sum_{k=0}^{3} \left[\Delta_{1k}^M(s) + \Delta_{1k}^G(s) + \Psi_{1k}^T(s)\right] \end{aligned} \qquad \text{(F12)}$$

## APPENDIX F

The coefficients $A_n^T$, $B_n^T$, $C_n^T$, $A_\gamma^T$, $B_\gamma^T$, and $C_\gamma^T$ appearing in equation (F12) are obtained from equations (E61) to (E68) for m = 1, except that the summations are now performed only over the outboard $(I_T-1)$ panels. The final expressions for the coefficients are

$$A_n^T = \rho \sum_{i=2}^{I_T} A_{\ell n}^N(y_i^T) \tag{F13}$$

$$B_n^T = \rho \sum_{i=2}^{I_T} [B_{\ell n}^N(y_i^T) + \phi_T(0) B_{\ell n}^C(y_i^T)] \tag{F14}$$

$$C_n^T = \rho \phi_T(0) \sum_{i=2}^{I_T} C_{\ell n}^C(y_i^T) \tag{F15}$$

$$A_\gamma^T = -\frac{\rho}{2} \sum_{i=2}^{I_T} C(y_i^T) b^2(y_i^T) a(y_i^T) \tag{F16}$$

$$B_\gamma^T = \frac{\rho}{2} b_R \sum_{i=2}^{I_T} C(y_i^T) b(y_i^T) \left[ 1 - 2\phi_T(0) [a(y_i^T) - \tfrac{1}{2}] \right] \tag{F17}$$

$$C_\gamma^T = \rho b_R^2 \phi_T(0) \sum_{i=2}^{I_T} C(y_i^T) \tag{F18}$$

where

$$C(y_i^T) = \Delta y(y_i^T) b(y_i^T) c_{\ell_\alpha}(y_i^T) \tag{F19}$$

## APPENDIX F

### B. Wing Loads Due to Wing Motion and Gust on the Wing

The mode acceleration method, discussed in References 15 and 17, is used in evaluating the wing structural loads due to wing motion and gust on the wing. The total structural loads are due to the inertial contributions (developed subsequently in Section IIA) and the aerodynamic contributions caused by wing motion and gust on the wing which are developed in this section. The assumption is made that the wing airloads associated with the response of the aircraft to the gust may be described in terms of the rigid-wing airload distribution required to produce the previously computed rigid-body vertical acceleration.

As the first step in the development of the wing structural load equations based on the mode acceleration method, a wing-induced rigid-body acceleration, $\ddot{\xi}_{1W}(t)$, is defined in terms of the airplane rigid-body acceleration, $\ddot{\xi}_1(t)$. For this purpose, the acceleration due to the tail lift is defined by dividing the tail lift by the airplane mass. This "tail-induced" vertical acceleration is then subtracted from the airplane acceleration to yield "wing-induced" acceleration.

$$\ddot{\xi}_{1W}(t) = \ddot{\xi}_1(t) - \left[-\frac{L_A(t)}{M_{11}/g}\right] \qquad \text{(F20)}$$

The tail lift outboard of the center line, $L_A(t)$, is evaluated from equations (F10) and (F11) as

$$L_A(t) = V_0 L_T(t) \qquad \text{where} \qquad V_0 = 1/V_1$$

The negative sign within the brackets arises from the fact that lift is defined as positive up whereas acceleration is defined as positive down. Finally, equation (F20) is

## APPENDIX F

rearranged as follows:

$$\frac{\ddot{\xi}_{1W}(t)}{g_a} = \left[ \frac{\ddot{\xi}_1(t)}{g} + \frac{L_A(t)}{M_{11}} \right] \frac{g}{g_a} \tag{F21}$$

where the acceleration constant, $g_a$, is introduced to non-dimensionalize each term.

The aerodynamic contributions to the wing structural loads are now defined in terms of "aerodynamic loading coefficients", which are the structural loads associated with the rigid-wing airload distribution required to produce a one "$g_a$" upward acceleration of 32.2 feet per second square. The shear (positive up) and bending moment (positive for compression in the top skin) at the $i^{th}$ load point may be expressed in terms of these coefficients and the wing-induced acceleration, $\ddot{\xi}_{1W}(t)$, as

$$S_i^{WA}(t) = -c_a^{\overline{S}}(Y_i) \frac{\ddot{\xi}_{1W}(t)}{g_a} \tag{F22}$$

$$M_i^{WA}(t) = -c_a^{\overline{M}}(Y_i) \frac{\ddot{\xi}_{1W}(t)}{g_a} \tag{F23}$$

where the negative signs arise from the opposite definition of the aerodynamic loading coefficients and direction of positive acceleration. The torque (positive nose up) may also be expressed in a form similar to equations (F22) and (F23). It is assumed that the aerodynamic loading coefficients for the torque are given about an arbitrary axis perpendicular to the airplane centerline, and that it is desired to calculate the torque about the reference axis. The torque about a perpendicular axis at the $i^{th}$ load point is given in terms of the known aerodynamic loading coefficient, $c_a^{\overline{T}}(Y_i, X_{PA})$, and the wing-induced

## APPENDIX F

acceleration as

$$t_A(Y_i, X_{PA}, t) = -c_a^T(Y_i, X_{PA}) \frac{\ddot{\xi}_{1W}(t)}{g_a} \qquad \text{(F24)}$$

Note that equations (F22) to (F24) reduce to the aerodynamic loading coefficients in the case where $\ddot{\xi}_{1W}(t) = -g_a$. To convert equation (F24) to the torque about the reference axis, use is made of Figure F2 in which the planform is divided into a number of panels. The torque at the $i^{th}$ load point about the perpendicular axis may be expressed in terms of the sum of the panel airloads, $f_A(\upsilon_j, t)$, outboard of the $i^{th}$ load point.

$$t_A(Y_i, X_{PA}, t) = -\sum_{j=i}^{J} \left\{ (\zeta_j - X_{PA}) f_A(\upsilon_j, t) \right\} \qquad \text{(F25)}$$

where the negative sign is due to the fact that an up load produces a nose-down torque. The torque about a point on the reference axis may also be obtained by summing up the torques outboard of the $i^{th}$ load point.

$$t_A(Y_i, X_i, t) = -\sum_{j=i}^{J} \left\{ (\zeta_j - X_i) f_A(\upsilon_j, t) \right\}$$

$$= -\sum_{j=i}^{J} \left\{ [(\zeta_j - X_{PA}) - (X_i - X_{PA})] f_A(\upsilon_j, t) \right\} \qquad \text{(F26)}$$

Equations (F25) and (F26) are combined and rearranged as follows,

$$t_A(Y_i, X_i, t) = t_A(Y_i, X_{PA}, t) + (X_i - X_{PA}) \sum_{j=i}^{J} f_A(\upsilon_j, t) \qquad \text{(F27)}$$

It is noted that the shear at the $i^{th}$ load point is given by

## APPENDIX F

$$S_i^{WA}(t) = \sum_{j=i}^{J} f_A(\upsilon_j, t) \tag{F28}$$

Equations (F22), (F24), (F27), and (F28) are now combined.

$$t_A(Y_i, X_i, t) = -[c_a^{\overline{T}}(Y_i, X_{PA}) + (X_i - X_{PA}) c_a^{\overline{S}}(Y_i)] \frac{\ddot{\xi}_{1W}(t)}{g_a} \tag{F29}$$

For brevity define the following identity,

$$T_i^{WA}(t) \equiv t_A(Y_i, X_i, t) \tag{F30}$$

Therefore, the final expression for the torque about the reference axis becomes

$$T_i^{WA}(t) = -[c_a^{\overline{T}}(Y_i, X_{PA}) + (X_i - X_{PA}) c_a^{\overline{S}}(Y_i)] \frac{\ddot{\xi}_{1W}(t)}{g_a} \tag{F31}$$

The equations for the shear, bending moment and torque at the elastic axis may be converted to the non-dimensional time, s, by use of equations (E11). The functions $L_A(t)$, $S_i^{WA}(t)$, $M_i^{WA}(t)$, and $T_i^{WA}(t)$ are expressed as $L_A(s)$, $S_i^{WA}(s)$, $M_i^{WA}(s)$ and $T_i^{WA}(s)$ after conversion from t to s. Equations (F22), (F23), and (F31) become after rearranging terms

$$\left.\begin{aligned} S_i^{WA}(s) &= \frac{g}{g_a} A_{ia}^{\overline{S}} \ddot{\xi}_{1W}(s) \\ M_i^{WA}(s) &= \frac{g}{g_a} A_{ia}^{\overline{M}} \ddot{\xi}_{1W}(s) \\ T_i^{WA}(s) &= \frac{g}{g_a} A_{ia}^{\overline{T}} \ddot{\xi}_{1W}(s) \end{aligned}\right\} \tag{F32}$$

where

$$\frac{g}{g_a} = 1 \frac{\text{pounds(mass)}}{\text{pounds(force)}}$$

## APPENDIX F

$$\left.\begin{aligned} A_{ia}^{\overline{S}} &= -C_V\, c_a^{\overline{S}}\,(Y_i) \\ A_{ia}^{\overline{M}} &= -C_V\, c_a^{\overline{M}}\,(Y_i) \\ A_{ia}^{\overline{T}} &= -C_V[\, c_a^{\overline{T}}(Y_i, X_{PA}) + (X_i - X_{PA}) c_a^{\overline{S}}(Y_i)\,] \end{aligned}\right\} \qquad \text{(F33)}$$

and the constant $C_V$ is given by equation (E19). The function $\overset{\circ\circ}{\xi}_{1W}(s)$ is similar in form to equation (F20) and is given below as

$$\left.\begin{aligned} \overset{\circ\circ}{\xi}_{1W}(s) &= \overset{\circ\circ}{\xi}_1(s) + \frac{V_0 L_T(s)}{C_V \overline{M}_{11}} \\ &= \overset{\bullet\bullet}{\xi}_1(s) + \frac{V_0 \ell_T(s)}{M_{11}} \end{aligned}\right\} \qquad \text{(F34)}$$

where the first expression is combined with equation (F11) to obtain the second expression.

# APPENDIX F

## II. Inertial Contributions to the Wing and Tail Structural Loads

### A. Wing and Tail Structural Loads Due to Motion

Whether the mode-acceleration or force-summation method is used in evaluating the total structural loads, the contribution of the inertial loads is formulated in the manner discussed below. The airfoil surfaces are subdivided into a number of chordwise strips or panels, which is not necessarily the same total number of panels as that used in the development of the generalized forces. The notation used in evaluating the inertial contributions to the total structural loads is shown in Figure F3. The vertical displacement of the $j^{th}$ panel center of gravity, $z(\bar{y}_j,t)$, positive down is given in terms of the vertical, $h(\bar{y}_j,t)$, and angular, $\alpha(\bar{y}_j,t)$, deflections at the reference axis by the following expression.

$$z(\bar{y}_j,t) = h(\bar{y}_j,t)+(\bar{x}_j-\bar{\chi}_j)\alpha(\bar{y}_j,t) \tag{F35}$$

The acceleration of the $j^{th}$ panel center of gravity is obtained from equation (F35) by taking the derivative with respect to real time, t.

$$\ddot{z}(\bar{y}_j,t) = \ddot{h}(\bar{y}_j,t)+(\bar{x}_j-\bar{\chi}_j)\ddot{\alpha}(\bar{y}_j,t) \tag{F36}$$

The incremental inertial load, $f_I(\bar{y}_j,t)$, on the $j^{th}$ panel due to a positive acceleration acting down is equal to the product of the panel mass, $m(\bar{y}_j)/g$, and the acceleration, $\ddot{z}(\bar{y}_j,t)$ where $m(\bar{y}_j)$ is given in pound mass units.

$$f_I(\bar{y}_j,t) = \frac{m(\bar{y}_j)}{g}[\ddot{h}(\bar{y}_j,t)+(\bar{x}_j-\bar{\chi}_j)\ddot{\alpha}(\bar{y}_j,t)] \tag{F37}$$

If an unbalance about the reference axis is defined as

$$s(\bar{y}_j,\bar{\chi}_j) = m(\bar{y}_j)(\bar{x}_j-\bar{\chi}_j) \tag{F38}$$

## APPENDIX F

where the unbalance is positive for a center of gravity location aft of the reference axis, equation (F37) becomes

$$f_I(\bar{y}_j,t) = \frac{1}{g}[m(\bar{y}_j)\ddot{h}(\bar{y}_j,t) + s(\bar{y}_j,\bar{x}_j)\ddot{\alpha}(\bar{y}_j,t)] \qquad (F39)$$

The vertical and angular accelerations may be expressed in terms of the contributions of the normal modes and converted from the real time independent variable, t, to the non-dimensional time, s, through the expressions

$$h(\bar{y}_j,t) = \sum_n f_{h_n}(\bar{y}_j)\xi_n(t) \qquad (F40)$$

$$\alpha(\bar{y}_j,t) = \sum_n f_{\alpha_n}(\bar{y}_j)\xi_n(t) \qquad (F41)$$

and equations (E11). The $j^{th}$ panel incremental inertial load, after combining equations (F39) through (F41) and equation (E11), becomes

$$f_I(\bar{y}_j,s) = C_V \sum_n [m(\bar{y}_j)f_{h_n}(\bar{y}_j) + s(\bar{y}_j,\bar{x}_j)f_{\alpha_n}(\bar{y}_j)]\ddot{\xi}_n(s) \qquad (F42)$$

where $C_V$ is given by equation (E19).

The incremental wing shear (positive up) at the $i^{th}$ load point is evaluated by summing the contributions, $f_I(\bar{y}_j,s)$, of all the panels outboard of the $i^{th}$ load point.

$$S_i^{WI}(s) = \sum_{j=i}^{J_W} f_I(\bar{y}_j^W,s) = C_V \sum_n A_{in}^{W\bar{S}}\ddot{\xi}_n(s) \qquad (F43)$$

where

$$A_{in}^{W\bar{S}} = \sum_{j=i}^{J_W} [m(\bar{y}_j^W)f_{h_n}(\bar{y}_j^W) + s(\bar{y}_j^W,\bar{x}_j^W)f_{\alpha_n}(\bar{y}_j^W)] \qquad (F44)$$

## APPENDIX F

and the letter W used as subscript or superscript designates the wing.

The incremental wing bending moment (positive for compression in the top surface) at the $i^{th}$ load point is dependent upon the summation of the incremental load, $f_I(\bar{y}_j,s)$, times the moment arm, $(\bar{y}_j-Y_i)$, outboard of the $i^{th}$ load point.

$$M_i^{WI}(s) = \sum_{j=i}^{J_W} f_I(\bar{y}_j^W,s)(\bar{y}_j^W-Y_i^W) = C_V \sum_n A_{in}^{W\bar{M}} \ddot{\xi}_n(s) \qquad (F45)$$

where

$$A_{in}^{W\bar{M}} = \sum_{j=i}^{J_W} [m(\bar{y}_j^W)f_{h_n}(\bar{y}_j^W) + s(\bar{y}_j^W,\bar{x}_j^W)f_{\alpha_n}(\bar{y}_j^W)][\bar{y}_j^W-Y_i^W] \qquad (F46)$$

The incremental torque (positive for nose-up) about an axis perpendicular to the airplane centerline which intersects the elastic axis at the $i^{th}$ load point is given by

$$T_i^I(s) = \sum_{j=i}^{J} [-(\bar{x}_j-X_i)f_I(\bar{y}_j,s) + t_I(\bar{y}_j,\bar{x}_j,s)] \qquad (F47)$$

where $t_I(\bar{y}_j,\bar{x}_j,s)$, the contribution of the $j^{th}$ panel due to the angular acceleration, $\ddot{\alpha}(\bar{y}_j,s)$, is given in terms of the center-of-gravity moment of inertia and the aforementioned acceleration as

$$t_I(\bar{y}_j,\bar{x}_j,s) = -C_V i(\bar{y}_j,\bar{x}_j)\ddot{\alpha}(\bar{y}_j,s) \qquad (F48)$$

At this time, the center-of-gravity moment of inertia for the $j^{th}$ panel is expressed in terms of the reference-axis moment of inertia, $i(\bar{y}_j,\chi_j)$, as follows,

## APPENDIX F

$$i(\bar{y}_j,\bar{x}_j) = i(\bar{y}_j,\bar{\chi}_j) - m(\bar{y}_j)(\bar{x}_j-\bar{\chi}_j)^2 \qquad \text{(F49)}$$

Also, equation (F47) is rewritten in the form,

$$T_i^I(s) = \sum_{j=i}^{J} [-(\bar{\chi}_j-X_i)f_I(\bar{y}_j,s) - (\bar{x}_j-\bar{\chi}_j)f_I(\bar{y}_j,s) + t_I(\bar{y}_j,\bar{x}_j,s)] \qquad \text{(F50)}$$

The final expression for the inertial contribution to the wing incremental torque at the $i^{th}$ load point is obtained by combining equations (F38), (F40) to (F42), and (F48) to (F50) and (E11).

$$T_i^{WI}(s) = C_V \sum_n A_{in}^{W\bar{T}} \xi_n(s) \qquad \text{(F51)}$$

where

$$A_{in}^{W\bar{T}} = -\sum_{j=i}^{J_W}\Big\{\Big[s(\bar{y}_j^W,\bar{\chi}_j^W)f_{h_n}(\bar{y}_j^W) + i(\bar{y}_j^W,\bar{\chi}_j^W)f_{\alpha_n}(\bar{y}_j^W)\Big] + [m(\bar{y}_j^W)f_{h_n}(\bar{y}_j^W) + s(\bar{y}_j^W,\bar{\chi}_j^W)f_{\alpha_n}(\bar{y}_j^W)][\bar{\chi}_j^W-X_i^W]\Big\} \qquad \text{(F52)}$$

Note that in the case where the reference axis is perpendicular to the airplane centerline, that is $\bar{\chi}_j^W = X_i^W$ for $i \le j \le J_W$, the second term in equation (F52) drops out.

For the tail loads, which are calculated at only a single point, the torque-tube fuselage juncture, the expressions are

## APPENDIX F

$$S_1^{TI}(s) = C_V \sum_n A_{1n}^{T\bar{S}} \ddot{\xi}_n(s) \tag{F53}$$

$$M_1^{TI}(s) = C_V \sum_n A_{1n}^{T\bar{M}} \ddot{\xi}_n(s) \tag{F54}$$

$$T_1^{TI}(s) = C_V \sum_n A_{1n}^{T\bar{T}} \ddot{\xi}_n(s) \tag{F55}$$

The coefficients appearing in equations (F53) to (F55) are given by expressions similar to equations (F44), (F46) and (F52), where in equation (F52) the second term drops out if the tail reference axis (torque tube) is perpendicular to the airplane center line as is assumed herein.

$$A_{1n}^{T\bar{S}} = \sum_{j=2}^{J_T} [m(\bar{y}_j^T) f_{h_n}(\bar{y}_j^T) + s(\bar{y}_j^T, \bar{x}_j^T) f_{\alpha_n}(\bar{y}_j^T)] \tag{F56}$$

$$A_{1n}^{T\bar{M}} = \sum_{j=2}^{J_T} [m(\bar{y}_j^T) f_{h_n}(\bar{y}_j^T) + s(\bar{y}_j^T, \bar{x}_j^T) f_{\alpha_n}(\bar{y}_j^T)](\bar{y}_j^T - Y_1^T) \tag{F57}$$

where $Y_1^T$ represents the fuselage station of the intersection of the torque tube.

$$A_{1n}^{T\bar{T}} = -\sum_{j=2}^{J_T} [s(\bar{y}_j^T, \bar{x}_j^T) f_{h_n}(\bar{y}_j^T) + i(\bar{y}_j^T, \bar{x}_j^T) f_{\alpha_n}(\bar{y}_j^T)] \tag{F58}$$

### B. Tail Loads Due to Stabilizer Rotation

The expressions for the inertial contributions to the tail structural loads due to stabilizer rotation will be

## APPENDIX F

similar to equations (F53) to (F55) with the variable $\overset{\infty}{\xi}_n(s)$ being replaced by $\overset{\circ\circ}{\gamma}(s)$.

$$S_1^{SI}(s) = C_V A_{1\gamma}^{T\bar{S}} \overset{\infty}{\gamma}(s) \tag{F59}$$

$$M_1^{SI}(s) = C_V A_{1\gamma}^{T\bar{M}} \overset{\infty}{\gamma}(s) \tag{F60}$$

$$T_1^{SI}(s) = C_V A_{1\gamma}^{T\bar{T}} \overset{\circ\circ}{\gamma}(s) \tag{F61}$$

where the coefficients in the above equations may be evaluated from equations (F56) to (F58) with the following values for the mode shapes,

$$\left.\begin{aligned} f_{h_n}(\bar{y}_j^T) &= 0 \\ f_{\alpha_n}(\bar{y}_j^T) &= 1 \end{aligned}\right\} \tag{F62}$$

$$A_{1\gamma}^{T\bar{S}} = \sum_{j=2}^{J_T} s(\bar{y}_j^T, \bar{x}_j^T) \tag{F63}$$

$$A_{1\gamma}^{T\bar{M}} = \sum_{j=2}^{J_T} s(\bar{y}_j^T, \bar{x}_j^T)[\bar{y}_j^T - Y_1^T] \tag{F64}$$

$$A_{1\gamma}^{T\bar{T}} = -\sum_{j=2}^{J_T} i(\bar{y}_j^T, \bar{x}_j^T) \tag{F65}$$

# APPENDIX F

## III. Total Wing and Tail Loads

The total structural loads at the $i^{th}$ wing load point are given by

$$\left.\begin{aligned} S_i^W(s) &= S_i^{WI}(s) + S_i^{WA}(s) \\ M_i^W(s) &= M_i^{WI}(s) + M_i^{WA}(s) \\ T_i^W(s) &= T_i^{WI}(s) + T_i^{WA}(s) \end{aligned}\right\} \qquad \text{(F66)}$$

where the component parts in equations (F66) have been developed in Sections IIA and IB, respectively.

Similarly, the total structural loads at the tail load point (defined by the intersection of the fuselage side and torque tube) are given by

$$\left.\begin{aligned} S_1^T(s) &= S_1^{TA}(s) + S_1^{TI}(s) + S_1^{SI}(s) \\ M_1^T(s) &= M_1^{TA}(s) + M_1^{TI}(s) + M_1^{SI}(s) \\ T_1^T(s) &= T_1^{TA}(s) + T_1^{TI}(s) + T_1^{SI}(s) \end{aligned}\right\} \qquad \text{(F67)}$$

where the component parts in equations (F67) are developed in Sections IA, IIA, and IIB, respectively.

Figure F1

DEFINITION OF MOMENT ARMS FOR AERODYNAMIC CONTRIBUTIONS TO TAIL BENDING MOMENT AND TORQUE

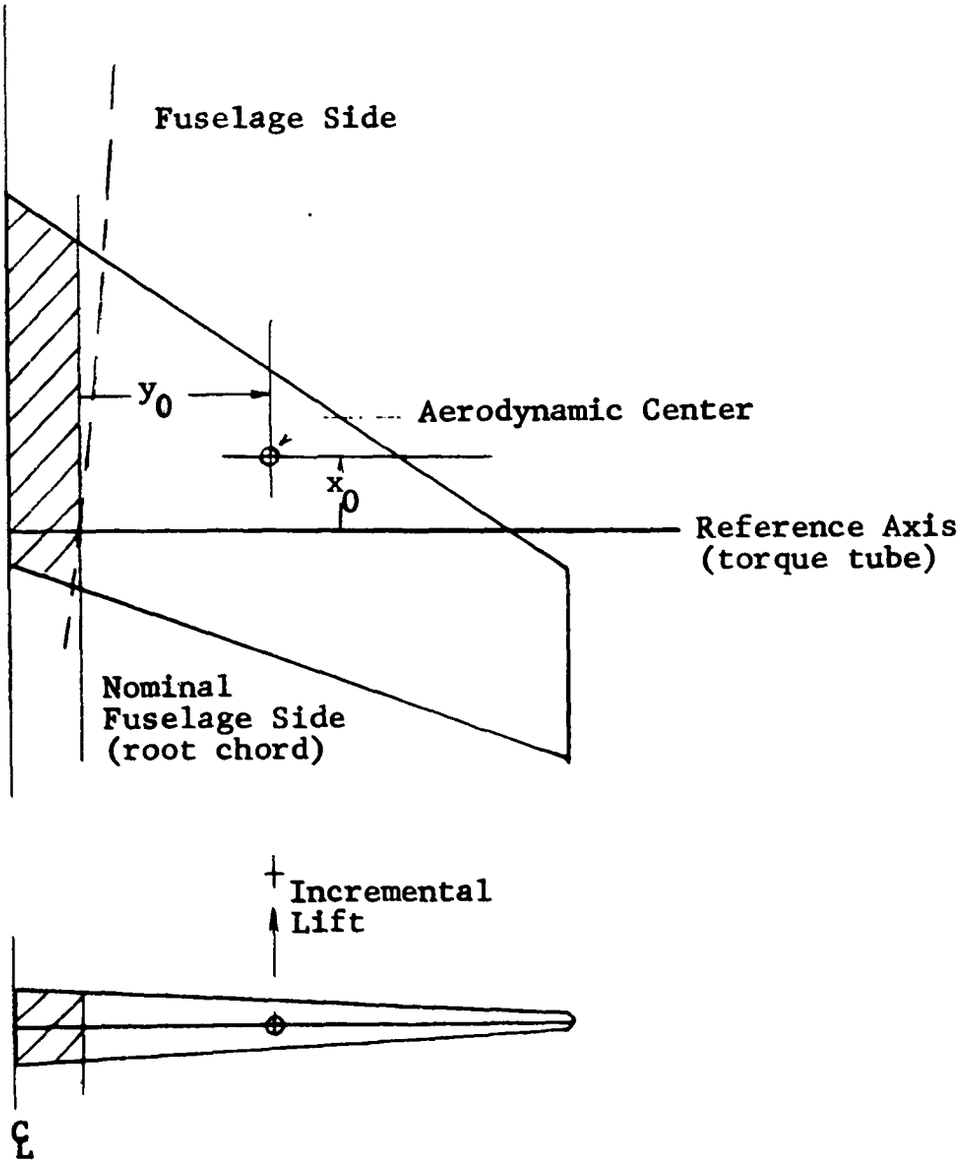

Figure F2

AXES NOTATION, PANEL BREAKDOWN, AND DEFINITION OF POSITIVE DIRECTIONS FOR EVALUATING THE AERODYNAMIC CONTRIBUTIONS TO THE STRUCTURAL LOADS (MODE ACCELERATION METHOD)

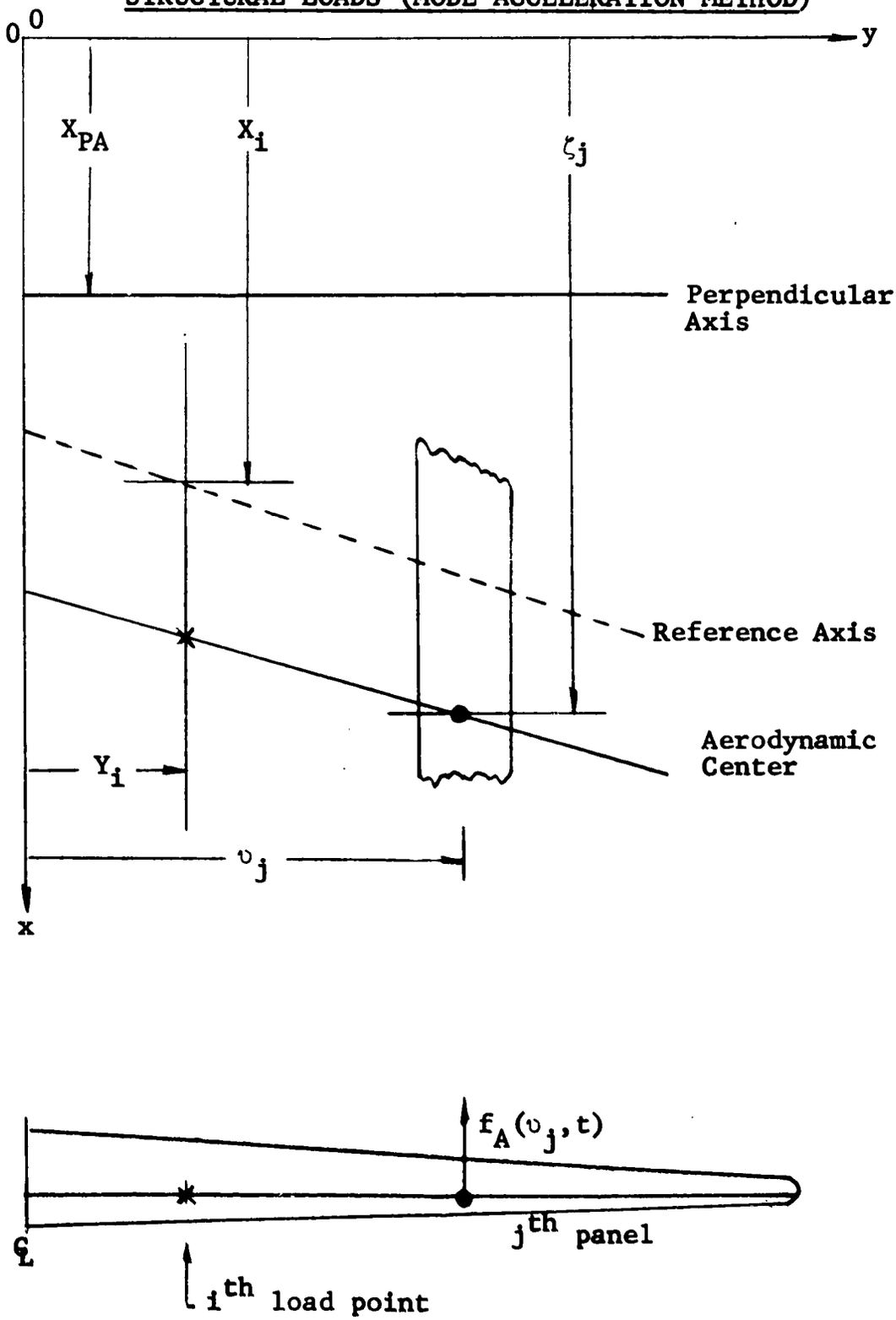

## Figure F3

## AXES NOTATION, PANEL BREAKDOWN, AND DEFINITION OF POSITIVE DIRECTIONS FOR EVALUATING INERTIAL CONTRIBUTIONS TO THE STRUCTURAL LOADS

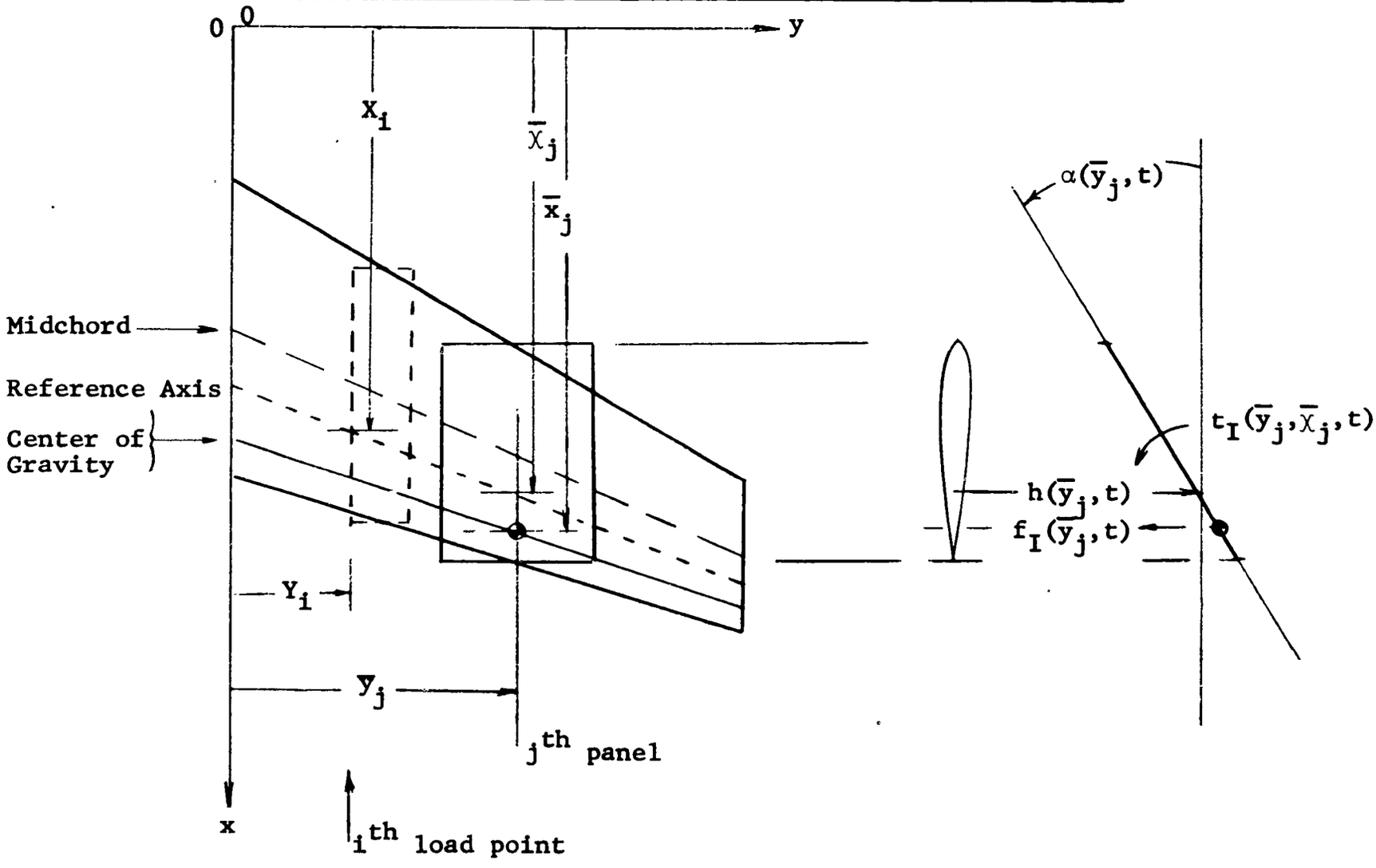

# APPENDIX G

## SYMBOLS

All symbols used in this volume are defined below. The symbols for the more important or fundamental quantities are defined verbally, and in addition, where appropriate, reference is made to equations and supporting figures. Other symbols which are of lesser importance or which represent intermediate quantities with less physical significance, are defined in terms of their analytical expressions by simply listing the corresponding equation or figure numbers.

### I. Unit Symbols

| Symbol | Units | |
|---|---|---|
| F | pounds | Force |
| I | inches | Linear dimension |
| L | feet | Linear dimension |
| P | pounds | Mass |
| R | radians | Angular dimension |
| S | semichords | Non-dimensional time |
| T | seconds | Real time |

## II. Roman Alphabet Symbols

| Symbol | Units | |
|---|---|---|
| $a$ | --- | Chordwise location of the reference axis of a two dimensional planform measured as a fraction of the semichord, positive for reference axis aft of midchord. |
| $a$ | --- | Subscript denoting amplitude of sinusoidal function (except in the coefficients $A_{ia}^{W\overline{S}}$, $A_{ia}^{W\overline{M}}$, $A_{ia}^{W\overline{T}}$, the constant $g_a$, and the parameters in Appendix A, Section II). |
| $a(y_i)$ | --- | Chordwise location of the reference axis at the spanwise center of the planform $i^{th}$ panel measured as a fraction of the planform local semichord, positive for a reference axis aft of midchord, (Figure C1) |
| $a_k$ | --- | Coefficient of $k^{th}$ exponential term in approximation for planform Kussner-type function, (Equation (B3)) |
| $a_{mk}$ | --- | Constant associated with the analytical approximation of the indicial generalized force functions, (Equation (C45)) |
| $a_\gamma$ | $T^2$ | Equation (A24) |

| | | |
|---|---|---|
| $A$ | --- | Subscript or superscript denoting aerodynamic contribution (except in the variable $L_A(s)$). |
| $A_{ia}^{\overline{M}}$ | $F^2S^2/P$ | Equation (F33) |
| $A_{ia}^{\overline{S}}$ | $F^2S^2/PL$ | Equation (F33) |
| $A_{ia}^{\overline{T}}$ | $F^2S^2/P$ | Equation (F33) |
| $A_{in}^{\overline{M}}$ | $PL$ | Equations (F46) and (F57) |
| $A_{in}^{\overline{S}}$ | $P$ | Equations (F44) and (F56) |
| $A_{in}^{\overline{T}}$ | $PL$ | Equations (F52) and (F58) |
| $A_{l\gamma}^{T\overline{M}}$ | $PL^2$ | Equation (F64) |
| $A_{l\gamma}^{T\overline{S}}$ | $PL$ | Equation (F63) |
| $A_{l\gamma}^{T\overline{T}}$ | $PL^2$ | Equation (F65) |
| $A_k$ | --- | Equation (C41) |
| $A_{\ell n}^{N}(y_i)$ | $L^3/R$ | Equation (E15) |
| $A_{mn}$ | $P$ | Equations (74), (E24), and (E61) |
| $A_{m\gamma}$ | $PL/R$ | Equation (75) |
| $A_n^T$ | $P/R$ | Equation (F13) |

| | | |
|---|---|---|
| $A^N_{tn}(y_i)$ | $L^4/R$ | Equation (E18) |
| $A^T_\gamma$ | PL/R | Equation (F16) |
| AR | --- | Planform aspect ratio |
| b | L | Semichord of two dimensional planform |
| $b(y_i)$ | L | Semichord at the spanwise center of the planform $i^{th}$ panel, (Figure C1). |
| $b_k$ | --- | Coefficient of $k^{th}$ exponential term in approximation for planform Wagner-type function, (Equation (B14)). |
| $b_{mk}$ | --- | Constant associated with the analytical approximation of the indicial generalized force functions, (Equation (C45)). |
| $b_R$ | L/S | Airplane reference semichord, (Figure B3). |
| $b_T$ | L/S | Tail reference semichord, half of tail mean aerodynamic chord, (Figures B1 and B3). |
| $b_W$ | L/S | Wing reference semichord, half of wing mean aerodynamic chord. |

| | | |
|---|---|---|
| $b_\gamma$ | T | Equation (A25) |
| $b_\eta$ | L | Reference semichord for an arbitrary planform, (Appendix B, Section IA). |
| B | --- | Scale parameter in the probability distribution of root-mean-square gust velocity, (Equation (113)). |
| $B_k$ | --- | Equation (C49) |
| $B_{\ell n}(y_i)$ | $L^3/RS$ | Equation (E15) |
| $B_{mn}$ | P/S | Equations (74), (E25), (E28), (E62), and (E63). |
| $B_{m\gamma}$ | PL/S | Equations (75), (E66), and (E67). |
| $B_n^M$ | S/T | Equation (E92) |
| $B_n^T$ | P/RS | Equation (F14) |
| $B_{tn}(y_i)$ | $L^4/RS$ | Equation (E18) |
| $B_\gamma^T$ | PL/RS | Equation (F17) |
| $c(y_i)$ | --- | Chordwise location of the aerodynamic center at the spanwise center of the planform $i^{th}$ panel measured as a fraction of the planform local semichord, positive for aerodynamic center aft of midchord, (Figure C1). |

| | | |
|---|---|---|
| $c_a^{\overline{M}}(Y_i)$ | FL | Bending moment at the $i^{th}$ wing load point due to wing airloads required to produce incremental one $g_a$ upward normal acceleration, positive for compression in the top skin. |
| $c_a^{\overline{S}}(Y_i)$ | F | Shear at the $i^{th}$ load point due to wing airloads required to produce incremental one $g_a$ upward normal acceleration, positive up. |
| $c_a^{\overline{T}}(Y_i, X_{PA})$ | FL | Torque at the $i^{th}$ load point, about the perpendicular axis $X_{PA}$, due to wing airloads required to produce incremental one $g_a$ upward normal acceleration, positive torque tends to twist the leading edge up. |
| $c_{\ell_\alpha}(y_i)$ | 1/R | Section rigid lift curve slope at the spanwise center of the planform $i^{th}$ panel. |
| C | --- | Gust power spectrum modifying constant, (Equation (125)). |
| C | --- | Superscript designating circulatory component. |
| $C(y_i)$ | $L^2/R$ | Equations (E8) and (E45) |
| $C(\kappa)$ | --- | Theodorsen's function. |

| | | |
|---|---|---|
| $C^{C}_{\ell n}(y_i)$ | $L^3/RS^2$ | Equation (E15) |
| $C_{mn}$ | $P/S^2$ | Equations (50), (E29), and (E64) |
| $C_{m\gamma}$ | $PL/S^2$ | Equations (50) and (E68) |
| $C^{M}_{n}$ | $1/T$ | Equation (E93) |
| $C^{T}_{n}$ | $P/RS^2$ | Equation (F15) |
| $C^{C}_{tn}(y_i)$ | $L^4/RS^2$ | Equation (E18) |
| $C_V$ | $FS^2/PL$ | $(V/b_R)^2/g$ |
| $C^{T}_{\gamma}$ | $PL/RS^2$ | Equation (F18) |
| $C_\eta$ | $LF/(R/T)$ | Angular damping constant of sprashpot system, (Figure A1). |
| $D_m$ | $PT/RS^2$ | Equations (D7), (D23), and (E84) |
| $E_{mn}$ | $P/S^2$ | Equation (77) |
| f(s) | Variable | General notation for a dependent variable (e.g., if the auto-pilot were being considered, f(s) would be replaced by $\mu(s)$). |
| $f^*(s)$ | Variable | 1-f(s) |

| | | |
|---|---|---|
| $\bar{f}(p)$ | Variable | Laplace transform of f(s). |
| $f(\omega)$ or $f(\Omega)$ | Variable | General notation for a sinusoidal function. |
| $f_a(\omega)$ | Variable | Amplitude of general sinusoidal function. |
| $f_{h_n}(x_a)$ | --- | Relative vertical deflection in the $n^{th}$ mode at the aft bobweight. |
| $f_{h_n}(x_f)$ | --- | Relative vertical deflection in the $n^{th}$ mode at the forward bobweight. |
| $f_{h_m}(y_i)$ or $f_{h_n}(y_i)$ | --- | Relative vertical deflection in the $m^{th}$ or $n^{th}$ modes of the planform reference axis at the spanwise center of the $i^{th}$ panel. |
| $f_{h_n}(\nu_i)$ | --- | Relative vertical displacement in the $n^{th}$ mode at the $i^{th}$ airplane location (either fuselage, wing, or tail). |
| $f_I(\bar{y}_j, t)$ | F | Equation (F39) |
| $f_{\ell\theta}(y_i^T, s)$ | $L^4/S^2$ | Equation (E50) |
| $f_{\ell\phi}(y_i, s)$ | $L^4/S^2$ | Equation (E14) |

| | | |
|---|---|---|
| $f_{t\theta}(y_i^T, s)$ | $L^5/S^2$ | Equation (E51) |
| $f_{t\phi}(y_i, s)$ | $L^5/S^2$ | Equation (E17) |
| $f_A(v_j, t)$ | F | Equations (F25) to (F28) |
| $f_\alpha(\omega)$ | R | Phase angle of general sinusoidal function. |
| $f_{\alpha_n}(x_a)$ | R/L | Relative pitching rotation in the $n^{th}$ mode at the aft bobweight. |
| $f_{\alpha_n}(x_f)$ | R/L | Relative pitching rotation in the $n^{th}$ mode at the forward bobweight. |
| $f_{\alpha_n}(x_s)$ | R/L | Relative pitching rotation in the $n^{th}$ mode at the stick pivot point. |
| $f_{\alpha_n}(x_\mu^\alpha)$ | R/L | Relative pitching rotation in the $n^{th}$ mode at the autopilot pitch angle sensing device. |
| $f_{\alpha_n}(x_\mu^{\dot{\alpha}})$ | R/L | Relative pitching rotation in the $n^{th}$ mode at the autopilot pitch rate sensing device. |
| $f_{\alpha_m}(y_i)$ or $f_{\alpha_n}(y_i)$ | R/L | Relative pitching rotation in the $m^{th}$ or $n^{th}$ modes about an axis perpendicular to the airplane center line at the intersection of the planform reference axis and the spanwise position of the center of the $i^{th}$ panel. |

| | | |
|---|---|---|
| $f_{\alpha_n}(\nu_i)$ | R/L | Relative pitching rotation in the $n^{th}$ mode at the $i^{th}$ airplane location (either fuselage, wing, or tail). |
| $f_\delta(s)$ | --- | Equation (E78) |
| $f_\theta(y_i^T, t)$ | L/T | Equation (E46) |
| $f_\phi(t)$ | L/T | Equations (E3) and (E5) |
| $f_\phi(y_i, t)$ | L/T | Equation (E9) |
| $f_\psi(s)$ | --- | Equation (D2) |
| $F_1$, $F_2$ | 1/S | Equation (77) |
| $F_3$ | --- | |
| $F(j)$, $F_j$ | --- | Equations (C27) and (C47) |
| $F(s)$ | --- | Equations (C22) and (C42) |
| $F_m(s)$ | $PL/S^2$ | Equations (E27) and (E60) |
| $F_M(s)$ | L/T | Equation (E91) |

| | | |
|---|---|---|
| $F_{mn}$ | $P/S^3$ | Equation (77) |
| g | $PL/FT^2$ | Gravitational constant which includes conversion from mass to force units. |
| $g_a$ | $L/T^2$ | Acceleration constant 32.2 feet/second squared. |
| G | --- | Subscript or superscript denoting gust or downwash due to gust. |
| h(t) | L | Vertical displacement of reference axis of two-dimensional airfoil section, positive down. |
| $\ddot{h}(x_a,t)$ | $L/T^2$ | Vertical acceleration at the aft bobweight, positive down. |
| $\ddot{h}(x_f,t)$ | $L/T^2$ | Vertical acceleration of the forward bobweight, positive down. |
| $h(y_i,t)$ | L | Vertical displacement of reference axis at the spanwise center of the $i^{th}$ panel, positive down. |
| $h(\bar{y}_j,t)$ | L | Vertical displacement of reference axis at the spanwise center-of-gravity position of the $j^{th}$ panel, positive down. |

| | | |
|---|---|---|
| $h_i(s)$ | L | Vertical displacement, velocity, and acceleration at the $i^{th}$ airplane location, positive down. |
| $\dot{h}_i(s)$ | L/T | |
| $\ddot{h}_i(s)$ | $L/T^2$ | |
| $h_W(y^T_{mac}, s)$ | L | Vertical displacement of the wing reference axis at the spanwise position of the tail mean aerodynamic chord, positive down. |
| $H_{20}$ | 1/S | Equation (A27) |
| $H_{21}$ | $1/S^2$ | Equation (A28) |
| $H_{22}$ | $1/S^2$ | Equation (A29) |
| $H_{30}$ | $1/S^2$ | Equation (A19) |
| $H_{3n}$ | 1/L | Equation (A20) |
| $H_{3\eta}$ | 1/S | Equation (A19) |
| $H_{40}$ | 1/S | Equation (A21) |
| i | --- | General index. |
| i | --- | $\sqrt{-1}$ |

| | | |
|---|---|---|
| $i(\bar{y}_j, \bar{x}_j)$ | $PL^2$ | Moment of inertia of planform $j^{th}$ panel about an axis perpendicular to the airplane centerline passing through the panel center of gravity. |
| $i(\bar{y}_j, \bar{\chi}_j)$ | $PL^2$ | Moment of inertia of planform $j^{th}$ panel about an axis perpendicular to the airplane centerline passing through a point defined by the intersection of the spanwise location of the $j^{th}$ panel center of gravity and the reference axis, (Figure F3). |
| I | --- | Subscript or superscript denoting inertial contribution. |
| I | --- | Number of planform panels in generalized force calculations. |
| $I_a$ | $PL^2$ | Aft bobweight inertia about its pivot point. |
| $I_f$ | $PL^2$ | Forward bobweight inertia about its pivot point. |
| $I_{mn}$ | $P/S^2$ | Equation (79) |
| $I_{m\gamma}$ | $PL/RS^2$ | Equation (79) |
| $I_s$ | $PL^2$ | Control system inertia referred to stick pivot point, (Equation (A10)). |

| | | |
|---|---|---|
| $I_{s0}$ | $PL^2$ | Inertia of the control system about the stick pivot point without the bobweight contribution, (Equation (A10)). |
| $I_{s1}$ | $PL^2$ | Inertia of the bobweight system about the stick pivot point, (Equation (A9)). |
| $I_{y_k}$ | Variable | Integral defined by Equation (114). |
| j | --- | General index. |
| J | --- | Number of planform panels in load calculations. |
| $J_1$, $J_2$ | $1/S$ | Equation (79) |
| $J_3$ | --- | |
| $J_{mn}$ | $P/S^3$ | Equation (79) |
| $J_{mγ}$ | $PL/RS^3$ | Equation (79) |
| k | --- | General index. |
| $k_7$ | $R/(R/T)$ | Pitch rate autopilot gain. |
| $k_8$ | $R/R$ | Pitch displacement autopilot gain. |

| | | |
|---|---|---|
| $k_\tau$ | --- | Stabilizer to control stick linkage ratio. |
| $K_\eta$ | LF/R | Angular spring constant of sprashpot, (Figure A1). |
| $K_\tau$ | LF/R | Angular spring constant of stick feel spring, (Figure A1). |
| $K_\phi$ | --- | Number of exponential terms in approximation to indicial lift function for planform motion, (Equation (B14)). |
| $K_\psi$ | --- | Number of exponential terms in approximation to indicial lift function for gust on a planform, (Equation (B3)). |
| $\ell_T(s)$ | $PL/RS^2$ | Equation (F12) |
| $\ell_\delta(y_i^T, s)$ | F | Equation (E76) |
| $\ell_\theta(y_i^T, s)$ | F | Equation (E48) |
| $\ell_\phi(t)$ | F/L | Equation (E1) |
| $\ell_\phi(y_i, s)$ | F | Equation (E13) |
| $\ell_\psi(y_i, s)$ | F | Equation (D1) |

| | | |
|---|---|---|
| L | L | Scale of turbulence parameter. |
| $L_{10}$ | 1/S | Equation (A6) |
| $L_{1n}$ | S/L | Equation (A6) |
| $L_{2n}$ | 1/L | Equation (A6) |
| $L_{3n}$ | 1/LS | Equation (A6) |
| $L_A(s)$ | F | Tail lift per side based on area from airplane center line to tail tip, positive up, (Equation (F8)). |
| $L_T(s)$ | F | Tail lift per side based on area from fuselage juncture to tail tip, positive up, (Equation (F11)). |
| m | --- | Normal mode index. |
| $m(\bar{y}_j)$ | P | Mass of planform $j^{th}$ panel. |
| $m_a$ | P | Mass of aft bobweight. |
| mac | --- | Mean aerodynamic chord. |
| $m_f$ | P | Mass of forward bobweight. |
| M | --- | Airplane Mach number. |

| | | |
|---|---|---|
| $M$ | --- | Subscript or superscript denoting motion or downwash due to motion. |
| $\overline{M}$ | --- | Superscript denoting bending moment. |
| $M_g$ | --- | Gust front Mach number. |
| $M_1^W(s)$ | FL | Total incremental bending moment at the $i^{th}$ wing load point positive for compression in the top skin, (Equation (F66)). |
| $M_{mm}$ | P | Normal-mode generalized masses based on half the airplane. |
| $M_{m\gamma}$ | PL | Normal-mode stabilizer-rotation generalized mass coupling terms based on half the airplane. |
| $M_{\gamma\gamma}$ | $PL^2$ | Stabilizer-rotation on-diagonal generalized mass term based on half the airplane (stabilizer pitching inertia about reference axis). |
| $M_1^{SI}(s)$ | FL | Inertial contribution to $M_1^T(s)$ due to stabilizer rotation, (Equation (F60)). |
| $M_1^T(s)$ | FL | Total tail incremental bending moment at the intersection of the fuselage and the torque tube, positive for compression in the top skin, (Equation (F67)). |

| | | |
|---|---|---|
| $M_{1\tau}(t)$ | FL | Equation (A11) |
| $M_{2\tau}(t)$ | FL | Equation (A13) |
| n, $\bar{n}$ | --- | Normal mode index ($1 \leq n \leq N$, $1 \leq \bar{n} \leq N + 1 \equiv \gamma$. |
| N | --- | Number of symmetric normal modes. |
| N | --- | Superscript designating non-circulatory component. |
| $N_{0_y}$ | 1/T | Characteristic frequency, average number of times per second that the variable y crosses the value zero with a positive slope, (Equation (111)). |
| N(y) | 1/T | Average number of times per second that the variable crosses a given value of y with a positive slope; an approximation for the average number of positive peaks per second exceeding a given value of y, (Equation (113)). |
| $N_a$ | --- | Ratio of aft bobweight angular motion to control stick angular motion. |
| $N_f$ | --- | Ratio of forward bobweight angular motion to control stick angular motion. |
| $N_{mi}$ | ---, i=7<br>1/S, i=1-5, 8<br>$1/S^2$, i=6 | Equation (72) |

| | | |
|---|---|---|
| $O_i$ | ---, i=7<br>1/S, i=1-5, 8<br>$1/S^2$, i=6 | Equation (67) |
| p | 1/S<br>1/T | Laplace transform differential operator. |
| $p_m(y_i,\infty)$ | $L^2/R$ | Equation (C7) |
| $P_m(\infty)$ | $L^2/R$ | Equation (C11) |
| $P_1$ | --- | Percentage of total flight time or distance in turbulence. |
| $q_{rm}(y_i,s)$ | F | Generalized force on the $i^{th}$ panel in the $m^{th}$ mode due to the $r^{th}$ contribution, (Equations (C5), (C6), (D3), and (E20)). |
| $Q_i$ | ---, i=7<br>1/S, i=1-5, 8<br>$1/S^2$, i=6 | Equation (62) |
| $Q_m(s)$ | F | Total generalized force in the $m^{th}$ mode, (Equations (36) and (57)). |
| $Q_{rm}(s)$ | F | Generalized force in the $m^{th}$ mode due to the $r^{th}$ contribution, (Equations (C8) and (D5)). |

| | | |
|---|---|---|
| r | --- | Index denoting generalized force contributions:<br>r=1, wing motion<br>2, tail motion and stabilizer rotation<br>3, downwash on tail due to wing motion<br>4, downwash on tail due to gust on the wing<br>5, gust on the tail<br>6, gust on the wing |
| $R_a$ | L | Moment arm of the aft bobweight from its pivot point, (Figure A1). |
| $R_f$ | L | Moment arm of the forward bobweight from its pivot point, (Figure A1). |
| $R_i$ | ---, i=7<br>1/S, i=1-5, 8<br>$1/S^2$, i=6 | Equation (56) |
| s | S | Non-dimensional time based on airplane reference semichord, (Equation (B5)). |
| $s_G$ | S | Transport time delay between airplane zero time reference point and assumed start of stabilizer lift build up due to downwash resulting from gust on the wing. |
| $s_M$ | S | Transport time delay between wing motion and assumed start of resulting stabilizer lift build up due to downwash. |

| | | |
|---|---|---|
| $s_T$ | S | Transport time delay between airplane zero time reference point and start of tail lift build up due to gust on the tail. |
| $s_T^x$ | S | Non-dimensional horizontal distance from the midchord of the wing mean aerodynamic chord to the leading edge of the tail mean aerodynamic chord, (Figures B1 and B6). |
| $s_T^z$ | S | Non-dimensional vertical distance between the planes containing the wing and the tail, (Figure B1). |
| $s_{TD}$ | S | General expression for transport time delay. |
| $s_W$ | S | Transport time delay between airplane zero time reference point and assumed start of wing lift build up due to gust on the wing. |
| $s(\bar{y}_j, \bar{X}_j)$ | PL | Unbalance of planform $j^{th}$ panel about an axis perpendicular to the airplane centerline passing through a point defined by the intersection of the spanwise location of the $j^{th}$ panel center of gravity and the reference axis, positive for center of gravity aft of reference axis, (Equation (F38)). |
| $\bar{S}$ | --- | Superscript denoting shear. |
| S | --- | Superscript denoting stabilizer rotation. |

| | | |
|---|---|---|
| $S_i^W(s)$ | F | Total incremental shear at the $i^{th}$ wing load point, positive up, (Equation (F66)). |
| $S_1^{SI}(s)$ | F | Inertial contribution to $S_1^T(s)$ due to stabilizer rotation, (Equation (F59)). |
| $S_1^T(s)$ | F | Total tail incremental shear at the inersection of the fuselage and the torque tube, positive up, (Equation (F67)). |
| t | T | Real time. |
| $t_A(Y_i,X_i,t)$ | FL | Equation (F26) |
| $t_A(Y_i,X_{PA},t)$ | FL | Equation (F25) |
| $t_I(\bar{y}_j,\bar{x}_j,s)$ | FL | Equation (F48) |
| $t_\delta(y_i^T,s)$ | FL | Equation (E79) |
| $t_\theta(y_i^T,t)$ | FL | Equation (E44) |
| $t_\phi(t)$ | F | Equation (E2) |
| $t_\phi(y_i,t)$ | F | Equation (E7) |
| $t_\psi(y_i,\eta)$ | FL | Equation (C4) |
| T | --- | Subscript or superscript denoting tail. |

| | | |
|---|---|---|
| $\overline{T}$ | --- | Superscript denoting torque. |
| $T(s)$ | FL | Kinetic energy in terms of normal velocity coordinates and generalized masses, (Equation (34)). |
| $T_i^W(s)$ | FL | Total incremental torque about a wing axis perpendicular to the airplane centerline passing through a point defined by the intersection of the spanwise location of the $i^{th}$ load point and the reference axis, positive nose up, (Equation (F66)). |
| $T_1$, $T_2$ | T | Equations (A22) to (A25) |
| $T_1^{SI}(s)$ | FL | Inertial contributions to $T_1^T(s)$ due to stabilizer rotation, (Equation (F61)). |
| $T_1^T(s)$ | FL | Total tail incremental torque about the torque tube at the intersection of the fuselage and torque tube, positive nose up, (Equation (F67)). |
| $\overline{T}_y(\omega)$ | Variable | Frequency-response function of arbitrary variable, (Equation (110)). |
| $V$ | L/T | Airplane forward velocity. |
| $V_0$ | --- | $1/V_1$ |

| | | |
|---|---|---|
| $V_1$ | --- | Equation (F10) |
| $V_2$ | $PT/RS^2$ | Equation (F9) |
| $V(s)$ | FL | Potential energy in terms of normal coordinates and generalized spring terms, (Equation (35)). |
| $w_G$ | L/T | Vertical gust velocity. |
| $w(M_g, M, AR_W, s_T^x, s_T^z, s)$ | --- | Indicial downwash function, normalized unsteady downwash build up on the tail due to either a step change in wing motion or a step change in gust velocity on the wing, (Equation (26)). |
| $w_\delta(s)$ | L/T | Equation (E75) |
| $w_\theta(y_i^T, t)$ | L/T | Equation (E47) |
| $w_\phi(t)$ | L/T | Downwash at the three-quarter chord of a two-dimensional planform, (Equation (E4)). |
| $w_\phi(y_i, t)$ | L/T | Downwash at the three-quarter chord at the spanwise center of the $i^{th}$ panel of a three-dimensional planform, (Equation (E10)). |

| | | |
|---|---|---|
| $w_{\phi}^{W}(y_{mac}^{T},t)$ | L/T | Equation (E71) |
| W | --- | Subscript or superscript denoting wing. |
| x | L or I | Fuselage station, positive aft of nose. |
| $x_0$ | L | Tail torque arm, longitudinal distance between tail aerodynamic center and tail reference axis, positive for aerodynamic center forward of reference axis, (Figure F1). |
| $x_a$ | L or I | Location of the aft bobweight pivot point, (Figure A1). |
| $x_{cg}$ | L or I | Location of airplane center of gravity, (Figure A1). |
| $x_f$ | L or I | Location of the forward bobweight pivot point, (Figure A1). |
| $\bar{x}_j$ | L | Longitudinal location of $j^{th}$ panel center of gravity, (Figure F3). |
| $x_s$ | L or I | Location of stick pivot point, (Figure A1). |
| $x_{TT}$ | L or I | Fuselage station of stabilizer torque tube. |

| | | |
|---|---|---|
| $x_\mu^\alpha$ | L or I | Location of the autopilot pitch angle sensing device. |
| $x_\mu^{\dot{\alpha}}$ | L or I | Location of the autopilot pitch rate sensing device. |
| $X_i$ | L | Longitudinal location of the reference axis at the $i^{th}$ load point, (Figures F2 and F3). |
| $X_{PA}$ | L | Longitudinal location of an axis perpendicular to the fuselage centerline about which the torque components of the data for the aerodynamic loading coefficients used in the mode-acceleration method are provided, (Figure F2). |
| $y$ | L or I | Spanwise coordinate measured from the airplane centerline perpendicular to the plane of symmetry, positive outboard, (Figure C1). |
| $y_i$ | L or I | Spanwise location of the center of the $i^{th}$ panel, (Figure C1). |
| $\bar{y}_j$ | L or I | Spanwise location of the $j^{th}$ panel center of gravity, (Figure F3). |
| $y_{mac}$ | L or I | Spanwise location of the planform mean aerodynamic chord, (Figure B3). |

| | | |
|---|---|---|
| $y_{max}$ | L or I | Planform semispan. |
| $y_0$ | L | Tail bending moment arm, spanwise distance between tail aerodynamic center and nominal fuselage side, positive for aerodynamic center outboard of fuselage, (Figure F1). |
| $Y_i$ | L or I | Spanwise location of the $i^{th}$ load point, (Figures F2 and F3). |
| $z(\overline{y}_j, t)$ | L | Vertical displacement of the $j^{th}$ panel center of gravity, (Equation (F35)). |

## III. Greek Alphabet Symbols

| Symbol | Units | |
|---|---|---|
| $\alpha$ | --- | Subscript denoting phase angle of sinusoidal function. |
| $\alpha(t)$ | R | Angular displacement about the reference axis of two-dimensional airfoil section, positive nose up. |
| $\ddot{\alpha}(x_a,t)$ | $R/T^2$ | Angular acceleration at the aft bobweight pivot point, positive nose up. |
| $\ddot{\alpha}(x_f,t)$ | $R/T^2$ | Angular acceleration at the forward bobweight pivot point, positive nose up. |
| $\ddot{\alpha}(x_s,t)$ | $R/T^2$ | Angular acceleration at the stick pivot point, positive nose up. |
| $\alpha(x_\mu^\alpha,t)$ | R | Angular displacement at the location of the autopilot pitch attack sensing device, positive nose up. |
| $\dot{\alpha}(x_\mu^{\dot{\alpha}},t)$ | R/T | Angular velocity at the location of the autopilot pitch rate sensing device, positive nose up. |

| | | |
|---|---|---|
| $\alpha(y_i, t)$ | R | Angular displacement about an axis perpendicular to the airplane centerline passing through a point defined by the intersection of the planform reference axis and the spanwise position of the center of the $i^{th}$ panel, positive nose up. |
| $\alpha(\bar{y}_j, t)$ | R | Angular displacement about an axis perpendicular to the airplane centerline passing through a point defined by the intersection of the planform reference axis and the spanwise center-of-gravity position of the $j^{th}$ panel, positive nose up. |
| $\alpha_i(s)$ | R | Angular displacement, velocity and acceleration about an axis perpendicular to the airplane centerline at the $i^{th}$ airplane location, positive nose up. |
| $\dot{\alpha}_i(s)$ | R/T | |
| $\ddot{\alpha}_i(s)$ | $R/T^2$ | |
| $\alpha_k$ | 1/S | Exponent of the $k^{th}$ exponential term in approximation for planform Küssner-type function based upon the non-dimensional time, s, (Equations (B9) and (B12)). |
| $\bar{\alpha}_k$ | 1/S | Exponent of the $k^{th}$ exponential term in approximation for planform Küssner-type function based upon the non-dimensional time, $\eta$, (Equations (B9) and (B12)). |

| | | |
|---|---|---|
| $\alpha_{mk}$ | 1/S | Constant associated with the analytical approximation of the indicial generalized force functions, (Equations (C45) and (C52)). |
| $\alpha_{A_k}$ | 1/S | Equation (C37) |
| $\alpha_W(y^T_{mac}, s)$ | R | Angular displacement about an axis perpendicular to the airplane centerline passing through a point defined by the intersection of the wing reference axis and the spanwise position of the tail mean aerodynamic chord, positive nose up. |
| $\beta_k$ | 1/S | Exponent of the $k^{th}$ exponential term in approximation for planform Wagner-type function based upon the non-dimensional time, s, (Equations (B16) and (B18)). |
| $\bar{\beta}_k$ | 1/S | Exponent of $k^{th}$ exponential term in approximation for planform Wagner-type function based upon the non-dimensional time, $\eta$, (Equations (B16) and (B18)). |
| $\gamma$ | --- | Subscript denoting stabilizer rotation. |
| $\gamma(s)$ | R | Stabilizer rotation, positive for trailing edge down. |

| | | |
|---|---|---|
| $\gamma_s(t)$ | R | Total signal input to stabilizer. |
| $\delta(s)$<br>$\delta(M_g, M, AR_W, AR_T, s_T^x, s_T^z, s)$ | --- | Tail indicial lift function due to downwash caused by wing motion ($M_g = \infty$) or gust on the wing ($M_g = 0$), (Equations (26), (B19), (B20), and (B21)). |
| $\delta_m^G(s)$ | --- | Indicial generalized force function for the $m^{th}$ mode due to downwash on the tail caused by gust on the wing, (Equations (C18) and (C19)). |
| $\delta_m^M(s)$ | --- | Indicial generalized force function for the $m^{th}$ mode due to downwash on the tail caused by wing motion, (Equations (C16) and (C17)). |
| $\Delta_m^G(s)$ | L/T | Generalized force variation due to downwash on the tail caused by gust on the wing, (Equation (D24)). |
| $\Delta_{mk}^G(s)$ | L/T | Component parts of $\Delta_m^G(s)$, (Equations (D25) to (D27)). |
| $\Delta_m^M(s)$ | L/T | Generalized force variation due to downwash on the tail caused by wing motion, (Equation (E87)). |

| | | |
|---|---|---|
| $\Delta^{M}_{mk}(s)$ | L/T | Component parts of $\Delta^{M}_{m}(s)$, (Equations (E88) to (E90)). |
| $\Delta s$ | S | Non-dimensional time increment. |
| $\Delta y(y_i)$ | L | Width of the $i^{th}$ panel whose center is located at $y_i$, (Figure C1). |
| $\partial\varepsilon/\partial\alpha$ | --- | Steady-state downwash slope. |
| $\varepsilon$ | --- | Exponent defining rate of decay of frequency-response function at high frequencies, (Equations (119) to (121)). |
| $\varepsilon_k$ | --- | Coefficients in equation (C30). |
| $\zeta_j$ | L | Longitudinal location of the aerodynamic center of the $j^{th}$ panel, (Figure F2). |
| $\eta$ | S | Non-dimensional time based on planform reference semichord, (Equation (B1)). |
| $\eta(t)$ | R | Motion of spring-damper attachment point in sprashpot, positive for positive stick rotation, (Figure A1). |

| | | |
|---|---|---|
| $_i$ | --- | Subscript denoting imaginary component. |
| $\kappa$ | R/S | Reduced frequency, (Equation (3)). |
| $\lambda_k$ | --- | Equations (C28) and (C34) |
| $\Lambda_k$ | --- | Equation (C24) |
| $\Lambda_{LE}$ | R | Sweep angle of planform leading edge, (Figure C1). |
| $\mu(s)$ | R | Autopilot signal to stabilizer, positive for nose up pitch attitude and pitch rate, (Equation (A5)). |
| $\nu_k^j$ | --- | Equation (C50) |
| $\xi_m(s)$ or $\xi_n(s)$ | L | Normal coordinates. |
| $\ddot{\xi}_{1W}(s)$ | $L/S^2$ | Wing-induced rigid-body vertical acceleration, (Equation (F34)). |

| | | |
|---|---|---|
| $\rho$ | --- | Subscript denoting real component. |
| $\rho$ | $P/L^3$ | Air density. |
| $\sigma$ | --- | Dummy variable of integration in Duhamel's integral. |
| $\sigma(y_i)$ | S | Transport time delay in terms of airplane reference semichords to the leading edge of the midspan of the $i^{th}$ panel measured from the planform apex, (Figure C1). |
| $\overline{\sigma}(y_i)$ | S | Transport time delay in terms of planform reference semichords to the leading edge of the midspan of the $i^{th}$ panel measured from the planform apex, (Equation (C2)). |
| $\sigma_{max}$ | S | Transport time delay in terms of airplane reference semichords to the tip chord leading edge measured from the planform apex. |
| $\sigma_{w_G}$ | L/T | Root-mean-square gust velocity. |
| $\sigma_y$ | Variable | Root-mean-square value of variable y, (Equation (112)). |

| | | |
|---|---|---|
| $\tau(s)$ | R | Stick rotation, positive for stick movement towards the pilot, (Equation (A17)). |
| $\upsilon_j$ | L or I | Spanwise location of the center of the $j^{th}$ panel, (Figure F2). |
| $\phi(s)$ | --- | Exponential approximation to the planform Wagner-type function, including compressibility and aspect ratio effects and based upon the airplane reference semichord, (Equations (B15) and (B17)). |
| $\phi(M,AR,\eta)$ | --- | Planform indicial lift function due to motion, including compressibility and aspect ratio effects, and based upon the planform reference semichord; Wagner-type function, (Equation (B13)). |
| $\phi(\eta)$ | --- | Exponential approximation to the planform Wagner-type function, including compressibility and aspect ratio effects, and based upon the planform reference semichord, (Equation (B14)). |
| $\Phi_m(s)$ | $PL/S^2$ | Unsteady contribution to the circulatory generalized force variation due to motion, (Equations (E39) and (E57)). |

| | | |
|---|---|---|
| $\Phi_m^C(s)$ | $PL/S^2$ | Circulatory contribution to the total generalized force variation due to motion, (Equations (E26), (E38), and (E56)). |
| $\Phi_m^N(s)$ | $PL/S^2$ | Non-circulatory contribution to the total generalized force variation due to motion, (Equations (E23) and (E55)). |
| $\Phi_{mk}(s)$ | $PL/S^2$ | Component parts of $\Phi_m(s)$, (Equations (E41) and (E59)). |
| $\overline{\Phi}_{w_G}(\omega)$ | $L^2/RT$ | Power-spectral-density function of vertical gust velocity in terms of circular frequency, (Equations (107) and (108)). |
| $\overline{\Phi}^*_{w_G}(\omega)$ | $L^2/RT$ | Modified power-spectral-density function of vertical gust velocity in terms of circular frequency, (Equation (125)). |
| $\tilde{\Phi}_{w_G}(\Omega)$ | $L^3/RT^2$ | Power-spectral-density function of vertical gust velocity in terms of reduced frequency, (Equation (106)). |
| $\overline{\Phi}_y(\omega)$ | Variable | Power-spectral-density function of response variable in terms of circular frequency, (Equation (110)). |

| | | |
|---|---|---|
| $\tilde{\Phi}_y(\Omega)$ | Variable | Power-spectral-density function of response variable in terms of reduced frequency, (Equation (109)). |
| $\chi(s)$ | L/T | Vertical gust velocity. |
| $\bar{\chi}_j$ | L | Longitudinal location of reference axis at a spanwise position corresponding to the center of gravity of the $j^{th}$ panel, (Figure F3). |
| $\psi(M,AR,\eta)$ | --- | Planform indicial lift function due to gust, including compressibility and aspect ratio effects, and based upon the planform reference semichord; Küssner-type function, (Equation (B2)). |
| $\psi(s)$ | --- | Exponential approximation to the planform Küssner-type function, including compressibility and aspect ratio effects and based upon the airplane reference semichord, (Equations (B7) and (B10)). |
| $\psi(\eta)$ | --- | Exponential approximation to the planform Küssner-type function, including compressibility and aspect ratio effects, and based upon the planform reference semichord, (Equation (B3)). |

| | | |
|---|---|---|
| $\psi_m(s)$ | --- | Indicial generalized force function for the $m^{th}$ mode due to gust, (Equations (C12), (C13), (C14), and (C15)). |
| $\Psi_m(s)$ | L/T | Generalized force variation due to gust, (Equations (D8) and (D17)). |
| $\Psi_{mk}(s)$ | L/T | Component parts of $\Psi_m(s)$, (Equations (D18) to (D20)). |
| $\omega$ | R/T | Circular frequency. |
| $\omega_b(L)$ | L/T | Breakpoint frequency in approximation of power-spectral-density function of vertical gust velocity, (Equation (117)). |
| $\omega_m$ | R/T | Natural frequency of the $m^{th}$ mode. |
| $\omega_{mk}$ | 1/S | Constant associated with the analytical approximation of the indicial generalized force functions, (Equations (C45) and (C52)). |
| $\Omega$ | R/L | Reduced frequency, (Equation (105)). |

## IV. Mathematical Symbols

### Symbols

| | |
|---|---|
| $(\dot{})$, $(\ddot{})$ | Dots above symbols denote differentiation with respect to real time, t. |
| $(\mathring{})$, $(\mathring{\mathring{}})$ | Circles above symbols denote differentiation with respect to non-dimensional time, s, (Equations (9), (10), and (E11)). |
| $(\,)'$ | Prime after symbol denotes differentiation with respect to independent variable. |
| $\lvert\ \rvert$ | Absolute value. |
| $\frac{\partial}{\partial \alpha}$ | Partial derivative with respect to $\alpha$. |
| $\mathcal{L}[\ ]$ | Laplace transform of [ ]. |

## INITIAL DISTRIBUTION FOR FINAL REPORT UNDER CONTRACT NOw 60-0449-c

**NOTE:** The military addressees listed below non-government addresses (marked "A") receive a copy of the forwarding document but not a copy of the report.

| | Addressee | Copy Number(s) |
|---|---|---|
| 1 | Bureau of Naval Weapons (RAAD-22) | 1, 2 plus the reproducible |
| 2 | Bureau of Naval Weapons (DLI-302) | 3 through 24 |
| 3 | Naval Air Engineering Center<br>Aeronautical Structures Laboratory<br>Naval Base, Philadelphia, Pennsylvania | 25 |
| 4 | Director, Air Force Flight Dynamics Laboratory<br>Wright-Patterson Air Force Base, Ohio 45433<br>Attention: FDT | 26, 27 |
| 5 | National Aeronautics and Space Administration<br>600 Independence Ave. S.W.,<br>Washington, D. C. | 28 |
| 6 | National Aeronautics and Space Administration<br>Ames Research Center,<br>Moffett Field, California | 29 |
| 7 | National Aeronautics and Space Administration<br>Langley Research Center,<br>Langley Field, Virginia | 30 |
| 8 | National Aeronautics and Space Administration<br>Flight Research Center, Box 273,<br>Edwards, California, 93523 | 31 |
| 9 | Federal Aviation Agency,<br>Dynamics and Loads Section,<br>Aircraft Engineering Division,<br>Washington, D. C. | 32 |

| | Addressee | Copy Number |
|---|---|---|
| 10 | Beech Aircraft Corporation<br>9709 East Central Ave.,<br>Wichita, Kansas | 33 |
| 10A | Headquarters,<br>Central Contract Management Region<br>Wright-Patterson Air Force Base, Ohio 45433 | |
| 11 | Bell Aerosystems Company<br>100 Connecticut Ave.,<br>Buffalo 5, New York | 34 |
| 11A | Headquarters,<br>Eastern Contract Management Region<br>Olmstead Air Force Base,<br>Middletown, Pennsylvania | |
| 12 | The Boeing Company<br>Post Office Box 3707<br>Seattle, Washington | 35 |
| 12A | Headquarters,<br>Western Contract Management Region<br>Mira Loma Air Force Station,<br>Mira Loma, California | |
| 13 | The Boeing Company<br>3801 South Oliver Street<br>Wichita, Kansas | 36 |
| 13A | Headquarters,<br>Central Contract Management Region<br>Wright-Patterson Air Force Base, Ohio 45433 | |
| 14 | Cessna Aircraft Company<br>5800 East Pawnee Road,<br>Wichita, Kansas | 37 |
| 14A | Bureau of Naval Weapons Representative<br>Box 516,<br>St. Louis, Missouri | |

| | Addressee | Copy Number |
|---|---|---|
| 15 | Cornell Aeronautical Laboratory, Inc.<br>of Cornell University<br>4455 Genesee St.,<br>P. O. Box 235,<br>Buffalo 21, New York | 38 |
| 15A | Inspector of Naval Materiel<br>1021 Main Street<br>Buffalo 3, New York | |
| 16 | Douglas Aircraft Company, Inc.,<br>Aircraft Division, 3855 Lakewood Boulevard,<br>Long Beach, California | 39 |
| 16A | Bureau of Naval Weapons Representative<br>Long Beach, California | |
| 17 | General Dynamics Corporation<br>Convair Division<br>3302 Pacific Highway<br>San Diego 12, California | 40 |
| 17A | Bureau of Naval Weapons Representative<br>San Diego, California | |
| 18 | General Dynamics Corporation,<br>Fort Worth Division<br>Grants Lane,<br>Fort Worth, Texas | 41 |
| 18A | Headquarters<br>Central Contract Management Region<br>Wright-Patterson Air Force Base, Ohio 45433 | |
| 19 | Lockheed-California Company,<br>A Division of Lockheed Aircraft Corp.<br>2555 North Hollywood Way,<br>Burbank, California | 42 |
| 19A | Bureau of Naval Weapons Representative<br>Burbank, California | |

| | Addressee | Copy Number |
|---|---|---|
| 20 | Lockheed-Georgia Company<br>86 South Cobb Drive,<br>Marietta, Georgia | 43 |
| 20A | Headquarters,<br>Eastern Contract Management Region<br>Olmstead Air Force Base,<br>Middletown, Pennsylvania | |
| 21 | McDonnell Aircraft Corporation<br>Post Office Box 516,<br>St. Louis 3, Missouri | 44 |
| 21A | Bureau of Naval Weapons Representative<br>Box 516,<br>St. Louis 3, Missouri | |
| 22 | Martin Marietta Corporation<br>Middle River<br>Baltimore, Maryland | 45 |
| 22A | Headquarters,<br>Eastern Contract Management Region<br>Olmstead Air Force Base,<br>Middletown, Pennsylvania | |
| 23 | Massachusetts Institute of Technology<br>Division of Sponsored Research<br>77 Massachusetts Ave.,<br>Cambridge, Massachusetts | 46 |
| 23A | Commanding Officer,<br>Office of Naval Research Branch Office<br>Boston, Massachusetts | |
| 24 | North American Aviation, Inc.,<br>Columbus Division<br>4300 East Fifth Avenue,<br>Columbus 16, Ohio | 47 |
| 24A | Bureau of Naval Weapons Representative<br>4300 East Fifth Avenue,<br>Columbus 16, Ohio | |

| | Addressee | Copy Number |
|---|---|---|
| 25 | North American Aviation, Inc.,<br>Los Angeles Division<br>Los Angeles International Airport,<br>Los Angeles 45, California | 48 |
| 25A | Headquarters,<br>Western Contract Management Region<br>Mira Loma Air Force Station,<br>Mira Loma, California | |
| 26 | Northrop Corporation<br>Norair Division<br>3901 West Broadway,<br>Hawthorne, California | 49 |
| 26A | Headquarters,<br>Western Contract Management Region<br>Mira Loma Air Force Station<br>Mira Loma, California | |
| 27 | Republic Aviation Corporation<br>Farmingdale, Long Island, New York | 50 |
| 27A | Headquarters,<br>Eastern Contract Management Region<br>Olmstead Air Force Base,<br>Middletown, Pennsylvania | |